MUSSEL-INSPIRED MUCOADHESIVE HYDROGELS FOR DRUG DELIVERY

By

Jinke Xu

A Thesis Submitted to the Faculty of Graduate Studies and Research in Partial Fulfillment of the Requirements for the Degree of Doctor of Philosophy

June, 2015

Department of Mining and Materials Engineering

McGill University

Montreal, Canada

ABSTRACT

A controlled drug delivery system can deliver a drug with the right dose, control its release rate and time, and target the site of action in the body. Chitosan (CS) and its derivatives have been extensively used in drug delivery. Additionally, CS is mildly mucoadhesive, i.e. it can stick to mucus. Many drug delivery routes such as oral, buccal, and rectal delivery exploit the presence of a mucosa to deliver the drug. Drug delivery systems made from mucoadhesive materials can stick to the mucosa, thus prolonging the retention of drugs on site and allowing a sustained release of the loaded drugs. CS-based mucoadhesive drug delivery systems have shown improved therapeutic effects in many applications.

Recently, the strong adhesion of marine mussels under the sea inspired the development of several water-resistant adhesives. The catechol groups present in large amount in the mussel adhesive proteins contribute to the outstanding adhesion of mussels on many different surfaces. Catechols also interact with biological surfaces, including mucus. These findings inspired us to use catechol-CS mucoadhesive systems to facilitate drug delivery. This was the first time that catechol groups were used to improve the mucoadhesion and thus the efficacy of a drug delivery system.

In this work, we developed three types of catechol-containing CS hydrogels as mucoadhesive drug delivery systems for oral, buccal and rectal drug delivery. We introduced catechols into CS hydrogels by simple physical mixing or covalent conjugation. We assessed the efficacy of catechol-containing hydrogels as drug delivery systems and their mucoadhesion both in vitro and in vivo.

Our first study showed that simple physical mixing of hydrocaffeic acid in CS-based hydrogels enhanced the mucoadhesion of the gels. The electrostatic interaction between hydrocaffeic acid and CS caused a slow release of this molecule from the CS hydrogel, and enhanced the adhesion of CS on mucus. The mucoadhesion of this hydrogel can be further increased in the presence of oxidizing agents during the contact with mucin. However, if the gel is oxidized before contacting mucin, there is no mucoadhesion enhancement.

In our second study we developed a chemically conjugated catechol-CS (Cat-CS) hydrogel crosslinked by genipin. In this case, the immobilized catechols were not released from the gel. This system showed good mechanical properties and great mucoadhesion both in vitro and in vivo. Using this mucoadhesive hydrogel, we succeeded in delivering lidocaine to rabbits through the buccal mucosa. Differently from gels made with unmodified CS, this system established an intimate contact with the rabbit buccal mucosa, achieved a sustained release of the drug, and maintained the drug concentration in the blood at a relatively high level during the 2 h experiment.

In our third study we developed an injectable sulfasalazine (SSZ) loaded Cat-CS hydrogel formulation for rectal treatment of ulcerative colitis (UC). In UC mice, rectal SSZ/Cat-CS formulation showed better therapeutic effects with only 50% of the normal oral dose. Most importantly, this formulation reduced the plasma levels of the SSZ metabolite sulfapyridine, which is associated with many side effects of SSZ and toxicity. Thus, these results proved the great potential of mucoadhesive SSZ/Cat-CS rectal formulation in UC treatment.

Overall, we developed mussel-inspired catechol-containing CS hydrogels that improved the mucoadhesion and thus the drug efficacy and therapeutic effects in drug delivery.

RÉSUMÉ

Un système de délivrance contrôlée de médicaments peut délivrer un médicament à une dose précise, contrôler son temps et son taux de libération, et cibler son site d'action. Le chitosane (CS) et ses dérivés ont été largement utilisés dans la délivrance de médicaments notamment pour leurs propriétés mucoahdésives. De nombreuses voies, telles que la voie orale, buccale, et réctale, exploitent la présence d'une muqueuse pour administer des médicaments. Les systèmes de délivrance de médicaments fabriqués à partir de matériaux mucoadhésifs peuvent coller au mucus, prolongeant ainsi la rétention du médicament sur le site d'action, et permettant une libération prolongée du médicament. Les systèmes de délivrance de médicaments mucoahdésifs à base de CS ont montré une amélioration des effets thérapeutiques dans de nombreuses applications.

Récemment, la forte adhésion des moules marines sous la mer a inspiré le développement de plusieurs adhésifs résistants à l'eau. Les groupes catéchols présents en grande quantité dans les protéines adhésives de moule contribuent à l'adhérence des moules sur de nombreuses surfaces. Les groupes catéchols intéragissent avec les surfaces biologiques, y compris le mucus. Ces résultats nous ont incité à utiliser des systèmes mucoadhésifs CS-catéchol pour faciliter la délivrance de médicaments. C'était la première fois que les groupes catéchols été utilisés pour améliorer la mucoadhésion, et donc l'efficacité d'un système de délivrance de médicament.

Dans ce travail, nous avons développé trois types d'hydrogels CS-cathécol comme systèmes d'administration mucoadhésifs de médicaments par voie orale, buccale et rectale. Nous avons introduit des catéchols dans les hydrogels de CS par simple mélange physique ou par conjugaison covalente. Nous avons évalué l'efficacité de ces hydrogels et leurs propriétés mucoadhésives in vitro et in vivo.

Notre première étude a montré que le simple mélange physique de l'acide hydrocaféique dans les hydrogels de CS permettait d'améliorer leur mucoadhésion. L'intéraction électrostatique entre l'acide hydrocaféique et le CS a provoqué une libération lente de cette molécule à partir de l'hydrogel, et a amélioré l'adhérence du CS sur le mucus. La mucoadhésion de cet hydrogel peut être encore augmentée en présence d'agents oxydants durant le contact avec les mucines. Cependant, si le gel est oxydé avant le contact avec les mucines, il n'y a aucune amélioration de la mucoadhésion.

Dans notre seconde étude, nous avons développé chimiquement un hydrogel conjugué catéchol-CS (Cat-CS) réticulé par la génipine. Dans ce cas, les catéchols immobilisés n'ont pas été libérés à partir du gel. Ce système a montré de bonnes propriétés mécaniques et une excellente mucoadhésion in vitro et in vivo. Cet hydrogel mucoadhésif a permis de délivrer un médicament modèle, la lidocaïne, à des lapins à travers la muqueuse buccale. Ce système a permis d'établir un contact intime avec la muqueuse buccale de lapin, permettant une libération prolongée et un maintient de la concentration du médicament dans le sang à un niveau relativement élevé pendant deux heures.

Dans notre troisième étude, nous avons développé une formulation injectable d'hydrogel Cat-CS chargé en sulfasalazine (SSZ) pour le traitement rectal de la colite ulcéreuse (UC). Dans des souris présentant une UC, induite par le dextran sulfate de sodium (DSS), la formulation rectale SSZ/Cat-CS a montré de meilleurs effets thérapeutiques avec seulement 50% de la dose orale normale. De plus, cette formulation a diminué les niveaux sanguins du métabolite de la SSZ, la sulfapyridine, qui est associé à de nombreux effets secondaires et à la toxicité de la SSZ. Ainsi, ces résultats ont prouvé le grand potentiel de la formulation rectale SSZ/Cat-CS mucoadhésive dans le traitement de la UC.

Dans l'ensemble, nous avons développé des hydrogels Cat-CS qui ont amélioré la mucoadhésion, et donc l'efficacité et les effets thérapeutiques du médicament.

ACKNOWLEDGEMENTS

Four years and a half, one thousand six hundred days, a man from 23 to 28. It was a long journey, but fortunately, I was never alone.

Prof. Marta Cerruti, my supervisor in research, my rainbow in life. As a supervisor, you gave me the chance to start this journey, you taught me how to walk and talk when I was new to this scientific world, you guided me all along the road making sure I wouldn't go into the wrong direction, you motivated me when I was down, and you threw me a bottle of water when I was crawling in the desert. And now, you are waiting for me at the finishing line – THANK YOU. As a friend outside research, you are my rainbow. You have so many colors, and always show up after thunder storms – THANK YOU.

Prof. Jake Barralet, my strict co-supervisor. You guided me to start my journey, and always encouraged me to run faster. Sometimes you gave me surprises and heart attacks, especially when I was reckless in front of you. I finally understood until recently: these are also part of the training. Confucius said "A teacher for a day is a father for a lifetime", this was something I always kept in mind during my journey – THANK YOU.

Prof. Julian X.X. Zhu, Prof. Mary Stevenson and Prof. Sophie Lerouge, my wisdom advisors, thank you for your support and advice helping me reach one milestone after another. Dr. Xuan Tuan Le, Dr. David Bassett, Dr. Ghareb Soliman, Dr. Elena Varoni, Dr. Satu Strandman and Dr. Mifong Tam, my knowledgeable mentors, thank you for sharing your precious experience on the road. I have learnt so much from you. I would also like to thank Ms. Barbara Hanley, Ms. Terry Zatylny and Ms. Courtney Jelaco from my department for your kind support during these days.

Dr. Hesam Mahjoubi, Dr. Mandana Bornapour and Dr. Jilani Ghulam, my dearest buddies in the lab. Thank you for your supports, encouragements, and birthday surprises. Having all of you in this journey was definitely a bonus, you made my journey much less boring – THANK YOU. I would like to specially thank Dr. Ophélie Gourgas for the kind help with the French translation of my abstract. As you may notice, each of you has the "Dr." title. That is my wish to you: the title is right "ahead" of you, go and get it soon.

Dr. Rui Li, Dr. Di Lin, Dr. Zhaomin Liu & Ms. Wenjia Yang, Dr. Kaiwen Hu, and Dr. Huaifa Zhang, my brothers and sisters. Thank you for your company during the sunniest days and the darkest nights. You gave me the feeling of family in Montreal – THANK YOU.

Dr. Guangsheng Yu, my uncle. You have been extremely supportive during these years. Your positive attitude towards difficulties, and love and forgiveness to people will influence me for the rest of my life – THANK YOU. I would also like to thank Dr. Xun He for your support and care during my PhD study.

Dad and mom, my parents, my ultimate source of energy and my reason of doing PhD. You gave me a life, and taught me to become a person with integrity, loyalty, and kindness – THANK YOU. This thesis is dedicated to you. You have been waiting for this day for too long.

TABLE OF CONTENTS

LIST OF FIGURES

LIST OF TABLES

CONTRIBUTION OF AUTHORS

This thesis contains three manuscripts written by me under the supervision of Prof. Marta Cerruti. They are presented in Chapters 3, 4, and 5, respectively. Chapter 3 has been published in the peer-reviewed journal "Langmuir". Chapter 4 has been published in the peer-reviewed journal "Biomaterials". Chapter 5 will be submitted shortly to a peer-reviewed journal.

I am the first author of all three manuscripts. My responsibilities included designing experiments, conducting tests, collecting and analyzing data, and writing the manuscripts.

My supervisor Prof. Marta Cerruti guided me throughout my entire PhD study. Her contributions to these manuscripts include initiating the projects, providing funds and facilities for the experiments, building the collaboration with various institutions and facilities, supervising the experiments, leading the discussion and analysis, offering recommendations, and extensively revising the manuscripts. My co-supervisor Prof. Jake Barralet's contributions to these manuscripts include providing facilities for the experiments, offering discussions and recommendations, and revising most of the manuscripts.

I worked closely with a few collaborators during my PhD study. Their contributions to the manuscripts are listed below:

Chapter 3.

Dr. Ghareb Soliman was a postdoctoral fellow in Prof. Marta Cerruti's and Prof. Jake Barralet's lab in McGill University. He helped me with the experimental design, data analysis, and manuscript writing.

Chapter 4.

Dr. Satu Strandman was a postdoctoral fellow at Prof. Julian X.X. Zhu's lab in Université de Montréal. She helped me with the experimental design, data analysis, and manuscript writing in the rheology section.

Prof. Julian X.X. Zhu is a professor in Université de Montréal. His contributions to this manuscript include providing rheology facilities and revising the manuscript.

Chapter 5.

Dr. Mifong Tam is a research associate at Prof. Mary Stevenson's lab in McGill University. She helped me with the experimental design, animal experiments, data collection and analysis, and manuscript revision.

Prof. Mary Stevenson is a professor in the Faculty of Medicine at McGill University. Her contributions to this manuscript include initiating the project in collaboration with Prof. Marta Cerruti, proposing animal experiments, providing animal-related facilities, offering discussions and recommendations, and revising the manuscript.

Prof. Sophie Lerouge is a professor in the Department of Mechanical Engineering at École de Technologie Supérieure (ÉTS). Her contributions to this manuscript include providing rheology and injection force measurement facilities, offering discussions and recommendations, and revising the manuscript.

CHAPTER 1. GENERAL INTRODUCTION

1.1 Background and rationale

People use drugs to treat diseases or stay healthy since ancient times. Modern pharmaceutic strategies aim at developing drugs with good efficacy, good patient compliance, and low side effects. To achieve these goals, most drug formulations use controlled drug delivery systems to control the delivery dose, time, and targets in the body [1-3]. Sustained release is a crucial feature of controlled drug delivery systems. A sustained release drug delivery system can prolong the drug release and maintain the drug concentration at the right level in the body, thus reducing the frequency of drug administration and the side effects caused by multiple-dose administration. The selection of a drug delivery system depends on the nature of the drug, the disease, and the administration route.

Drug delivery systems include hydrogels, tablets, capsules, liquid formulations, sprays, patches, films, particles, and microneedles [4-7]. Among these types, hydrogels are widely used as drug delivery systems due to their high biocompatibility and versatile functions. Chitosan (CS), a polycationic polymer derived from chitin, has been extensively used to form hydrogels for drug delivery. Many functionalized CS derivatives have shown success in drug delivery providing sustained release [8, 9], responsiveness to stimuli such as pH, temperature, and enzymes [10-15], and ability to target specific tissues [16-19].

An important property of CS and its derivatives is mucoadhesion. Mucoadhesion refers to the adhesion of a material with the mucus [20]. Using mucoadhesive materials, people developed drug delivery systems that could stick to mucosas, thus extending the drug retention at the site of application and prolonging its therapeutic effects [21-24]. Due to its cationic nature in

physiological pH, CS shows a weak mucoadhesion via electrostatic interactions with the anionic mucin [25, 26]. Some functionalization can enhance the mucoadhesion of CS. For example, thiolated CS can form disulfide covalent bonds with the cysteine subdomains in the mucin, thus showing a stronger mucoadhesion compared to CS [22, 27].

Recently, a series of catechol functionalized polymers including CS have shown superior adhesion to biological surfaces including skin [28-32] and cells [33]. The strategy of introducing catechol groups to enhance adhesion was inspired by the strong adhesion of the *Mytilus edulis* mussel under the sea. This mussel produces adhesive proteins that contain a large amount of an unusual amino acid, 3,4-dihydroxyphenyl-L-alanine (DOPA). The catechol groups in DOPA can interact with molecules on various surfaces by forming catechol-metal coordination, hydrogen bonds, or covalent bonds, thus contributing to the adhesion. Because of their good adhesion to biological tissues, catechol-modified polymers have found applications in wound healing and hemostatic [29-32]. Besides skin and cells, catechol modified polymers also showed some adhesion to mucus. For example, the mixture of mucin and catechol-modified poly(ethylene oxide)-poly(propylene oxide)-poly(ethylene oxide) block co-polymers was more viscous than the mixture of mucin with unmodified polymers [34]. Atomic force microscopy measured a high molecular pull-off force between DOPA-modified PEG and mucin [35]. Although these results directly or indirectly proved the interaction between catechol groups with mucin, the mechanism is still not fully understood. The interactions responsible for catechol mucoadhesion may include hydrogen bonds, hydrophobic interactions, π electron interactions, physical chain entanglement, and covalent bonds [34, 35]. Most importantly, so far no work has been down to show if catechol-enhanced mucoadhesion can be used to improve drug delivery.

1.2 Objectives

We hypothesized that introducing catechols into CS hydrogels would enhance CS mucoadhesion, thus prolonging its retention on a mucosa and in turn increasing the residence time and the therapeutic effects of drugs loaded in the gels. Mucosa layers cover the surfaces of many organs that can be used to perform drug delivery. In this work we focus on oral, buccal and rectal mucosas. We hypothesize that drug delivery through any of these routes can benefit from a mucoadhesive system made from catechol-modified CS hydrogels.

Thus, the objectives of this study are:

I. *To develop catechol-containing CS hydrogels by physical mixing CS with three catechol compounds: DOPA, hydrocaffeic acid (HCA) and dopamine (DA), and evaluate their potential as mucoadhesive oral drug delivery systems in vitro.*

Oral drug delivery is the most common and convenient drug administration method. It involves the ingestion of drugs through the gastrointestinal tract, which is covered by mucus. This layer provides the sites for mucoadhesive drug delivery systems to bind. We aim at developing catechol-containing mucoadhesive CS hydrogels for oral drug delivery. We selected three catechol-containing compounds: DOPA, HCA and DA. We physically mixed CS with each catechol-containing compound, vacuum dried the mixtures, and re-hydrated them to form the hydrogels. These three catechol molecules have different charges in physiological pH; in this work we explore how this affects hydrogel properties such as swelling ratio, release rate of the catechol molecules, and catechol-induced mucoadhesion. In addition, catechols undergo various reactions in presence of oxidizing agents. Some diseases in the gastrointestinal tract such as ulcerative colitis cause the formation of a large amount of reactive oxygen species in the mucus layer. Thus, in this paper we also studied how the oxidation of catechols affects the mucoadhesion of the hydrogels.

This information provides some insights to help the design of catechol-modified CS mucoadhesive gels for oral drug delivery.

II. *To develop a catechol-CS (Cat-CS) hydrogel by chemical conjugation of HCA to CS, and evaluate it as a mucoadhesive drug delivery system for buccal drug delivery both in vitro and in vivo.*

Based on the encouraging in vitro results from Objective I, we extended our work to in vivo studies. Compared to oral drug delivery, buccal drug delivery has advantages including prolonged localized drug effect, and avoidance of gastrointestinal drug metabolism and first pass elimination. One crucial challenge of buccal drug delivery is how to retain the drug formulations on the buccal mucosa. Movements of the mouth and tongue, and the flush of food, water, and saliva may eliminate the buccal drug delivery system quickly. Mucoadhesive systems can stick to the buccal mucus layer and prolong the retention time of the drug on site. Thus, we proposed to use catechol-introduced mucoadhesive CS hydrogels for this application. We covalently conjugated the catechol groups to CS molecules (Cat-CS) instead of simply mixing them together, as we did in Objective I. We hypothesized that the immobilized catechol groups in Cat-CS can provide better mucoadhesion than catechol groups simply mixed with CS. We loaded a model drug lidocaine in the hydrogels, and after evaluating the system from a physico-chemical point of view, we tested the gels for lidocaine buccal delivery in rabbit models.

III. *To develop a novel sulfasalazine-loaded injectable rectal mucoadhesive formulation made from the previously developed Cat-CS hydrogels, and evaluate its therapeutic effect in mice models affected by ulcerative colitis.*

The results from Objectives I and II supported our hypothesis: catechol-modified CS hydrogels are promising mucoadhesive drug delivery systems. We further exploited the possibility

of using this mucoadhesive system to treat ulcerative colitis (UC). UC is an inflammatory bowel disease involving recurring inflammation and ulcers at the mucosal layer of the colon [36]. Both oral and rectal formulations can treat mild to moderate UC in patients. Rectal formulations such as liquid suppositories and foams have shown better therapeutic effects than oral formulations, due to the enhanced local efficacy directly at the surfaces of the inflamed mucosa. In addition, rectal formulations can reduce the side effects associated with oral formulations [37, 38]. However, such rectal formulations are difficult to retain in the colon, thus limiting the therapeutic effects. We hypothesized that the mucoadhesive Cat-CS hydrogels can overcome this challenge by sticking to the colon mucosa. Thus, we loaded sulfasalazine (SSZ), a conventional oral drug for UC treatment, inside Cat-CS hydrogels forming SSZ/Cat-CS gels. We injected this formulation rectally in mice treated with dextran sulfate sodium (DSS), which is a method to induced UC in mice. We evaluated the therapeutic effect of this formulation in comparison with an oral formulation, in terms of body weight recovery rate, colon length, histology and expression of inflammation-related cytokine TNF-α. In addition, we compared the plasma concentration of the drug metabolite related to SSZ side effects, to compare the safety of our proposed formulation and the oral one.

1.3 Thesis structure

This thesis is written in a manuscript-based format. Chapter 1 (i.e. this chapter) introduces the general background, rationale and the objectives of the whole study. Chapter 2 reviews the literature in topics related to this research, including drug delivery, chitosan hydrogels, mucoadhesion, and mussel-inspired mucoadhesion. Chapters 3, 4, and 5 are three manuscript-based chapters showing the results of our Objectives I, II, and III, respectively. Chapter 6 summarizes the contributions to original knowledge, and discusses future perspectives. Appendix summarizes all the methods that we used in this thesis.

CHAPTER 2. LITERATURE REVIEW

2.1 Drug delivery

2.1.1 Introduction

Humans have been using drugs to treat diseases and improve health quality since ancient times. Ancient Chinese Shen Nong documented the use of plants for medication as early as 3,500 B.C. [39]. Herbal mixtures made from leaves and roots of medical plants represented the early drug formulation [1]. Such formulations contained not only the active ingredients, but also some non-effective or even toxic components. The doses of the active ingredients in such systems lacked of consistency. In the 18th century, scientists started attempting to deliver therapeutics at a uniform and consistent dose. They formulated the medical plant extracts into pills, syrups, capsules, tablets, solutions, suspension, lozenges, and powders [1]. With the development of medicinal chemistry technologies, people succeeded to extract the effective components from natural plants [40]. For instance, Friedrich Sertürner isolated the active ingredient morphine from opium as an analgesic drug in 1815 [41]. Later, in early 1900s, Paul Ehrlich and his research group synthesized the first man-made antibiotic drug called arsphenamine, and used it to treat syphilis by injection. This discovery started a new chapter of rational synthetic drug development.

Although researchers made tremendous progress in the field of drug design and development, the optimization of drug formulation did not attract enough research interest. Traditional formulations lacked a mechanism to control the drug release or distribution. Thus, frequent doses, low drug bioavailability, low drug efficacy, severe side-effects and potential toxicity often limited their use [1].

In the mid-1960s, Judah Folkman introduced the original concept of controlled drug delivery. He used a drug-loaded silicone rubber tubing as an implant to achieve a sustained drug release [42]. The study successfully prolonged therapeutic effects of a number of drugs, including digitoxin, triiodothyronine, thyroid I125, isoproterenol, sodium ethylenediamine tetraacetic acid (EDTA) and tyrosine [43]. His concept started the development of controlled drug delivery systems. By definition, a controlled drug delivery system refers to a formulation or a device that delivers a drug with the right dose, controls the rate and time of the drug release, and targets the site of action in the body [1-3]. Such systems can control the mechanism of delivery in chemical, physiochemical or mechanical ways independently or collaboratively [44]. At early times, the reservoir and the matrix system were the two main types of diffusion-controlled drug delivery systems (Figure 2.1). A reservoir system contains a polymeric core with drug loaded inside, while a matrix system is a polymeric bulk with drug distributed homogeneously in the structure [1]. Both systems can achieve a controlled release drug delivery, but their release profiles can be quite different. The release profiles of these drug delivery systems depend on the type of polymer, degradation properties, size and structure of the system, and nature of the loaded drug.

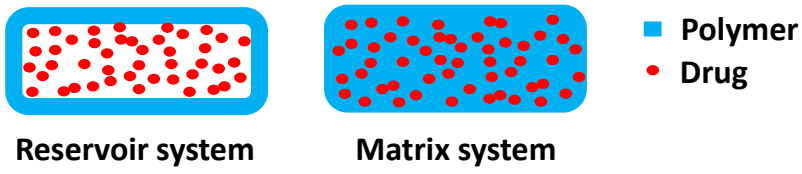

Figure 2.1. Schematic of diffusion-controlled drug delivery systems: a reservoir system and a matrix system.

A crucial feature of controlled drug delivery systems is that they can achieve sustained drug release, which means that the drug remains at the correct concentration at the site of action

for an extended time. This feature can reduce the potential toxicity caused by drug overdosing, lower the frequency of administration, and increase the drug efficacy. When people inject or ingest a drug formulation without a controlled release mechanism, the drug concentration in local tissue or plasma can increase sharply after initial administration, following a burst release kinetics (see dash-dotted curve in Figure 2.2). Eventually, the drug will be metabolized in our body and its concentration will decrease. However, the peak drug concentration may exceed the safety threshold and reach the toxic concentration range. This will result in potential toxicity and adverse effects. To avoid such hazard, we usually take drugs at relatively low doses multiple times per day (see dashed curve in Figure 2.2). Each dose will ensure that the drug concentration in our body does not reach toxic concentration range. When the drug is gradually metabolized and its concentration drops close to the lowest therapeutic concentration, we take another dose. Such an approach maintains the drug concentration within the therapeutic concentration window, thus reducing the toxicity risk and increasing drug efficacy. However, this approach requires frequent doses, thus reducing ease of administration and patient compliance. A sustained release drug delivery system provides an ideal alternative solution. The system gradually releases the drug to the site of action, and maintains the concentration at a constant level within the therapeutic concentration range (see solid curve in Figure 2.2). Instead of multiple doses, we can use one dose only, and yet achieve a prolonged therapeutic effect. At the same time, we reduce the toxicity risk caused by overdosing.

Systemic and local drug administration are the two main approaches to treat diseases [1]. A controlled drug delivery system can improve drug efficacy and safety in both strategies. In conventional systemic drug administration, we either inject therapeutics intravenously or administrate drugs orally. Systemic blood circulation transports the therapeutics to the sites of

action. A controlled drug delivery system prolongs the drug release from the carrier, and reduces the risk of systemic overdosing. Still, since the therapeutics go through the entire blood circulation in the body, accumulation of therapeutics at tissues other than the site of action may bring unintended side effects or toxicity. To prevent this, we can use a targeted drug delivery system. Although still systemic, a targeted drug delivery system can selectively bind to the tissue or cells that need treatment, thus preventing the presence of drugs at non-targeted regions. There are many systemic drug delivery systems in the formats of nanoparticles, liposomes, and degradable matrices.

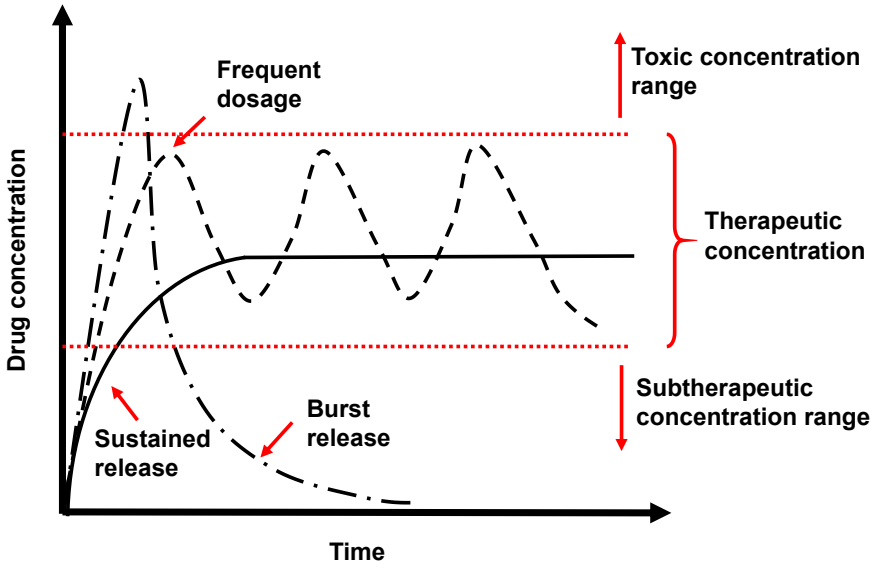

Figure 2.2. Schematics of drug release profiles in the body: a burst release, a frequent dosage, and a sustained release.

Differently from systemic administration, local administration aims at delivering drugs directly to the site of application. Local administration can provide a high drug concentration at the local tissue or organ. The advantage of this approach is the reduced systemic toxicity. However, if uncontrolled, the high drug concentration may damage the local tissue. A controlled drug release system can prevent a burst drug release and lower the risk of toxicity on the site of action.

Hydrogels, patches, and implantable micro-devices are commonly used local drug delivery systems, for example in anti-cancer and anti-inflammatory drug delivery.

A controlled drug delivery system can also increase the bioavailability of drugs. Our bodies have various mechanisms to protect ourselves from foreign materials, including drug molecules. When a drug enters the gastrointestinal tract, it has to pass through the harsh acidic gastric environment and intestinal environment rich in digestive enzymes. The metabolism in the liver can significantly reduce the concentration of drugs participating in the systemic circulation. In the plasma, metabolic reactions are very active due to the presence of enzymes and cells. All these conditions may reduce or eliminate the activity of therapeutic compounds, thus challenging the bioavailability of these drugs. If a drug has low bioavailability, the body may metabolize the drug before its concentration reaches the effective therapeutic level. As a result, the drug shows low or no efficacy. This problem limits the use of a large number of drugs. For example, insulin is a peptide drug widely used for diabetes treatment. Insulin has very low bioavailability if administrated orally, due to the intensive metabolism of the drug in gastrointestinal tract. Currently, the common administration method is subcutaneous injection. This method complicates the administration procedures and reduces patient compliance. A nanoparticle drug delivery system resisting gastric acid and enzyme metabolism could protect insulin against the degradation in the gastrointestinal tract, thus enhancing its bioavailability in oral delivery [45].

Modern strategies aim at designing multifunctional, target-oriented drug delivery systems. Research in drug delivery systems is a multi-disciplinary field involving knowledge of chemistry, pharmacology, biology, physiology, and material science [46]. The material and formulation of a drug delivery system can greatly affect the drug efficacy. Our limited understanding of the

interaction between complex materials and the body remains one of the major challenges in this field [47].

2.1.2 Drug delivery routes

The choice of a proper drug delivery system depends on the nature of the disease, the kinetics of the drug, and its metabolism profile. These factors further narrow down the choices of drug delivery routes. Oral ingestion and intravenous injection are the most commonly used drug delivery methods. The advantages of oral drug administration include ease of administration, good patient compliance, and low cost [46]. Orally delivered drugs enter the body through the mouth, pass by the esophagus, and reach the stomach. Depending on the target site, therapeutics may act locally in the gastrointestinal tract, or participate in the systemic circulation [15]. Different from oral delivery, intravenous injection only offers the systemic pathway [48]. The drugs reach the blood stream through a needle inserted into a vein, and from there, they rapidly reach the entire body via the systemic circulation [48]. Besides oral drug delivery and intravenous drug delivery, other drug delivery routes include buccal, rectal, pulmonary, ocular, intranasal, transdermal, intramuscular, and subcutaneous drug delivery.

Many organs that can be targeted for drug delivery, such as eyes, nose, mouth, respiratory tract, gastrointestinal tract, and reproductive tract, are covered by a mucosa layer [24, 49]. This is a 5 – 200 μm thick layer protecting against unfavorable chemicals, bacteria or virus [23]. Mucus is composed of 95% water, 0.5 – 5% glycoproteins (also known as mucin), and small amounts of lipids, mineral salts and free proteins [23]. Mucin is secreted by goblet cells in human body; it has a protein core with heavily glycosylated oligosaccharide side chains (Figure 2.3) [23, 50]. At pH higher than 2.8, mucin is negatively charged due to the sialic acids and sulphate residues in the

oligosaccharide side chains [49]. The mucin chains are linked terminally with many crosslinking including disulphide bonds.

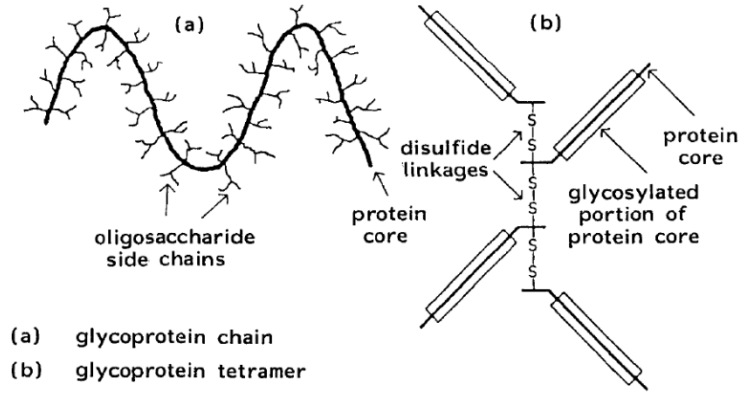

Figure 2.3. Schematic of mucin [23].

In this work, we will focus on oral, buccal and rectal drug delivery. We will exploit the mucosa layer that covers the organs involved as a site for our drug delivery system to bind to, thus prolonging drug residence time and achieving sustained drug release. In this section, we review the physiological structure and provide examples of applications of these three drug delivery routes.

2.1.2.1 Oral drug delivery

The human gastrointestinal tract includes the esophagus, the stomach, the small intestine and the colon (large intestine) (Figure 2.4). A layer of mucus covers the surface of the luminal side of the gastrointestinal tract [51]. The gastrointestinal mucus layer is 100 – 150 μm thick, mainly composed of mucin and water. It serves as a protective layer as well as lubricant. Therapeutic molecules have to penetrate this layer to enter systemic circulation. Below the mucus layer, an epithelial layer consisting of tightly joined epithelia cells and intercellular junctions provides a further barrier.

Most drugs targeting a systemic effect are absorbed at the proximal part of the small intestine [46, 52]. Other drugs may target local regions within the gastrointestinal tract, such as stomach and colon [52].

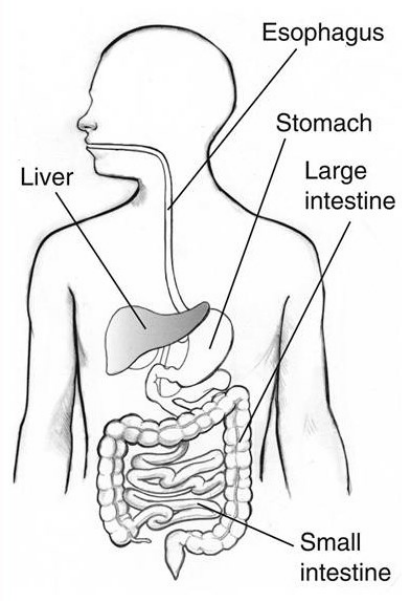

Figure 2.4. Schematic of the human gastrointestinal tract.

(Source: http://i.ehow.com/images/a05/0n/u3/lower-left-stomach-pain-children-800x800.jpg)

Stomach-specific drugs target diseases such as ulcer and stomach cancer; these drugs need to stay long enough in the stomach for their action to take place. However, the regular emptying of the stomach caused by gastric movements and flow of food and water may shorten the presence of these drugs in the stomach. These factors challenge the efficacy of stomach-specific oral drugs. A suitable oral drug delivery system should thus prevent this rapid elimination. Shishu et al. designed an oral formulation which was able to float in the gastric fluid. They loaded an anti-stomach cancer drug into calcium alginate beads containing carbon dioxide gas bubbles [53]. When the beads reached the stomach, they floated in the gastric fluid due to the presence of carbon

dioxide gas bubbles, and did not get eliminated when the stomach was emptied. As a result, this system showed better anti-stomach tumor efficacy compared to conventional oral tablets.

Inflammatory bowel diseases such as ulcerative colitis, Crohn's disease and colon cancer can greatly benefit from local drug treatment. Oral drugs for these diseases have to pass through the stomach and small intestine prior to the targeting site of action in colon [54]. Early degradation or absorption of these drugs in the upper gastrointestinal tract may reduce or eliminate drug efficacy before reaching the colon. A colon-specific oral drug delivery system protects the drugs through the upper gastrointestinal tract, and releases them specifically in the colon. One strategy is to conjugate the drug molecule to a parent molecule forming a prodrug. The prodrug will tolerate the degradation and absorption in the stomach and the small intestine. Once the prodrug reaches the colon environment, enzymes or bacteria trigger the release of the active therapeutics. Other strategies include designing pH or time-dependent controlled release formulations to achieve colon-specific oral drug delivery [55].

2.1.2.2 Buccal drug delivery

Buccal drug delivery acts on the surface of the luminal side of the oral cavity. It can show therapeutic effects either locally at the site of application, or systemically through the blood stream. Figure 2.5 shows a schematic of the human buccal mucosa [56]. Human oral mucosa consists of oral epithelium, lamina propria and sub-mucosa [57]. A layer of mucus covers the surface of the epithelium towards the luminal side of the oral cavity. The human buccal epithelium is non-keratinized and about 500-800 μm, 40-50 cells in thickness [57, 58]. The permeability of the oral mucosa is in the order of sublingual > buccal > palatal [59]. The buccal mucosa has a surface area of approximately 30 cm^2 [60].

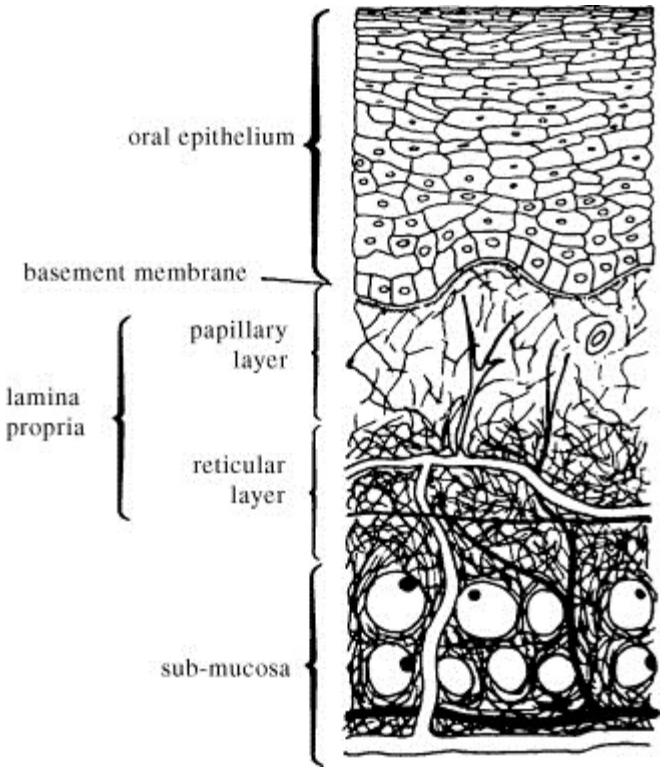

Figure 2.5. Schematic of the human oral mucosa [56].

In buccal drug delivery, a film or a tablet containing the drug can bind to the mucosal surface. Buccal drug delivery receives good patient compliance because of such easy and non-invasive administration method. Buccal drug delivery can treat local diseases in oral cavity, such as lichen planus, oral cancer, oral candidiasis, oral mucositis and periodontal diseases [59, 61-63]. In these cases, buccal drug delivery systems release the therapeutics directly on top of the disease sites.

Besides local treatments, buccal drug delivery can also achieve systemic treatment through transmucosal pathways. The oral cavity is rich in micro blood vessels under the mucosa [57, 58]. The released drugs penetrate the mucosal membrane and join the blood stream circulation. Different from oral drug delivery, buccal drug delivery does not require drugs to pass through the stomach or small intestine, thus it avoids the severe digestive reaction and hepatic first-pass

elimination. Therefore, buccal drug delivery can improve the efficacy of drugs with low oral bioavailability.

Flushing of saliva and food as well as movement of the mouth limits the retention time of drugs in the oral cavity. These factors can cause loss of drugs and non-uniform drug distribution, thus reducing drug efficacy. One way to avoid this is to develop a buccal drug delivery system that can stick to the oral mucosa and release the drugs progressively. These systems are called mucoadhesive. Researchers have developed many different mucoadhesive formulations for buccal drug delivery, such as adhesive gels, tablets, films, patches, ointments, mouth washes, and pastes [64]. We will discuss in details about the use of mucoadhesive materials for buccal drug delivery in Section 2.3.4.2.

2.1.2.3 Rectal drug delivery

Figure 2.6 shows a schematic of the human rectum. Rectum is the distal part of colon, with a length of ~10 cm and surface area of ~300 cm^2 [64]. Different from other parts of gastrointestinal tract, the rectum has no villi on the surface, and therefore it has a relatively lower surface area [65]. Similar to buccal drug delivery, drugs delivered rectally can enter the blood stream circulation before passing through the stomach and liver metabolism. In addition, rectal drug delivery offers a safe absorption site for peptides and proteins due to lower proteolytic activity in colon compared to small intestine [15]. Researchers have developed gels, liquid suppositories, and solid formulations for rectal drug delivery [66-68].

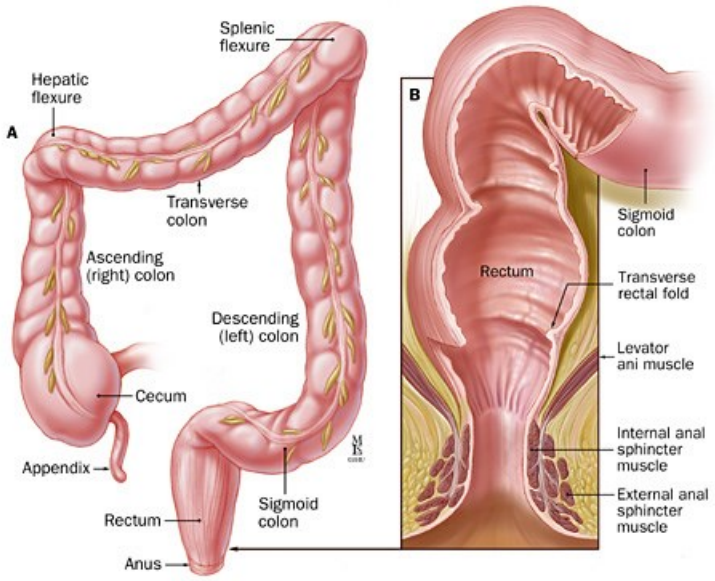

Figure 2.6. Schematic of the human rectum.

(Source: http://www.hopkinscoloncancercenter.org/Upload/200904141145_51605_000.jpg)

Rectal drug delivery can effectively treat some inflammatory bowel diseases such as ulcerative colitis. As we mentioned before, the conventional treatment for such diseases is to use an oral colon-targeting prodrug. For instance, sulfasalazine (SSZ), a potent oral formulation to treat ulcerative colitis, is a prodrug of the active compound 5-aminosalicylic acid (5-ASA). SSZ is composed of 5-ASA and sulfapyridine (SP) linked by an azo bond (Figure 2.7). 5-ASA has a low oral bioavailability because of the intensive absorption of the compound in the small intestine. SSZ protects 5-ASA from the intestinal absorption and metabolism. Once it reaches the colon, the bacterial enzymatic effect breaks the azo bond and releases 5-ASA (Figure 2.7) [69]. However, oral SSZ formulation has little control on the drug distribution. Thus, its therapeutic effect and consistency may vary depending on the location of the ulcers in the colon. In addition, the bowel movement and the fecal content may limit the retention time of the drug in the colon. Rectal

delivery of 5-ASA provides a topical treatment directly on the colon mucosa. This method does not need to deliver 5-ASA through the upper gastrointestinal tract, thus avoiding the use a prodrug to protect 5-ASA against early absorption in the small intestine. Prolonging the retention time of 5-ASA in the colon also improves its efficacy. 5-ASA rectal hydrogels and suppositories have shown a better therapeutic effect on ulcerative colitis than the oral SSZ formulation [70-74].

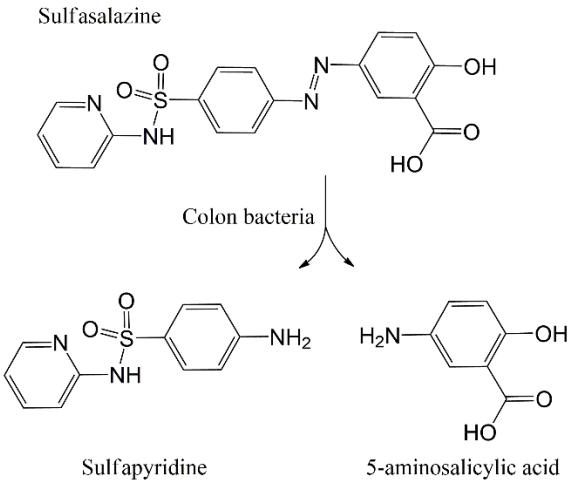

Figure 2.7. SSZ and its metabolites.

2.1.3 Hydrogels for drug delivery

Conventional drug delivery systems include tablets, capsules, liquid formulations, sprays, patches and films [4, 5]. More recently, researchers have developed particulate drug delivery systems, such as polymeric micro or nanoparticle systems and lipid-base nanoparticle systems. Such systems can encapsulate drugs, protect drug degradation, control drug release and enhance drug absorption [6, 7]. Due to its small size and high surface area, a nanoparticulate system can significantly increase the cellular contact and bioavailability [6, 75]. Lipid-based particulate systems (i.e., liposomes) are made from a phospholipid bilayer membrane with entrapped water [75]. Such particles are very biocompatible since phospholipids are natural components of biological membranes and

lipoproteins. Lipid-based particulate systems can facilitate the absorption of drugs with poor solubility [76]. Besides particulate systems, another recent technology that has gained much interest is microneedle arrays for transdermal delivery. These consist of multiple micron-sized needles coated or loaded with drugs. Microneedles can penetrate the first 10-15 μm of skin without irritating the nerves in the skin [77, 78]. The system passes the skin transport barrier and delivers the drugs to the skin microvascular networks. This easy and painless drug delivery method has found applications in vaccine delivery [79-81].

In the rest of this section we will review the use of hydrogels as drug delivery systems, since the experimental part of this work has focused on the development of hydrogel-based drug delivery systems.

Hydrogels are three dimensional hydrophilic polymeric networks containing large amounts of water [82, 83]. The polymeric network does not dissolve in water due to the presence of crosslinks between the polymer chains. These crosslinks can be chemical, through covalent bonds, or physical, including electrostatic interactions, hydrophobic interactions, hydrogen bonds, polymer chain entanglement and van der Waals interactions. Small ordered regions (crystallites) formed in an unordered amorphous polymer matrix may also keep together a hydrogel [83].

Hydrogels can swell and retain water, in amounts varying between 20% to as much as 99% by weight [84, 85]. They provide a water environment similar to the physiological conditions found in the body. In addition, hydrogels usually have low interfacial free energy in body fluids because of their hydrophilic nature, thus proteins and cells cannot bind to them easily [86]. Because of these properties, hydrogels often have very good biocompatibility, thus avoiding significant immune system reaction or toxicity when used in boi-related applications. Therefore, hydrogels can deliver bioactive drugs or genes.

Hydrogels can be made from natural polymers, synthetic polymers, or proteins [87]. Depending on the charges of the materials, hydrogels can be classified into cationic, anionic and neutral hydrogels. Changing the degree of crosslinking or polymer molecular weight can make the hydrogel very soft or very stiff to fit the needs of the applications. Using hydrogels, researchers have been able to achieve drug delivery at a controlled rate and to specific targets [83, 88-90].

Recently, people have developed stimuli-sensitive hydrogels, which behave differently upon environmental changes such as temperature, pH, electric signals, light, pressure, and specific ions [89]. For example, temperature increase can break hydrogen bonds in the hydrogel structure. In hydrogels made from hydrophobic polymers, this will cause the aggregation of polymer chains, leading to shrinkage of the hydrogels and drug release [88, 89].

People use biodegradable hydrogels in many drug delivery applications. In this study, we made our hydrogel drug delivery systems from a biodegradable natural polymer, chitosan (CS), and its derivatives. We discuss about CS-based hydrogel in the next section.

2.2 Chitosan hydrogels

2.2.1 Chitosan (CS)

CS is a linear polysaccharide consisting of randomly distributed repeating units of β-(1-4)-linked D-glucoamine and N-acetyl-D-glucoamine (Figure 2.8) [15]. In commercial productions, CS is derived from chitin, which is widely present in crab and shrimp shells as well as cell walls of fungi. Alkaline deacetylation of chitin can remove the acetyl groups and form CS. By controlling the molecular weight and the degree of deacetylation, it is possible to tune different properties of CS such as solubility, viscosity, biocompatibility, and biodegradation rate [91].

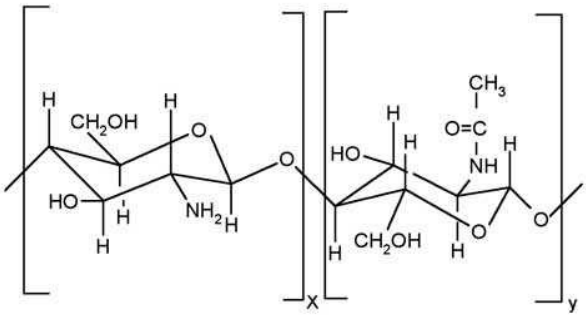

Figure 2.8. Chitosan

CS is biocompatible, non-toxic and biodegradable [92-94]. In the human body, enzymes such as lysozyme can metabolize CS without inducing an immune response [15, 95]. CS has a pKa of ~ 6.3. The primary amines in its structure get protonated under acidic conditions, making CS a cationic polymer. However, in physiological conditions where the pH is above 6, CS has little or no charge [15, 96]. When CS solution pH is elevated above 6, the repulsive electrostatic forces between the polymer chains are weakened due to the neutralization of amine groups. Meanwhile, attractive hydrophobic interaction and hydrogen bonds dominate, leading to CS precipitation [97]. To prevent this, some researchers used β-glycerophosphate as a mild base to increase solution pH. The amine groups from CS kept their charge in the presence of β-glycerophosphate, and CS did not precipitate until the pH increased up to 7.2 [98, 99].

2.2.2 CS hydrogel preparation methods

2.2.2.1 Physically crosslinked CS hydrogels

As discussed in Section 2.1.3, possible physical interactions include ionic interactions, polyelectrolyte interactions, hydrophobic interactions, and crystallite and secondary bonding [15, 91, 100] (Figure 2.9) [15]. We will illustrate these interactions in details in the following sections.

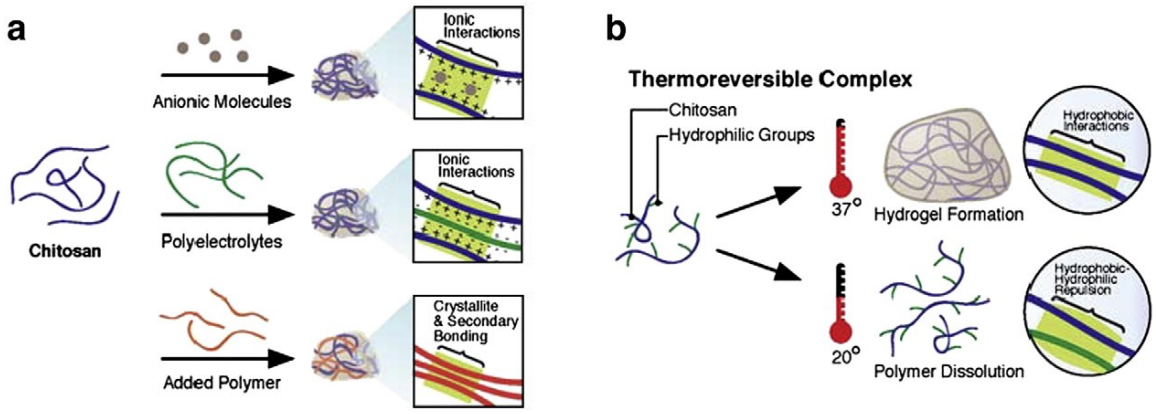

Figure 2.9. Schematic representation of CS hydrogel networks derived from different physical associations: (a) networks of CS formed with ionic molecules, polyelectrolyte polymers and neutral polymers; (b) thermoreversible networks of CS graft copolymer resulting in a semi solid gel at body temperature and a liquid below room temperature [15].

Ionic interaction

Due to the polycationic nature of CS, anionic molecules or ions can form crosslinks within the CS polymeric chains. These reversible ionic interactions require no purification steps [91]. Metallic anions such as Mo(VI) and Pt(II) anionic complexes can form ionic crosslinking with the protonated amino groups of CS. Brack et al. investigated changes in CS hydrogel viscosity due to $PtCl_2^{2-}$ ionic crosslinking [101]. Time of gelation decreased with the increase in concentration of $PtCl_2^{2-}$. Besides anionic metal complexes, small anionic molecules such as sulfates, citrates and phosphates can also crosslink CS ionically. Pieróg et al. studied the swelling properties of CS hydrogel membranes prepared by adding sulfuric acid, trisodium citrate, and sodium tripolyphosphate respectively, and they found that the swelling properties depended on both crosslinking agents and environmental pH [102].

Polyelectrolyte interaction

Polyelectrolyte interaction refers to the electrostatic interaction between a cationic polymer and an anionic polymer. It is stronger than other secondary bonds such as hydrogen bonding and van der

Waals interactions, and thus may lead to the formation of more mechanically stable physically crosslinked gels [15] Many studies used alginate, a polyanion, to form polyelectrolyte complexes with CS [103-105]. Other natural polyanions include carrageenan, pectin, hyaluronic acid, gelatin, and poly-γ-glutamic acid, etc [106]. Synthetic polyanions rich in COO^- groups such as Carbopol can also form polyelectrolyte interaction with the NH_3^+ groups in CS.

Hydrophobic interactions

CS hydrogels formed through hydrophobic interactions usually have interesting features such as thermosensitivity [15]. For example, Bhaattarai et al. prepared polyethylene glycol (PEG) modified CS with sol-gel transition point at above 25°C [13]. At low temperature, the hydrogen bonds between PEG and water molecules dominated, and the system was in solution state. When the temperature increased above the transition point, the hydrophobic interactions between polymer chains dominated, so the solution turned to gel (Figure 2.9). The transition point could be tuned by changing the percent of PEG.

Crystallite and secondary bonding

Another strategy to prepare hydrogels is by mixing CS and other water soluble nonionic polymers due to the formation of crystallites. One example is the formation of CS/poly(vinyl alcohol) (PVA) hydrogels through freeze-thaw cycles [107-110]. The repeated freeze-thaw procedure can gradually increase the degree of crystallization until ordered crystallites are formed between folded PVA chains. These crystallites enhance the chain-chain interaction, thus increasing the degree of crosslinking. Secondary bonds such as hydrogen bonds can also play a role in hydrogel preparation as reported by Qu et al. [111], who developed D,L-lactic acid and/or glycolic acid modified CS hydrogels with pH sensitivity.

2.2.2.2 Chemically crosslinked CS hydrogels

Chemical crosslinking in CS hydrogels refers to the formation of covalent bonds in the polymeric matrix. CS can crosslink with itself (Figure 2.10a) or with a copolymer forming a hybrid polymer network (Figure 2.10b). CS can also form a semi-interpenetrating network with another non-crosslinked polymer (Figure 2.10c). In this case, only CS is crosslinked by a crosslinker [91]. Chemically crosslinked CS hydrogels are more stable than physically crosslinked hydrogels. In the following sections, we will explain these three types in details.

CS crosslinked with itself

Small crosslinking molecules can form covalent bonds between CS polymeric chains. Typical crosslinkers are glutaraldehyde and formaldehyde. The mechanism relies on the covalent bond formation between the primary amines of CS and the aldehydes. However, due to the toxicity of these crosslinkers, extra purification steps are often necessary to remove the excess unreacted chemicals, thus limiting the biocompatibility of such CS hydrogels. An alternative to aldehydes is a natural crosslinker called genipin; since this molecule is much less toxic than glutaraldehyde, many studies used it as a CS crosslinker for bio-related applications [10-12].

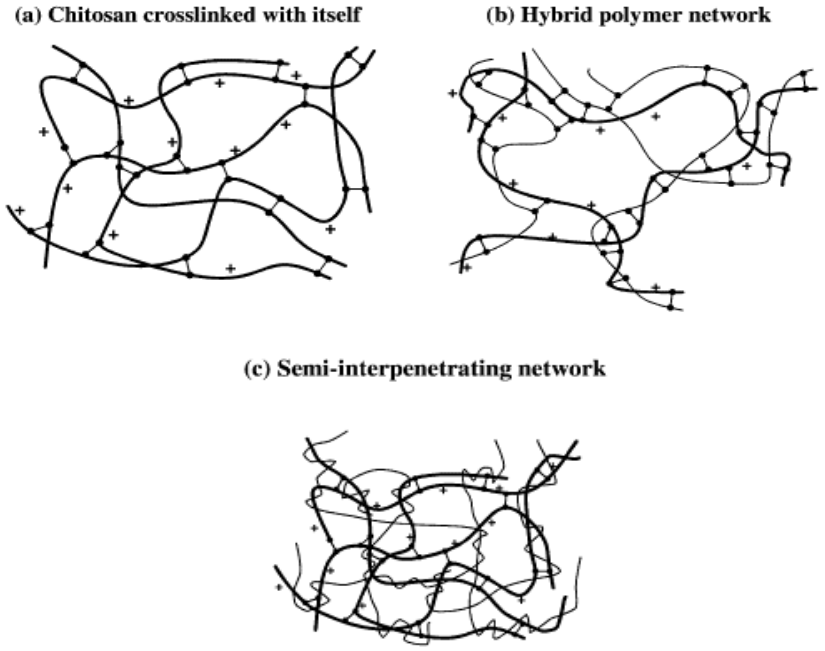

Figure 2.10. Structure of CS hydrogels formed by (a) CS crosslinked with itself; (b) hybrid polymer network; (c) semi-interpenetrating network [91].

CS crosslinked with copolymers

Another way to prepare covalently crosslinked CS hydrogels is to use copolymers with reactive functional groups. Sometimes, researchers need to modify CS in order to introduce certain functional groups necessary for the crosslinking. Tan et al. developed an injectable and biodegradable hydrogel made from water soluble N-succinyl-CS and aldehyde modified hyaluronic acid. The Schiff-base reaction between the amino and aldehyde groups of the polysaccharide derivatives formed covalent bonds between the polymers and turned the mixture into a hydrogel [112]. Thiol modification is another crosslinking strategy, based on the formation of disulfide bonds [113]. Inspired by mussel adhesive proteins, Ryu et al. developed CS/pluronic hydrogels for tissue adhesives [29]. They functionalized CS with catechol groups, and conjugated thiol groups on Pluronic F-127 triblock copolymer. When these two blends were mixed at body

temperature and physiological pH, instantaneous gelation occurred due to the crosslinking reaction of the catechol and thiol groups. We will discuss in detail the chemistry of catechol groups and their applications in Section 2.4.

Semi-interpenetrating network

Semi-interpenetrating networks are formed when a non-crosslinked polymer is entrapped within the matrix of crosslinked CS. If the non-reacting polymer is further crosslinked, it forms a full-interpenetrating network [15, 91]. The addition of the non-crosslinked polymer causes physical entanglement with CS chains, and it may enhance certain properties of the CS hydrogel. For instance, Lee et al. prepared semi-interpenetrating network CS hydrogel crosslinked by glutaraldehyde with the addition of PEG. The addition of non-crosslinked PEG decreased CS hydrogel degradation rate and tuned its mechanical strength for wound dressing application [114]. Other non-crosslinked polymers added in CS hydrogels include silk fibroin, PVA, etc., as summarized by Berger et al. [91].

2.2.3 CS hydrogels for oral, buccal and rectal drug delivery

CS hydrogels have been used extensively in drug delivery [15]. Here we provide a few examples of their use in the three delivery routes of interest to our work.

One of the challenges that CS hydrogels have to face in oral drug delivery is the large pH variations found in the gastrointestinal tract environment, which range from as low as 1 in the stomach to around 6 in the small intestine. A pH-sensitive CS hydrogel can protect sensitive drugs such as peptides and proteins from the harsh gastric environment and release them in the small intestine. For example, Chen et al. developed a semi-interpenetrating network hydrogel made from water-soluble N,O-carboxymethyl CS and alginate crosslinked by genipin [10]. At the stomach pH, the swelling of this hydrogel was minimal due to the hydrogen bonds between N,O-

carboxymethyl CS and alginate. When the pH increased to 7.4, the electrostatic repulsions between polymer chains due to the ionization of the acidic groups of alginate dominated. This caused the gel to swell, and allowed the release of loaded proteins (bovine serum albumin). Besides pH-sensitive CS hydrogels, enzyme-sensitive CS hydrogels can achieve targeted delivery to a specific site including stomach [16], small intestine and colon [17-19]. The bacteria or microorganisms in the gastrointestinal tract secrete various enzymes. These enzymes may degrade CS hydrogels, causing the release of the loaded drugs [14, 15].

CS hydrogels can also facilitate buccal drug delivery and rectal drug delivery. Senel and co-workers used 2% CS gel in dilute lactic acid solution to deliver a large bioactive peptide (transforming growth factor TGF-β) through porcine buccal mucosa [115]. Martin et al. developed physically cross-linked palmitoyl glycol CS hydrogels by freeze-drying, and achieved sustained release of denbufylline for 5 h through buccal mucosa in a rabbit model [8]. They detected the drug in the plasma as early as 0.5 h after the drug administration. Eman et al. loaded an anti-inflammatory drug (diclofenac sodium) in CS microspheres, and they made a hydroxypropyl methylcellulose and Carbopol 934 hydrogel containing these microspheres [67]. Such formulation provided a sustained release of the drug-loaded microspheres, which in turn released the drug to the rectal mucosa. This system reduced the rectal mucosal tissue irritation compared to other forms of the drug.

Besides the biocompatibility, biodegradability, pH and enzyme-sensitivity, the success of using CS hydrogels in oral, buccal and rectal drug delivery also relies on their mucoadhesion. Hydrogels made from CS or CS derivatives can stick to the mucosa surface in oral, buccal and rectal drug delivery routes. Such systems prevent the removal against organ movement and flow of body fluids, thus increasing the residence time of drugs at the site of action. In the next section,

we discuss in detail the concept of mucoadhesion and mucoadhesive materials. We also review the applications of mucoadhesive systems in oral, buccal and rectal drug delivery.

2.3 Mucoadhesion

2.3.1 Introduction

Despite the versatility of drug delivery systems for oral, buccal and rectal delivery, the drug retention time at the site of action may still be very short. For example, the movement of the tongue will interrupt the retention of a buccal drug delivery system in the oral cavity; the food and drink we ingest may shorten the retention of an oral drug delivery system in the gastrointestinal tract; bowel movements can accelerate the elimination of a rectal drug delivery system. In these cases, the drugs may not have enough time to act on the disease before being eliminated. Mucoadhesive drug delivery systems can attach to the mucus covering the drug delivery paths and increase the drug retention time.

Mucoadhesion refers to the adhesion between a material and a mucosal surface [20]. In addition to oral, buccal and rectal drug delivery, mucoadhesive systems have found applications in other mucosa-involving paths such as ocular, nasal, gingival, and vaginal administration [21]. Due to the prolonged drug retention time, the drug efficacy is higher when a mucoadhesive formulation is used compared to non-mucoadhesive formulations [116]. Other advantages include reduced administration frequency leading to better patient compliance, improved drug bioavailability, reduced dosage of administration, controlled release of drugs, and the possibility of targeting specific intestinal sites [21-24].

Early in 1947, Scrivener and Schantz first used a mixture of gum tragacanth and dental adhesive to administrate penicillin through the oral mucosa [117]. In the 1980s, Nagai prepared

mucoadhesive tablets loaded with drugs for the local treatment of aphthae [118]. Since then, people gradually accepted the importance of mucoadhesion in drug delivery. In this section, we introduce the theory of mucoadhesion, and we focus on the use of mucoadhesives in oral, buccal and rectal drug delivery.

2.3.2 Mechanism of mucoadhesion

The interactions between mucin and mucoadhesive materials include ionic, covalent, hydrogen bonds, van der Waals, and hydrophobic interactions [22]. Factors such as the molecular weight of the polymer, the flexibility of the polymer chains, environmental pH, charge, and functional groups in the polymer may affect the mucoadhesion strength [21, 22, 119]. Oxidation of some polymers functionalized by catechol groups can enhance mucoadhesion. We will discuss this in details in Section 2.4.

Several theories have been proposed to explain the mechanism of mucoadhesion. The wetting theory developed by Peppas and Buri attributes mucoadhesion to the surface tension of mucoadhesives: better spreading (i.e. low surface tension) induce better mucoadhesion [49]. Voiutskii suggested that mucoadhesion is due to the semi-permanent adhesive bond formed by interdiffusion between the polymer chains of the mucoadhesive materials and mucin [120]. Smart proposed a combined theory consisting of 3 steps. First, mucoadhesives get wet and start to swell. Then, they contact mucus and form non-covalent bonds at the interface. Finally, mucoadhesive polymer chains and mucin chains interpenetrate each other, and develop further entanglements [22]. Other theories include the adsorption theory [121] and the fracture theory [122]. Still, no single theory can fully explain the complex mechanism of mucoadhesion [21, 22].

2.3.3 Mucoadhesive materials

2.3.3.1 Cationic polymers

Cationic polymers are likely to demonstrate good mucoadhesion since they can form electrostatic interaction with the negatively charged mucin at the physiological pH [123]. For example, polylysine is a cationic polymer containing many amino groups in its polymer chains. These amino groups can be protonated at physiological pH, making polylysine a mucoadhesive polymer [124].

CS is a well-known cationic mucoadhesive. The mucoadhesion of CS mainly comes from the electrostatic interaction with the negatively charged mucin [25, 26]. CS is also a permeation enhancer due to the ability to open the tight junctions of the epithelial cells [125]. However, the mucoadhesion of CS is limited, and weaker compared to other polymers such as carbomer, polycarbophil and hyaluronic acid [126]. Various strategies have been tested to enhance the mucoadhesion of CS. For example, Werle et al. developed thiolated CS derivatives showing very strong mucoadhesion [27]. The enhancement is attributed to the formation of disulfide links between the thiol groups and cysteine-rich subdomains of mucus [22, 27]. After Werle, researchers have developed various thiolated CS derivatives, including CS-thioglycolic acid conjugates [127], CS-cysteine conjugates [128], CS-glutathione conjugate [129], CS-thioethylamidine conjugate [130] and CS-4-thio-butyl-amidine conjugate [131]. In addition to the mucoadhesion enhancement, thiolated CS derivatives also improved the cohesion of CS hydrogels due to inter- and intra-chain disulfide bonds formation. Trimethylation is another modification that provides enhanced mucoadhesion [132, 133]. Trimethylation of amino groups in CS increases the positive charge, and enhances the electrostatic interaction between CS and mucin. In another study by Jintapattanakit and co-workers, PEG-grafted CS showed even higher mucoadhesion compared to

trimethylated CS. The chain interpenetration of the PEG and the mucin contributed to the extra mucoadhesion enhancement [132].

2.3.3.2 Anionic polymers

A group of anionic polymers containing –COOH groups exhibit strong mucoadhesion. The mucoadhesion is attributed to hydrogen bonds formed between –COOH and the oligosaccharide side chains in mucin [134]. Alginate, poly(acrylic acid) (PAA), carboxymethylcellulose, and pectin belong to this category [21, 134]. For example, Kesavan et al. developed a mucoadhesive sodium alginate/sodium carboxymethylcellulose formulation to deliver antibacterial gatifloxacin through the ocular route [135]. They found that increasing the concentration of either mucoadhesive component caused an increase in mucoadhesion. The mucoadhesion of PAA have been intensively studied as well [136-139].

2.3.3.3 Non-ionic and amphoteric polymers

Different from cationic or anionic mucoadhesive polymers, some non-ionic polymers show mucoadhesive properties due to chain entanglement with mucin [134]. In general, chain entanglement is weaker than polyelectrolyte interaction [21]. Non-ionic polymers in this class include hydroxypropylmethylcellulose (HPMC) [140, 141], poly(ethylene oxide) (PEO) [142] and PVA [143].

Amphoteric polymers contain both cationic and anionic substructures. Some amphoteric polymers have shown mucoadhesion. The cationic substructures can form electrostatic interactions with the negatively charged mucin, while the anionic substructures can form hydrogen bonds with the –COOH groups in mucin. Gelatin is a typical example belonging to this category [144, 145].

2.3.4 Mucoadhesives for oral, buccal and rectal drug delivery applications

2.3.4.1 Oral mucoadhesive drug delivery systems

An oral mucoadhesive drug delivery system prolongs the drug retention time in the stomach or small intestine, thus allowing for sustained release at the target site [52]. In addition, the intimate contact of the mucoadhesive device with the mucosal surface provides a high concentration gradient which facilitates passive drug uptake [116].

For stomach-targeting drug delivery, a mucoadhesive drug delivery system can adhere to the stomach mucosa, which gives a better local efficacy due to the increased drug retention time in the stomach [52]. For example, Majithiya and Murthy developed CS-based mucoadhesive microspheres containing an antibiotic drug (clarithromycin) for the treatment of stomach ulcers [146]. The system increased the drug accumulation in the stomach, and achieved a four-fold improvement in drug bioavailability compared to a plain drug suspension.

For drugs targeting or being absorbed in the small intestine, a mucoadhesive drug delivery system can improve the local therapeutic effect or drug absorption by increasing its retention time in the small intestine. Yin et al. developed a thiolated trimethyl CS nanoparticulate system for insulin oral delivery [147]. The formation of disulfide bonds between thiol functional groups and mucin enhanced the mucoadhesion by up to 4.7 folds compared to non-thiolated nanoparticles. Again using thiolated CS, Millotti and co-workers made mucoadhesive tablets containing insulin for oral delivery [148]. This formulation increased the mucoadhesion by a factor of about 80 in comparison with unmodified tablets, and the bioavailability of the drug in a rat model was also remarkably increased about 21 folds. A few reviews have summarized different types of oral mucoadhesive drug delivery systems [64, 116, 149, 150].

2.3.4.2 Buccal mucoadhesive drug delivery systems

Mucoadhesive drug delivery systems can stick to the oral mucosa and prevent the removal of drugs against mouth movement or the flow of saliva. Both local and systemic therapeutic effects can benefit from buccal mucoadhesive drug delivery systems. Buccal mucoadhesive formulations include tablets, patches, films and gels [59]. In recent years, buccal mucoadhesive drug delivery systems have been extensively studied [9, 151-174]. We summarize some examples in Table 2.1.

Table 2.1. Summary of buccal mucoadhesive drug delivery systems.

Mucoadhesive drug delivery system formulation	Type	Drug	Application	In vivo model	Ref.
Chitosan-EDTA	Hydrogel	Insulin	Transmucosal	Rat	[9]
Hakea gibbosa gum	Tablet	Salmon calcitonin	Transmucosal	Rabbit	[151]
PEO, HPMC	Tablet	Lercanidipine HCl	Hypertension	Human & rabbit	[152]
EC. HPC	Film	Lidocaine HCl	Regional anesthetic	Human	[153]
Tamarind gum	Film	Benzydamine Lidocaine	Anti-inflammatory Local anesthetic	-	[154]
Carbopol, Poloxamer, PEG, Methocel	Patch	Lidocaine	Local anesthetic	-	[155]
NaCMC, Chitosan, polycarbophil, glycerol, propyleneglycol,	Semi-solid	Sucralfate, lidocaine	Anti-inflammatory	Human	[156]
Carbopol, HPC	Tablet	Nicotine	Smoking cessation	Human	[157]
Carbopol, sodium aliginate	Tablet	Nicotine	Smoking cessation	-	[158]
Carbopol, HPMC	Patch	Nicotine	Smoking cessation	Human	[159]
Xanthan gum, Carbopol	Patch	Nicotine	Nicotine replacement therapy	-	[160]
Chitosan-gelatin	Film	Propranolol HCl	Hypertension	Human	[161]
Sodium alginate, Carbopol	Tablet	Propranolol HCl	Hypertension, cardiovascular disorders	Rabbit	[162]
Carbopol, HPMC	Patch	Pravastatin sodium	Vascular disease	Rabbit	[163]
Carbopol, silicone	Patch	Oxytocin	Inadequacy of breast feeding	Rabbit	[164]
Hakea gibbosa gum	Tablet	Chlorpheniramine maleate	Anti-histamine	Rabbit	[165]
HPC, Carbopol	Disk	Nalbuphine	Analgesic	-	[166]
NaCMC, chitosan, PVA, HEC, HPMC	Patch	Miconazole nitrate	Anti-fungal	Human	[167]
HEC, carbomer	Tablet	Metronidazole	Periodontal disease	Human	[168]
PVP	Film	Fentanyl	Analgesic	-	[169]
PVP, NaCMC	Film	Ibuprofen	Anti-inflammatory, analgesic	Human	[170]

Sodium alginate, HPMC, magnesium oxide and croscarmellose sodium	Tablet	Omeprazole	Inhibition of gastric acid secretion	Golden hamster	[171]
Mucoadhesive wax-film composite	Film	Testosterone	Hormone therapy	Rabbit	[172]
poly(sodium methacrylate, methylmethacrylate), HPMC and MgCl2	Tablet	Clobetasol propionate	Oral lichen planus	Human	[173]
Eudragit RL-PO/solubilizer	Patch	Fenretinide	Head and neck squamous cell carcinoma (HNSCC), oral cancer	Rabbit	[174]

* EDTA: Ethylenediaminetetraacetic acid; PEO: polyethylene oxide; HPMC: hydroxypropyl methylcellulose; EC: ethylcellulose; HPC: hydroxypropyl cellulose; PEG: polyethylene glycol; NaCMC: sodium carboxymethylcellulose; PVA: polyvinyl alcohol; HEC: hydroxyethyl cellulose; PVP: polyvinylpyrrolidone.

2.3.4.3 Rectal mucoadhesive drug delivery systems

Mucoadhesive drug delivery systems can decrease their displacement in the rectum. For example, Choi et al. developed a formulation to deliver acetaminophen using poloxamer-based mucoadhesive liquid suppository [175]. This system achieved a strong mucoadhesion in the rat rectum and achieved a higher acetaminophen concentration in plasma compared with conventional suppositories. In another study, a similar system was used to rectally deliver propranolol, a drug with low bioavailability if delivered orally. The enhanced mucoadhesion of the drug delivery system reduced the displacement of the suppository and increased the drug bioavailability [176]. We summarize some applications of rectal mucoadhesive drug delivery systems in Table 2.2.

Table 2.2. Summary of rectal mucoadhesive drug delivery systems.

Mucoadhesive drug delivery system formulation	Type	Drug	Application	In vivo model	Ref.
Poloxamer, polycarbophil	Liquid suppository	Acetaminophen	Anti-pyretic, analgesic	Rat	[175, 177]
Poloxamer, HPC, PVP, Carbopol, polycarbophil, sodium alginate	Liquid suppository	Propranolol HCl	Hypertension	Rat	[176]
Poloxamer, sodium alginate	Liquid suppository	Acetaminophen	Anti-pyretic, analgesic	Human	[68]
Poloxamer	Liquid suppository	Ketorolac tromethamine	Analgesic	Rabbit	[178]
Poloxamer, HPMC	Liquid suppository	Ondansetron	Nausea and vomiting	Rat	[179]
Carbopol	Liquid suppository	Metronidazole	Anti-biotic	Rabbit	[180]
Poloxamer, HPMC, PVP, MC, HEC, Carbopol	Liquid suppository	Etodolac	Anti-inflammatory	Rat	[181]
HPMC, Carbopol, chitosan	Hydrogel with chitosan microspheres	Diclofenac sodium	Anti-inflammatory	Rat	[67]
Mucin, gelatin	Microspheres	Ceftriaxone sodium	Anti-bacteria	-	[66]

* HPC: hydroxypropyl cellulose; PVP: polyvinylpyrrolidone; HPMC: hydroxypropyl methylcellulose; MC: methylcellulose; HEC: hydroxyethyl cellulose.

2.4. Mussel-inspired mucoadhesion

2.4.1 Introduction to marine mussel adhesion

In the previous section, we have discussed different types of mucoadhesive materials, and their applications in drug delivery. Many studies used CS to develop mucoadhesive drug delivery systems because of its abundant availability and good biocompatibility. However, the weak electrostatic interactions between CS and mucin limit CS mucoadhesion. To enhance CS mucoadhesion, researchers have functionalized CS with various groups or polymers, among which thiols are particularly attractive [147, 148].

Recently, the strong underwater adhesion of blue marine mussels (*Mytilus edulis*) has attracted the attention of material scientists. These mussels stick to many surfaces under the sea, such as rocks and boats, thus avoiding being removed by the waves [182]. Mussels can adhere to many different surfaces: organic and inorganic, hydrophilic and hydrophobic, smooth or rough, and even the inert Teflon [182-184]. To adhere under water, mussels secrete proteins called *Mytilus edulis* foot proteins (Mefps). Mefps can rapidly solidify in the seawater and form the so-called byssus. Figure 2.11a shows a schematic of the *Mytilus edulis* mussel and byssus structures [185]. The distal part of the byssus is called the byssal plaque. Mussels use the strong adhesion of the byssal plaques to attach themselves to various solid surfaces. Further investigation unveiled the presence of an unusual amino acid, 3,4-dihydroxyphenyl-L-alanine (DOPA), highly expressed in Mefp sequence (Figure 2.11b) [186]. DOPA contains catechol functional groups, which have been shown to participate in the formation of byssal plaques and in the adhesion to solid surfaces under the sea [186, 187].

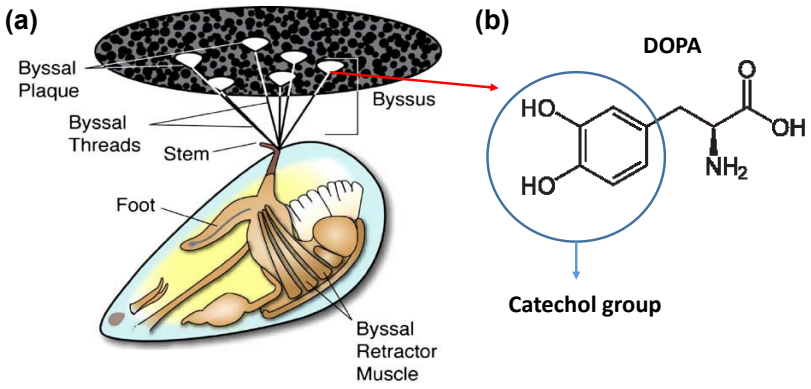

Figure 2.11. *Mytilus edulis* mussel and byssus structure (a) and the structure of DOPA (b) [185].

The catechol-induced underwater adhesion inspired many researchers to develop novel catechol-containing adhesives. In our work, we used hydrogels made of catechol-functionalized CS as mucoadhesive drug delivery systems. In this section, we review Mefps, catechol chemistry and the applications of catechol functionalized materials, with a specific focus on mucoadhesion.

2.4.2 Mefps

A byssus consists of four parts: the root attached to the byssal retractor muscle, the stem, the byssal threads, which can expand, spread and reach solid surfaces, and the adhesive attachment plaques in contact with the foreign surfaces (Figure 2.11a) [185, 188]. An organ called mussel foot produces the Mefps, and releases them through the so-called byssal grooves, where Mefps are molded into threads. The threads remain attached to the root, radiating up to 5-6 cm in mature mussels.

Figure 2.12 shows a schematic of a single byssal thread [189]. A plaque contains an outside layer called cuticle and a foam-like core made of open pores interconnected by channels. The cuticle is 2-5 μm thick, and serves as an inert protective barrier for the inner core from seawater and microbes. The size of the pores in the inner core varies depending on the location within the

plaques. At the interface between plaque and substrate, small pores with a diameter of ~ 200 nm are dominant, whereas in the upper part connecting the thread and the plaque the pore diameters are a few microns [185, 189]. In this section, we introduce the proteins found in plaques. Figure 2.13 shows a schematic illustration of Mefps distribution in the byssus [185].

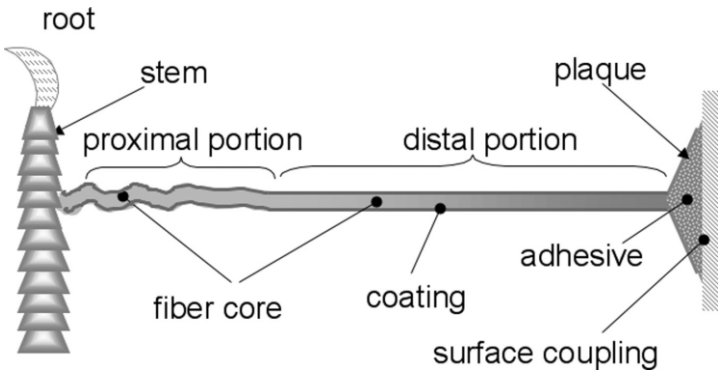

Figure 2.12. Schematic of a single byssal thread [189].

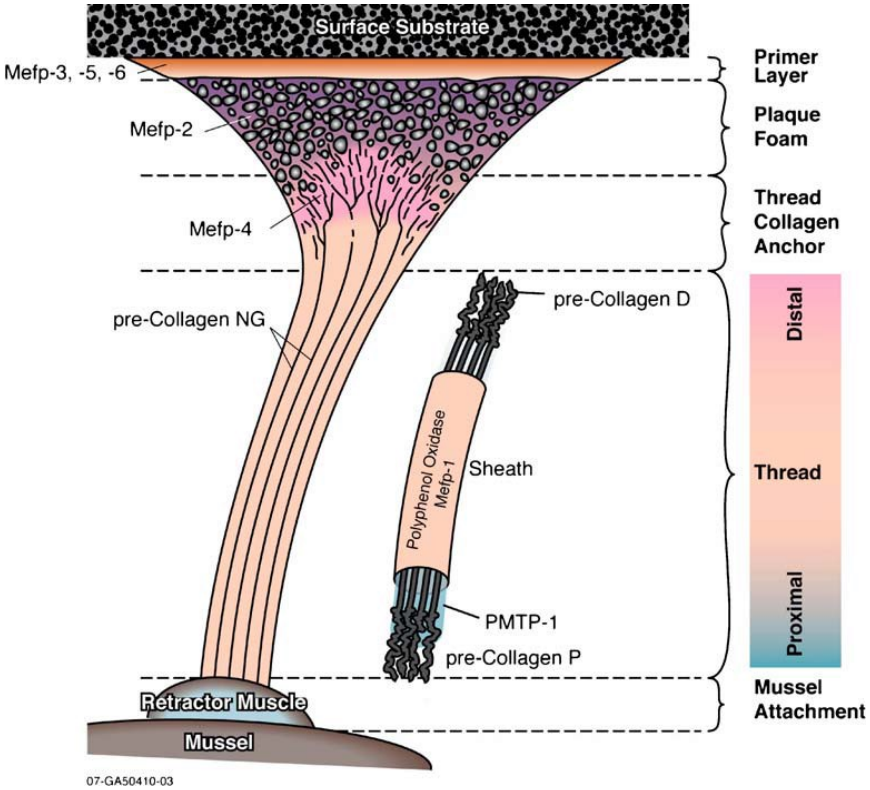

Figure 2.13. Schematic illustration of Mefp distribution [185].

2.4.2.1 Byssal thread protein

The cuticle of the byssal threads is composed of a polyphenolic protein called Mefp-1 (Figure 2.13) [185]. This is by far the most studied mussel adhesive protein. Mefp-1 is a large, basic, hydrophilic protein consisting of 897 amino acids with a molecular weight of ~108 kDa. It contains 15 mol% of DOPA in the protein sequence. Catechol oxidase enzyme triggers the oxidation of DOPA in Mefp-1, leading to the formation of the hard cuticle [185].

2.4.2.2 Byssal plaque polyphenolic proteins

Five proteins are only present in the byssal plaques, namely Mefp-2, Mefp-3, Mefp-4, Mefp-5 and Mefp-6 (Figure 2.13) [185]. Mefp-2 contains less than 5 mol% of DOPA, but contributes to 25 – 40% of the entire plaque proteins. It is smaller (45 kDa) than Mefp-1. Mefp-2 contains a repeated motif similar to the epidermal growth factor [190]. Mefp-3 has a molecular weight of ~6 kDa and is the smallest Mefp. Mefp-3 has many different sequence variants, and its DOPA concentration can reach 20 mol% or above. Mefp-3 is responsible for mussel adhesion on different surfaces [183, 184]. Mefp-4 contains only ~2 mol% of DOPA, but has a repeated histidine-rich decapeptide, which allows it to form copper complexes with histidine-rich ends of prepolymerized collagens in the byssus. Mefp-5 and Mefp-6 contain high levels of lysine, tyrosine and glycine. While Mefp-5 contains 28 mol% of DOPA, Mefp-6 contains only less than 2 mol% of it. Mefp-5 serves as a primer for interfacial adhesion [184], while Mefp-6 may form cysteinyl-DOPA crosslinking with other proteins in the plaques during the byssal formation.

2.4.2.3 Byssal thread collagen

The fibrous core of a byssal thread is made of different prepolymerized collagen variants, including proximal prepolymerized collagen (preCollagen-P), distal prepolymerized collagen (preCollagen-D) and pepsin-resistant nongradient prepolymerized collagen (preCollagen-NG), and the proximal

thread matrix protein (PTMP-1) (Figure 2.13) [185]. These collagens contain little DOPA (< 3 mol%). preCollagen-P and preCollagen-D are present in the byssal threads in gradient, while preCollagen-NG distributes evenly along the threads. The water soluble PTMP-1 appears in the proximal part of the thread, interconnecting other proteins in thread formation [191].

2.4.3 Catechol chemistry

Mussel adhesion to foreign surfaces and byssal formation (the solidification of secreted Mefps) are both attributed to DOPA reactions [184, 192]. To understand the mechanisms of these processes, we have to understand catechol chemistry.

DOPA can transform to semi-quinone radicals and ortho-benzoquinone (DOPA-quinone) through redox reactions [193]. The redox reactions are triggered by oxidizing agents, enzymes, or a basic pH condition [193, 194]. DOPA-quinone can further react according to three main pathways: self-crosslinking, involving coupling of two DOPA molecules, Michael addition with –SH or $–NH_2$ group, and Schiff-base reaction with $–NH_2$ [190, 192, 193, 195] (Figure 2.14).

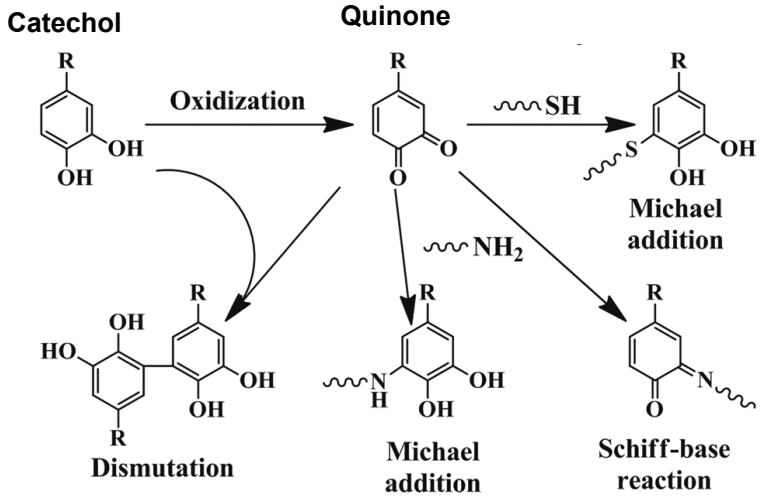

Figure 2.14. Catechol oxidative chemistry [195].

In addition, DOPA can form strong metal coordination complexes [193, 194]. For example, catechols can form mono, bis or tris-catecholate complexes with Fe^{3+} depending on the pH and the ratio between catechols and metal ions (Figure 2.15) [193, 196, 197]. Other metal ions include Fe^{2+}, Cu^{2+}, Al^{3+}, Zn^{2+}, Ti^{4+}, and Mn^{3+} [189, 198].

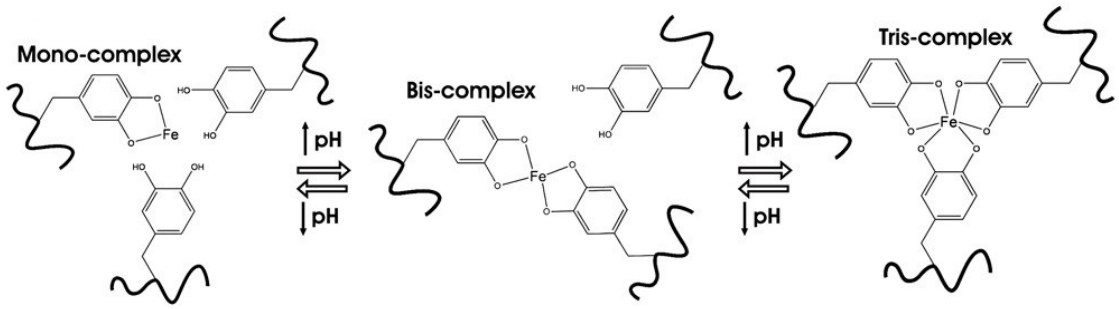

Figure 2.15. Schematic of the formation of catechol-iron complexes [196].

During the formation of the byssal threads, DOPA is oxidized into DOPA-quinone by different factors, including basic pH, enzymes, and metal ions in the seawater. DOPA-quinones can actively participate in intermolecular crosslinking, leading to the formation of bulk protein matrix [184]. The concentration of metal ions in mussel byssus is significantly higher than in the surrounding seawater [199]. This indicates that stable complexes formed by DOPA and metal ions also contribute to the byssal thread formation [200].

2.4.4 Mefp adhesion mechanism

Different Mefps exhibit different adhesive behaviors depending on environmental factors such as the nature of the surface and the environmental pH. Numerous studies have attempted to explain the mechanism of Mefp adhesion on a wide variety of surfaces.

Lin et al. found that both Mefp-1 and Mefp-3 could adhere to mica due to hydrogen bonds formed between DOPA and mica [183]. However, while they measured a strong adhesion when

they put together two mica pieces both coated with Mefp-3, they found little adhesion if the two mica pieces were coated with Mefp-1. This was attributed to differences in the molecular structures of Mefp-1 and Mefp-3. Mefp-1 has a high molecular weight and can absorb on the surface via DOPA-hydrogen bonds, with unbound segments facing outside. Thus, it could only link to one mica surface but could not link to another. On the contrary, Mefp-3 is a small protein with high mobility and flexibility. Therefore, it is capable to diffuse into the narrow junctions of two mica surfaces and build more hydrogen bond binding sites. Thus, Mefp-1 serves as a protective layer on each mica piece, while Mefp-3 can function as an adhesive between mica surfaces [183].

Yu et al. investigated the adhesion of Mefp-3 on TiO_2 at different pHs using a surface force apparatus (SFA) [194]. In an acidic environment (pH 3) where DOPA did not undergo oxidation, the adhesion force was attributed to the hydrogen bonds formed between the two hydroxyl groups and the O atoms on the TiO_2 surface (Figure 2.16a). When the pH was higher than 5.5, hydroxyl groups started to dissociate and formed a charge transfer complex with Ti atoms, called DOPA-Ti coordination [194]. One (Figure 2.16b) or both (Figure 2.16c) of the hydroxyl groups in DOPA could participate in the DOPA-Ti coordination. DOPA-Ti coordination was stronger than the hydrogen bonds. However, DOPA also turned to DOPA-quinone via auto-oxidation at pH 5.5, and this reduced the adsorption of Mefp-3 on the TiO_2 surface. Thus, the auto-oxidation of DOPA to DOPA-quinone provided a competing effect on the overall adhesion.

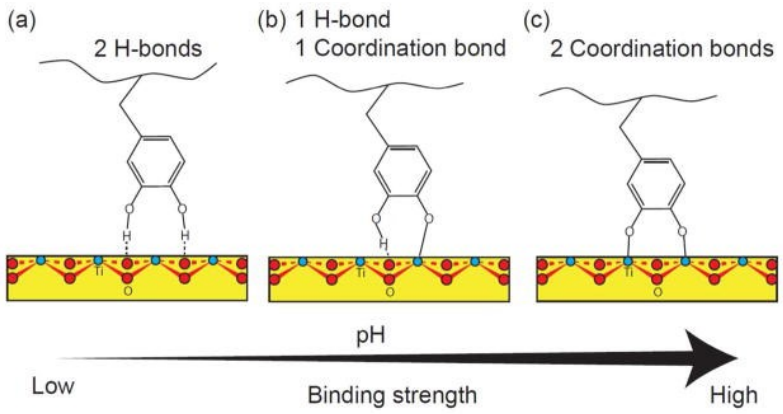

Figure 2.16. Schematic of DOPA-Ti coordination with (a) two hydrogen bonds; (b) one hydrogen bond and one DOPA-Ti coordination bond; (c) two DOPA-Ti coordination bonds [194].

Lee et al. designed single-molecule measurements of the pull-off force between DOPA molecule and different surfaces using atomic force microscopy (AFM), aiming to unveil the adhesion mechanism at the interface [184]. An AFM tip was modified by a single DOPA residue and brought in contact with different surfaces; repeated pull-off tests were performed. On the Ti surface, the authors measured a high and reversible strength of ~805 ± 131 pN attributed to the DOPA-Ti coordination mentioned above (Figure 2.16). This high pull-off force disappeared when the DOPA residues were oxidized. On the other hand, oxidized DOPA exhibited an irreversible 2.2 nN pull-off force when in contact with an amine-functionalized silicon surface. This was likely due to the covalent bonds formed between DOPA-quinones and amino groups.

2.4.5 Mussel inspired materials

Inspired by mussel adhesion, researchers used the versatile catechol chemistry in many applications. For example, catechols were used to conjugate proteins and polysaccharides. Ayyadurai et al. developed a method to conjugate a model protein (green fluorescent protein) and CS by DOPA [201]. Their strategy was to first modify the protein with DOPA by residue specific incorporation. Then, the DOPA-protein recombinant was oxidized by periodate, leading to the

formation of DOPA-quinones. The reactive DOPA-quinones further bonded to the amino groups in the CS through Michael addition and achieved the protein-CS conjugation.

Catechols were also used in antioxidant materials, since they act as free-radical scavengers by donating an electron or a hydrogen atom to a free radical. Nunes et al. modified CS with a catechol-containing molecule caffeic acid. The film made from CS-caffeic acid showed high antioxidant activity [202]. In addition, catechols form strong complex with metal ions such as iron, so they have been used in iron chelating applications [203]. Catechol functionalized materials have been shown to improve the cell adhesion to culture scaffolds, facilitating cell proliferation and differentiation. Thus, catechol functionalization can find applications in cell culture and tissue engineering as well [33, 204].

Besides these applications, most mussel inspired materials are made into adhesives, coatings, hydrogels and films. In this section, we review these mussel inspired materials and their applications.

2.4.5.1 Adhesives

Many studies mimicked the mussel adhesion mechanism to design new adhesives. Inspired by the high concentration of DOPA in Mefps, researchers functionalized different polymers with catechol groups. For example, Matos-Pérez and co-workers synthesized the mussel inspired adhesive polymer poly[(3,4-dihydroxystyrene)-co-styrene, with catechol groups distributed throughout the polymer backbone [205]. They tested the bulk adhesion of this new adhesive on different surfaces. They found that the polymer containing ~33% of catechol groups could achieve the strongest adhesion, comparable to commercial cyanoacrylate “Krazy Glue”. Yamada et al. created a water-resistant adhesive made from CS crosslinked by dopamine in presence of tyrosinase [206]. The modified CS solution showed an increased viscosity compared to unmodified CS solution. In water,

the two pieces of glass slides adhered strongly with this adhesive, giving more than 400 kPa of shear strength. Lee et al. synthesized amphiphilic block copolymers containing from 2 to 10 wt% of catechol groups [207]. The polymers could gel rapidly by photopolymerization. The presence of catechol groups significantly increased the adhesion of the gel on the titanium surface, with the highest work of adhesion at 410 mJ/m^2 achieved by the polymer containing 10 wt% of catechols. They also noticed that pre-oxidation of catechol reduced the adhesion, most likely because of the loss of ability to form the metal coordination. Another study from the same research group reported similar findings on titania surfaces [208].

2.4.5.2 Coatings

Catechols can functionalize a wide range of materials as surface coatings. For example, Ochs et al. made degradable capsules with dopamine-conjugated poly(L-glutamic acid) (PGA) [209]. The dopamine-PGA assembled on the surface of silica particles, and capsules were obtained when the silica cores were removed. The authors controlled the degradation rate of dopamine-PGA capsules by tailoring the degree of dopamine functionalization in the polymer.

Polydopamine is obtained by self-polymerization of the catechol-containing dopamine molecules. Although the exact polymerization mechanism is still unknown, the formation of DOPA-quinones can initiate the polymerization and lead to the deposition of the polydopamine on the substrates [187]. When immersed in diluted dopamine aqueous solutions in mild basic condition (pH 8.5), substrates can be coated by a thin adhesive layer of polydopamine. Figure 2.17 shows a schematic of the polydopamine coating method [210]. This method is almost universal, since polydopamine can coat many different surfaces, including adhesion-resistant surfaces such as poly(tetrafluoroethylene) [187]. The thin layer of polydopamine coating contains a large number of catechol groups, which can be further functionalized via catechol interactions with other

molecules [187]. For example, Sileika et al. coated a polycarbonate substrate by polydopamine, and added on top of it a further antifouling layer of PEG [211]. The substrate was immersed in a solution containing Ag^+. The catechol groups in the polydopamine layer reduced Ag^+ and caused the deposition of Ag nanoparticles on the coating. Due to the presence of both Ag nanoparticles and PEG, the surface exhibited both antimicrobial and antifouling properties. Other examples include the use of polydopamine mediated Ag coating to enhance photocatalysis [212], improve photon scattering [213], and for biosensing [214].

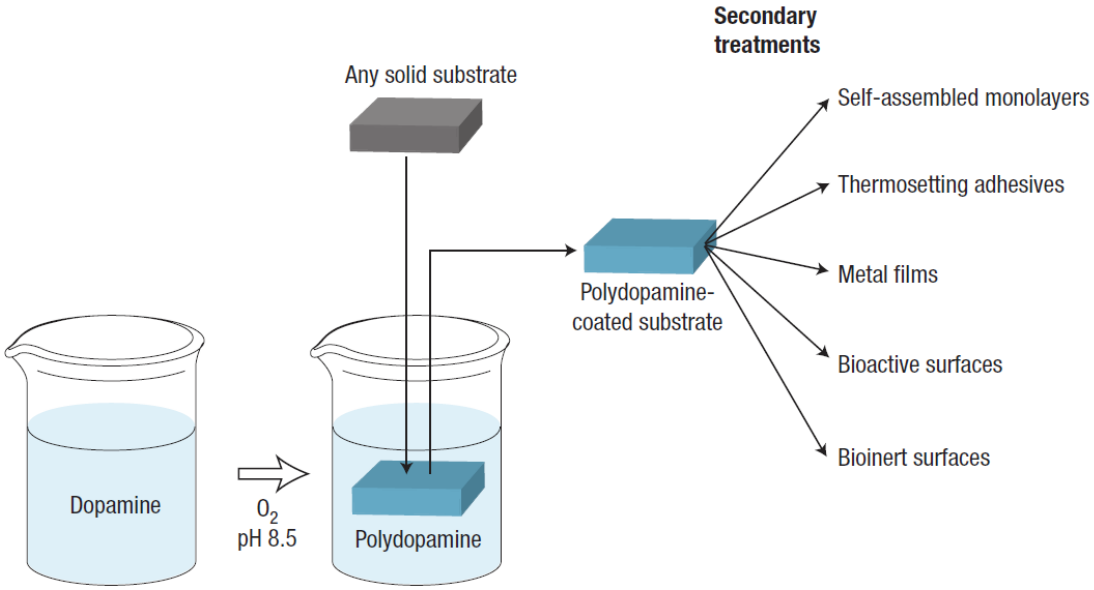

Figure 2.17. Schematic of the polydopamine coating method [210].

2.4.5.3 Hydrogels and films

We discussed in Section 2.4.3 that catechols can create crosslinks with themselves or other functional groups. We can use such catechol-induced crosslinks to make hydrogels or films.

Lee and co-workers synthesized a series of DOPA-functionalized linear and branched PEGs [215]. They used three oxidizing agents including sodium periodate, horseradish peroxidase,

and mushroom tyrosinase to initiate transformation from DOPA to DOPA-quinone. DOPA-quinones crosslinked the polymers and resulted in a rapid gelation. Their proposed crosslinking mechanism involved DOPA-quinone self-crosslinking and the interaction with amino groups [215].

Min and Hammond developed films with catechol functionalized branched poly(ethyleneimine) and PAA through layer-by-layer (LbL) technology [216]. Without modification, LbL assembly could be achieved due to the interaction between the two polyelectrolytes with opposite charges. The incorporation of catechols brought additional intermolecular interactions between the polyelectrolyte chains, including H-bonding, π-π stacking interactions, and various covalent bonds formed by oxidized catechols at pH 7.4. These additional crosslinking interactions significantly enhanced the stability of the films.

Similarly, Wu et al. fabricated a multilayer made from catechol functionalized poly(acrylic acid) (polyanion) and poly(allylamine hydrochloride) (polycation) through electrostatic LbL assembly [195]. They immersed this multilayer in a mild oxidative condition, allowing catechol groups to transform to DOPA-quinones. DOPA-quinones induced covalent intermolecular crosslinkings and stabilized the multilayer. The crosslinks included interactions between DOPA-quinones and $-NH_2$ groups by Michael addition and Schiff base reaction, as well as catechol self-crosslinking by quinone-phenol dismutation [195].

To trigger catechol crosslinking, most of the studies used $NaIO_4$, enzymes, or heavy metal ions. Fullenkamp and co-workers, instead, used $AgNO_3$ as an oxidizing agent [217]. $AgNO_3$ not only initiated the catechol oxidation of four-armed catechol modified PEG leading to gel formation, but also embedded Ag nanoparticles from the reduction of Ag^+ . The film so obtained could achieve a sustained release of Ag for at least 2 weeks, and therefore, exhibited excellent antibacterial properties.

Oh et al. synthesized catechol modified hyaluronic acid and lactose modified CS respectively [218]. The mixture of these two polymers formed a re-moldable hydrogel with interpenetrating network structure. Two types of crosslinks contributed to the interpenetrating network formation: inter-molecular polyelectrolyte complexes between the negatively charged hyaluronic acid and the positively charged CS, and covalent bonds between oxidized catechol groups and $-NH_2$ groups [218].

2.4.6 Mussel inspired mucoadhesives

Besides the applications mentioned above, catechol induced adhesion can expand to biological surfaces for medical applications. Here, the surfaces are tissue, mucosa, or cell membranes instead of glass or metal. Such adhesion is attributed to the interactions between catechols and amine, thiol, and imidazole residues at biological surfaces. For example, the extracted Mefps from blue mussel (*Mytilus edulis*) showed high adhesion to the porcine skin, comparable to the commercial adhesive fibrin [28]. Researchers also developed surgical adhesives for fast wound healing and hemostatic by covalently conjugating catechol groups to polymers such as hyaluronic acid, CS and PEG [29-32].

In this section, we focus on catechol induced adhesion to the mucosa. Several catechol modified polymers have shown enhanced mucoadhesion compared to non-modified polymers [34, 35]. Catechol groups interact with mucin by hydrogen bonding, hydrophobic interactions, π electron interactions and physical chain entanglement, either independently or cooperatively [34, 35]. When catechol groups are oxidized to DOPA-quinones by oxidizing agents or enzymes, DOPA-quinones may form covalent bonds with the primary amino groups of mucin [219]. We classify these mussel inspired mucoadhesives into two categories: mucoadhesives containing extracted Mefp and mucoadhesives containing functionalized catechols.

2.4.6.1 Mucoadhesives containing extracted Mefps

Schnurrer and Lehr were the first investigators who attempted to evaluate the potential of Mefps as mucoadhesives or mucoadhesive enhancers [220]. They extracted Mefps from the blue mussel (*Mytilus edulis*) and tested the detachment force between Mefps-coated glass slides and the porcine intestinal mucosa. Mefps showed strong mucoadhesion, comparable to polycarbophil. More importantly, when they dried and stored the films in N_2 to prevent oxidation, the mucoadhesion was almost two times higher than for air-dried films, thus confirming the importance of avoiding catechol oxidation before testing. In another study, Deacon et al. also observed a strong interaction between Mefp-1 and mucin [221].

2.4.6.2 Mucoadhesives containing functionalized catechols

Using Mefps directly as mucoadhesives has limitations. For example, the extraction of Mefps requires complex procedures and high cost. Therefore, many studies have developed catechol modified polymers as mucoadhesives.

Huang et al. prepared DOPA-conjugated poly(ethylene oxide)-poly(propylene oxide)-poly(ethylene oxide) block polymers [34]. The presence of catechol groups increased the viscosity of the polymer and mucin mixture. Higher catechol concentration led to higher viscosity [34]. The authors suggested that catechol groups formed hydrogen bonds with the hydroxyl groups and the carbonyl groups in the mucin. Such increased polymer-mucin interactions resulted in the increase in viscosity.

Catron et al. synthesized four-armed PEG with one catechol group at the end of each arm [35]. This polymer showed a strong adsorption on mucin coated surfaces at pH values ranging from 4.5 to 8.5. In addition, the authors measured a high single molecular pull-off force between DOPA modified PEG and mucin by AFM. Interactions between catechol groups and the mucin

might include hydrogen bonds, hydrophobic interactions, π electron interactions and physical chain entanglement [35].

2.4.7 Catechol toxicity and biocompatibility

In all applications where catechol-modified materials are in contact with the body, the cytotoxicity of the reactive catechol groups is a concern. This limits the use of catechol functionalized materials for biomedical applications.

Free catechols can interact with biomolecules in the body, including DNA, proteins and membranes through multiple reaction paths [193]. Catechol oxidation by enzymes or heavy metals generates reactive oxygen species (ROS), which can cause DNA damage [222]. Oxidized catechols may also react with –SH or $–NH_2$ groups in proteins or enzymes, thus causing protein crosslinking and enzyme function failure [193]. In addition, catechols can interfere with electron transportation and cause an inhibitory effect on energy transducing membrane proteins [193, 223].

In spite of the toxic effects of free catechols, many catechol-functionalized materials showed great biocompatibility, without causing significant damage to cells or tissue [29, 32, 217, 224]. For example, Hong et al. coated polydopamine on poly-L-lactic acid films and CdSe quantum dots. The cytotoxicity of both materials were greatly reduced in vivo compared to the uncoated materials, in terms of inflammatory and blood immunological responses [225]. In another study, the same authors used catechol functionalized hyaluronic acid to facilitate cell culture of human neural stem cells (hNSCs) [33]. When they cultured hNSCs on a Ti surface coated by catechol-hyaluronic acid, they observed a significant increase in cell attachment on the coated substrate. The authors also made a catechol functionalized hyaluronic hydrogel by adding an oxidizing agent. Catechol groups formed intermolecular crosslinks when oxidized by the oxidizing agent. They also encapsulated hNSCs in a catechol-containing hyaluronic acid hydrogel,

synthesized by adding an oxidizing agent to catechol-functionalized hyaluronic acid, and found better cell viability than if the cells were cultured in methacrylate conjugated hyaluronic acid hydrogel.

Yang et al. also showed the biocompatibility of catechol functionalized materials [204]. They coated polystyrene and poly(lactic-co-glycolic acid) substrates with polydopamine. On top of the polydopamine coating, they immobilized adhesion peptides (fibronectin and laminin) and neurotrophic growth factors. The immobilized neurotrophic growth factors greatly enhanced the proliferation and differentiation of hNSCs on the substrates, and the polydopamine coating did not cause toxicity to the cells.

CHAPTER 3. MOLLUSK GLUE INSPIRED MUCOADHESIVES FOR BIOMEDICAL APPLICATIONS

Mussel adhesive proteins secreted by marine mussels (Mytilus edulis) show outstanding adhesion to various surfaces, even in wet conditions. A large amount DOPA, a catechol-containing amino acid, is present in these proteins. Catechol groups are responsible for mussel adhesion on almost all surfaces. Inspired by this, people developed catechol functionalized polymers in biomedical applications, such as surgical glues and hemostatic.

Recent studies have shown that catechol groups interact with mucin too. These findings inspired us to develop catechol functionalized mucoadhesive CS hydrogels for oral drug delivery. To start with our study, we proposed a simple approach to introduce catechols into CS hydrogels, by physically mixing three catechol-containing compounds (DOPA, HCA and DA), inside CS hydrogels. We attempted to answer the following questions:

i. How do catechol-containing molecules affect the properties of CS hydrogels, such as swelling ratio and catechol release rate?
ii. How do catechol-containing molecules affect the mucoadhesion of CS hydrogels?
iii. How does the mucoadhesion of catechol-functionalized CS hydrogels change in the presence of oxidizing agents?

This manuscript has been published in Langmuir in 2012:

Xu J, Soliman GM, Barralet J, Cerruti M. Mollusk Glue Inspired Mucoadhesives for Biomedical Applications. Langmuir. 2012;28:14010-7.

3.1 Abstract

Chitosan (CS), partially *N*-deacetylated chitin, is a biodegradable and biocompatible polymer that has shown great potential in drug delivery and tissue engineering applications. Although bioadhesive, CS has limited mucoadhesion in wet conditions due to weak interactions with biological surfaces. DOPA (3,4-dihydroxy-L-phenylalanine), a catechol-containing molecule naturally present in marine mussel foot proteins, has been shown to increase the mucoadhesion of several polymers. We report here a simple and bioinspired approach to enhance CS mucoadhesion in wet conditions by preparing mixed hydrogels including CS and different catechol-containing compounds, namely DOPA, hydrocaffeic acid (HCA), and dopamine (DA). We characterized the hydrogels for their swelling, release kinetics of the catechol compounds and mucoadhesive strength to rabbit small intestine. The swelling of the hydrogels was pH dependent with maximum swelling at pH 1. The hydrogel swelling was higher in the presence of the DOPA and DA, but lower in the presence of HCA. HCA/CS hydrogel also showed the slowest catechol release, most likely due to electrostatic interactions between CS and HCA. Lower hydrogel swelling and slower HCA release resulted in increased mucoadhesion: HCA/CS showed more than two-fold enhancement of mucoadhesion to rabbit small intestine compared to CS alone. Since it is known that catechol compounds can be oxidized, we analyzed the oxidation of DOPA, HCA and DA at different pH values, and its effect on mucoadhesion. We found that oxidation occurring before contact with the intestinal mucosa did not improve mucoadhesion, while oxidation occurring during the contact further increased the mucoadhesion of HCA/CS hydrogels. These results show that mucoadhesion of CS hydrogels can be increased with a simple bioinspired approach, which has the potential to be applied to other polymers since it does not require any chemical modification.

3.2 Introduction

Bioadhesion is a phenomenon occurring at the interface between a natural or a synthetic macromolecule and a biological substrate. The term mucoadhesion is used when the biological surface is a mucosal membrane [20]. Because of their ability to prolong residence time on biological surfaces, bioadhesive polymers have found several biomedical applications [226, 227], especially in the field of drug delivery: the increased residence time at the site of application or at absorption surfaces allows for sustained drug release, as well as improved bioavailability [228]. The first mucoadhesive drug delivery system was developed in the early 1980s by Nagai who prepared bioadhesive tablets for the local treatment of aphthae [118]. Many other mucoadhesive drug delivery systems have been developed after this, and several researchers have explored the factors influencing mucoadhesion [21, 229-231].

Many natural, synthetic or semi-synthetic polymers have been tested as mucoadhesive biomaterials [22, 231]. Among them, chitosan (CS) is one of the most widely used bioadhesive polymers for drug delivery and tissue engineering, due to its biocompatibility, biodegradability, and its absorption enhancing ability [232, 233]. CS is a linear polymer of β (1-4) linked $_D$-glucosamine and *N*-acetyl-$_D$-glucosamine units prepared by deacetylation of chitin [234]. The bioadhesive strength of CS decreases when CS is swollen, possibly because of its weak electrostatic interactions with mucus and the absence of entanglement between the interacting chains [25, 126]. Also, CS's hydrophilicity and solubility in acidic solutions limit its ability to control the release of encapsulated drugs [234]. These shortcomings motivated several researchers to modify CS to enhance its mucoadhesion and ability to control drug release.

One CS derivative that shows improved mucoadhesion is thiolated CS. The improved mucoadhesion of thiolated CS is attributed to the formation of disulfide bonds between the

polymer thiol groups and cysteine-rich domains of glycoprotein in the mucus layer [235]. The covalent disulfide bonds are stronger than non-covalent electrostatic interactions between positively charged CS and the anionic mucus layer. For example, CS-thioglycolic acid nanoparticles showed 14-fold higher adhesive strength on the urinary bladder mucosa under continuous bladder emptying in comparison to unmodified CS nanoparticles [236]. In addition to improved bioadhesive properties, thiolated CS nanoparticles also showed more sustained drug release, intracellular triggered drug release and more efficient delivery of antisense oligonucleotide [237]. *N*-Trimethyl CS is a partially quaternized derivative of CS that showed enhanced bioadhesion and absorption enhancement properties, as well as better solubility in neutral and alkaline media. Compared to unmodified CS, trimethyl CS showed faster permeation of a model hydrophilic macromolecule through porcine cheek epithelium [133]. *N,O*-carboxymethyl CS (NOCC) is a water-soluble CS derivative having carboxymethyl groups on some or both the amino and primary hydroxyl sites of the CS glucosamine units. NOCC exhibited greater biodegradability and higher mucoadhesion, and increased the bioavailability of drugs for ophthalmic preparations [10, 238].

Adhesion in wet conditions is challenging but several marine organisms have evolved to excel in this. Marine and fresh water mussels secrete proteinaceous material that mediate firm attachment of the organisms to inorganic and organic objects, such as rocks, metal ship hulls, and wood structures [239]. An amino acid, 3,4-dihydroxy-L-phenylalanine (DOPA), naturally present in marine mussel foot proteins, has been shown to be the key component responsible for the impressive adhesion attained by these molluscs. A key functional group of DOPA is the *ortho*-dihydroxyphenyl group (catechol), which forms strong covalent and non-covalent bonds with various surfaces [240, 241]. Inspired from the mussel adhesion mechanism, several new

bioadhesive hydrogels have been reported [29, 35, 220]. Among them, thermosensitive catechol-CS/pluronic hydrogels were recently synthesized and used as tissue adhesives and haemostatic materials. The hydrogels showed strong adhesiveness to soft tissues and mucus layers and had superior haemostatic properties [29]. In order to reduce the rapid drug release from the layer-by-layer (LBL) assembled structures, catechol-containing compounds were covalently bonded on polymer chains of the LBL components. The release rate of the incorporated drugs was significantly reduced [216].

One of the drawbacks of using catechol compounds is their instability—they are easily oxidized at elevated pH values (catechol autoxidation, defined as the process involves only parent catechol compound [242]) or in the presence of oxidizing agents or catalysts. The effect of oxidation on mucoadhesion is complex and somewhat controversial. Both non-oxidized catechol and oxidized *o*-quinone are responsible for strong water resistant adhesion while the oxidized *o*-quinone is also believed to play a role in crosslinking of the mussel adhesive proteins [190]. DOPA oxidation results in a semi-quinone (one-electron oxidation) or DOPA-quinone (two-electron oxidation) and consequently significant decreases the adhesion on inorganic surfaces [243]. Other reports suggested that reactive catechol quinones could form covalent bonds with amine, thiol, and imidazole residues found in extracellular matrix proteins and carbohydrates resulting in improved bioadhesion [244, 245].

Here we report three different bioinspired catechol/CS hydrogels for biomedical applications. In order to get insights into the effect of different functional groups on CS performance as a bioadhesive material, we selected three catechol-containing compounds: DOPA, hydrocaffeic acid (HCA), and dopamine (DA). These three compounds have the same *ortho*-dihydroxyphenyl backbone but different functional groups (both carboxylate and amino group in

DOPA, carboxylate group in HCA, and amino group in DA). We prepared the hydrogels simply by mixing different catechol compounds with CS, and we correlated their adhesion to rabbit intestine with the gel swelling, as well as with the release and oxidation of the catechol compounds. Our results show that the swelling of the hydrogels was dependent on the pH of the medium and the nature of the catechol compounds. HCA/CS hydrogel had the lowest degree of swelling, lowest catechol release rate and around two-fold increase in the mucoadhesion to rabbit intestine. The mucoadhesion of the hydrogels decayed after oxidation of the catechol compounds. However, the gels became more mucoadhesive if the catechol compounds were oxidized during the contact with the mucosal tissue.

3.3 Experimental section

3.3.1 Materials

Medium molecular weight CS (MW 190,000-300,000, degree of deacetylation 75%-85%) and three types of catechol-containing chemicals: DOPA, HCA, and DA were purchased from Sigma-Aldrich (USA). Glacial acetic acid (99.98%, Fisher Scientific, USA), hydrochloric acid (HCl, 36.5%-38.0%, Chimiques ACP Chemicals, Canada), sodium hydroxide (NaOH, ACROS, USA) were used as received. Rabbit small intestine was obtained from sacrificed rabbits and stored at -20 ˚C within 2 h of animal sacrifice. Before being used for experiments, samples were thawed at room temperature, followed by gentle removing of the non-digested matter. Oxidizing agent sodium periodate ($NaIO_4$) was purchased from Sigma-Aldrich (USA).

3.3.2 Hydrogel film preparation

CS powder (0.4 g) was dissolved in 20 ml of 1% v/v aqueous solution of acetic acid. DOPA, HCA, and DA were added to the CS solution under stirring so that the catechol/CS repeating unit molar

ratio was 0.5:1. The homogeneous solution was cast into a mold (opening area 25 cm^2) and stored in refrigerator at 4 ˚C overnight to remove air bubbles. The samples were then dried in vacuum at 55 ˚C for 24 h. The films so obtained (namely CS, DOPA/CS, HCA/CS, and DA/CS) were removed from the mold for further testing.

3.3.3 Hydrogel swelling

Dry films were cut into 1 × 1 cm^2 pieces and were immersed in 20 ml water with pH of 1, 5.5, 6.8 and 7.4 adjusted by 1 M HCl or 1 M NaOH, respectively. The three dimensional sizes of the swollen hydrogel films were measured by a digital caliper at time points of 0, 5, 10, 15, 20, 25, 30, 60 and 120 min. Total volumes were calculated and the swelling ratio (degree of swelling) was taken as the ratio of the volume in the swollen state to the volume in the dry state. Each experiment was repeated three times.

3.3.4 Catechol compound release

Release of catechol compounds from the hydrogels was tested by immersing small pieces of dry films (1 × 1 cm^2, containing ~3.2 mg/cm^2 of catechol compounds) into 40 ml deionized water of pH 5.5 maintained at 37 ˚C. At different time intervals, 3 ml samples were collected and replaced by 3 ml fresh medium. The concentrations of the catechol compounds were quantified by Cary 5000 UV-Vis-NIR Spectrophotometer (Agilent Technologies) by measuring the absorbance at 285 nm and using a calibration curve. The cumulative release percentage was calculated for each catechol compound and plotted as a function of the release time. Each experiment was repeated three times.

3.3.5 Catechol oxidation studies

We studied oxidation of HCA, DOPA and DA as a function of solution pH and exposure time using UV-vis spectroscopy. However, due to the multiple pathways of catechol oxidation and the formation of various intermediate products [246, 247], quantitative analysis is difficult. Indeed, most studies only qualitatively compared the UV-vis spectra evolution representative of catechol oxidation [215, 243, 248]. In this study, we compared the absorbance ratio of the oxidation peak A_{OX} (465 nm, 500 nm and 465 nm for DOPA, HCA and DA respectively) to the non-oxidized catechol peak at 285 nm (A_{285}) as a semi-quantitative measurement of catechol oxidation. DOPA, HCA and DA solutions (1 mM) were first prepared in phosphate buffered saline (PBS) (pH 7.4, buffer strength 50 mM) and their pH values were adjusted to 4, 5, 6, 6.8, 7.4 and 8 using 1 M HCl or 1 M NaOH. Aliquots of solutions were incubated at room temperature for 48 h and were scanned at different time intervals by UV-vis spectrophotometer from 200 to 700 nm. Each experiment was repeated three times.

3.3.6 Mucoadhesion test

The mucoadhesion of different CS hydrogels (CS, DOPA/CS, HCA/CS, and DA/CS) was evaluated by measuring the maximum detachment force (MDF) between the surface of the swollen hydrogel and intestinal mucosa using a tensile tester with a load cell of ±100N (Instron 5569, USA). Hydrogels used for all mucoadhesion tests were prepared by swelling the dry films in deionized water for 2h. This allowed complete swelling of all four types of hydrogels, thus allowing us to evaluate mucoadhesion in the absence of morphological and physico-chemical changes of the gels. A piece of rabbit small intestine (1 × 1 cm^2) was fixed to the probe using tissue glue (Vetbond, 3M, USA), and the hydrogel was placed on the sample holder. An initial contact force of 0.1 N was applied, and held for either 10 s or 3 min. The probe was elevated at a speed of 0.1 mm/s until

completely detached from the hydrogel surface. The force-displacement curve was recorded and the peak force was noted as the MDF. The effect of oxidation on mucoadhesion was tested on two groups: in the first group, four hydrogels were oxidized by immersing them in $NaIO_4$ (0.01 mol/L) for 10 min, and mucoadhesion was tested after this treatment; in the second group, four hydrogels were put in contact with a droplet of $NaIO_4$ (0.01 mol/L), and mucoadhesion was measured right after. In both groups, the contact force of 0.1 N was held for 3 min before detaching the probe to measure the MDF. Each experiment was repeated four times.

3.3.7 Statistical analysis

The statistical analysis was carried out using Student's t-Test. Error bars in the figures represent the standard deviation (SD). A value of $p \leq 0.05$ was considered significant in all tests.

3.4 Results and discussion

3.4.1 Hydrogel swelling

Swelling is known to affect the release rate of drugs incorporated in hydrogels, as well as their mucoadhesion strength [15, 249]. We evaluated the swelling of CS and mixed CS-catechol hydrogels in water at different pH values. The maximum swelling for pure CS gels occurred at pH 1 (Figure 3.1a), most likely because at pH ≤ 4.5 the amino groups of CS are completely protonated, thus causing electrostatic repulsion between the polymer chains and rapid swelling [250]. At any pH, swelling was higher for the hydrogels containing DOPA or DA compared to those with HCA or pure CS. The higher swelling in the presence of DOPA or DA may be attributed to their cationic nature, which allows more water to enter the films and make them swell. The lower swelling of the films containing HCA is presumably due to electrostatic interactions between HCA carboxylic

acid groups and CS amino groups. These interactions neutralize CS amino groups and reduce the electrostatic repulsion that is responsible for the swelling of pure CS gels [250].

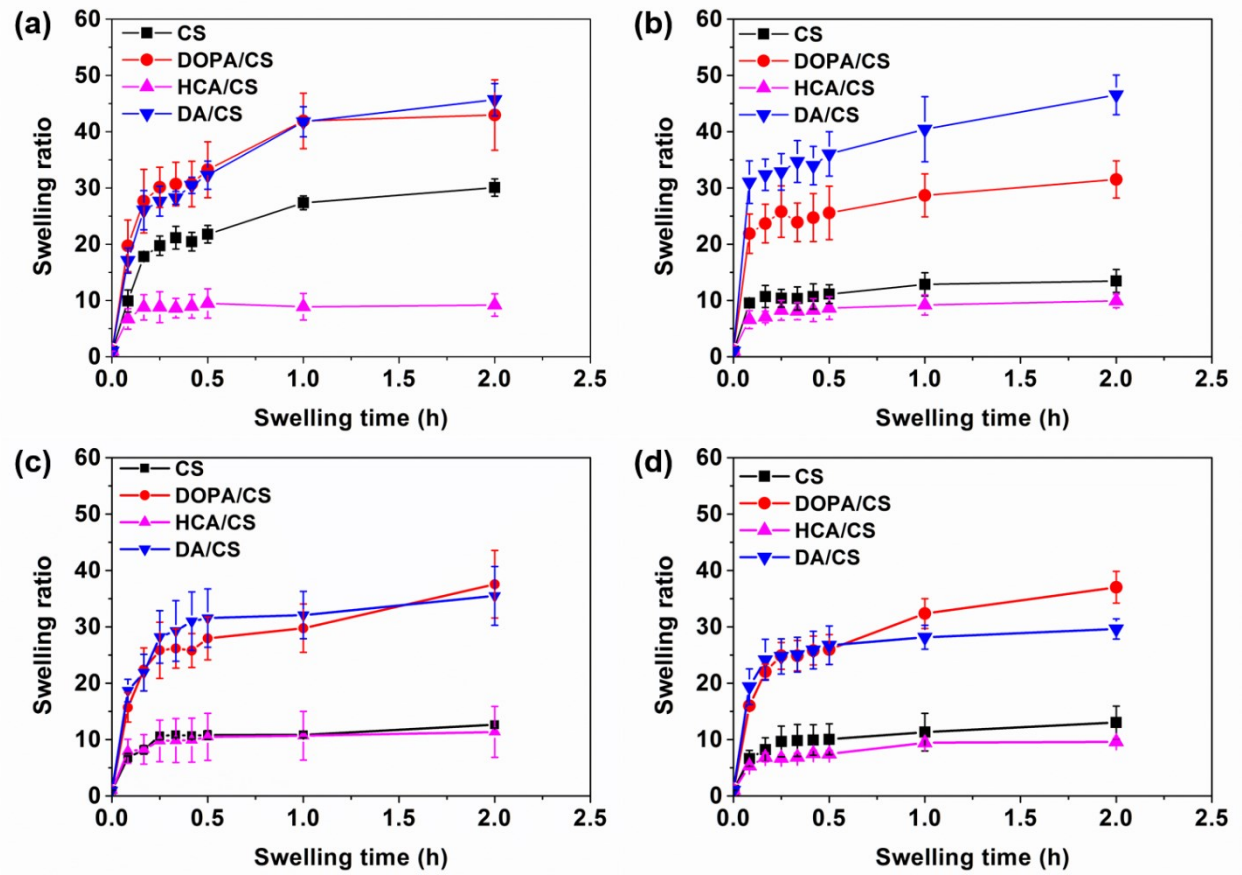

Figure 3.1. Swelling ratios of CS, DOPA/CS, HCA/CS and DA/CS hydrogels in water at different pH values as a function of time. (a) pH = 1; (b) pH=5.5; (c) pH=6.8; (d) pH=7.4.

3.4.2 Release of catechol compounds from the hydrogels

The properties of catechol/CS hydrogels are influenced by the catechol content in the hydrogel. We determined the amount of catechol remaining in the hydrogel as a function of time under conditions similar to those used in the swelling and adhesion tests. At pH 5.5, DOPA and DA showed rapid release from the hydrogels and almost 100% release was achieved in 30 min (Figure 3.2). In contrast, HCA was released from the hydrogels at a much slower rate. Around 50% HCA

was left in the hydrogel after 2 h. This difference in the release profile may be due to the difference in ionization status of the catechol compounds. DA and DOPA are cationic, while HCA is anionic at pH 5.5 [251, 252]. Therefore, only HCA can interact electrostatically with the positively charged CS at pH 5.5. Such electrostatic interactions are responsible for the slower release of HCA. The faster release of DA and DOPA correlates well with the larger swelling observed for the DA/CS and DOPA/CS gels compared with the HCA/CS gels: indeed, previous work showed that higher degrees of gel swelling result in rapid release of the incorporated drugs [253].

The release of catechols from the hydrogels raises a concern about any potential cytotoxic effect. Catehcol toxicity due to damage of DNA and proteins has been studied mostly *in vitro*[193], while its clinical toxic effect is still controversial [254]. Basma et al. showed that approximately 50% PC12 cells (a model system for neuronal differentiation) incubated with 100 μM DOPA were dead after 24h, and attributed this effect to DOPA autoxidation into highly reactive toxic free radicals and quinones [255]. However, in another study by Koshimura et al., DOPA and DA at low concentrations (< 30 μM) had a beneficial effect on PC12 cells – they protected the cells from death when cells were cultured without serum and nerve growth factor [256]. Moridani et al. reported the LD_{50} of catechol compounds after incubation with isolated rat hepatocytes for 2h: DOPA 7900 μM; HCA 6000 μM; DA 2000 μM [257]. On the other hand, Hong et al. showed that polydopamine coated CdSe quantum dots and poly($_L$-lactic acid) (PLLA) had reduced *in vivo* toxicity [225]. More recently, the same research group proposed an explanation for this phenomenon: they reported that during the formation of polydopamine, a significant amount of dopamine did not polymerize, but self-assembled forming the $(dopamine)_2$/5,6-dihydroxyindole complex, which was stable and tightly associated with the polydopamine layers. Thus, they suggested that the good biocompatibility of polydopamine coatings might be attributed to the

minimal release of the (dopamine)$_2$/5,6-dihydroxyindole complex [258]. Polydopamine coated polycaprolactone also exhibited fairly good biocompatibility and endothelial cell growth [259]. The reason for the different cytotoxicity observed for these catechol compounds is not well understood, and it may depend on many factors such as concentration, type of cells, catechol status, and whether catechol groups were free in solution or immobilized on a substrate.

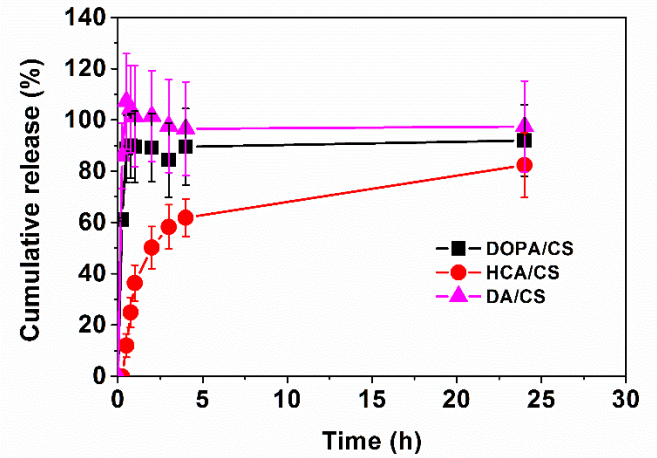

Figure 3.2. Cumulative release of DOPA, HCA and DA from the hydrogels as a function of time.

3.4.3 Catechol oxidation studies

Catechol oxidation has been studied by many researchers using oxidizers such as H_2O_2 and $NaIO_4$, or enzymes such as mushroom tyrosinase. Without oxidizers or enzymes, catechol compounds can undergo autoxidation at basic pH values [242, 243, 260]. DOPA and DA have similar oxidation pathways; they are first oxidized to DOPA-*o*-quinone or DA-*o*-quinone, and these compounds further develop to dopachrome or dopaminechrome through cyclization and oxidation [246-248]. HCA transforms to HCA-*o*-quinones and gradually to 6-OH-HCA in acidic conditions but does not form aminochrome because of the lack of amino groups [246]. Catechol quinones may also self-crosslink because of dismutations [195]. We studied catechol autoxidation as a function of

solution pH and time. Catechol oxidation induced a change in color from transparent to dark brown of the catechol solutions even at very low concentration (1 mM). UV-vis spectra allowed for a semi-quantitative comparison of the level of oxidation of these compounds (see spectra of oxidized and non-oxidized HCA in Figure 3.3a as an example). None of the catechol compounds showed much oxidation in PBS of pH <6 for 2 h, as indicated by the absence of new peaks in their UV-vis spectra. In contrast, the spectra of DOPA in PBS solutions at pH ≥ 6 show the appearance of broad peaks at around 465 nm, indicating oxidation of DOPA to dopachrome [215, 261]. The peak of HCA oxidation products is centered at around 500 nm, and it may be attributed to the formation of various HCA oxidized products, including HCA-quinone, HCA-lactone-*o*-quinone, 6-OH-HCA-*p*-quinone and HCA dehydrodimers [262, 263]. DA spectra show a less defined broad peak centered at around 465 nm increasing in absorbance with increasing pH indicating the formation of dopaminechrome. The semi-quantitative estimation of catechol oxidation was obtained by plotting the ratio of dopachrome absorbance to the absorbance of non-oxidized compounds (λ_{max}~285 nm) versus pH at 2h and 48h (Figure 3.3b and 3.3c, respectively). Higher oxidation was observed at higher pH at both times of analysis for all compounds; however only after 48 h did oxidation occur to a large extent. Compared to DOPA and DA, HCA showed the lowest extent of oxidation after 48 h at pH 8.

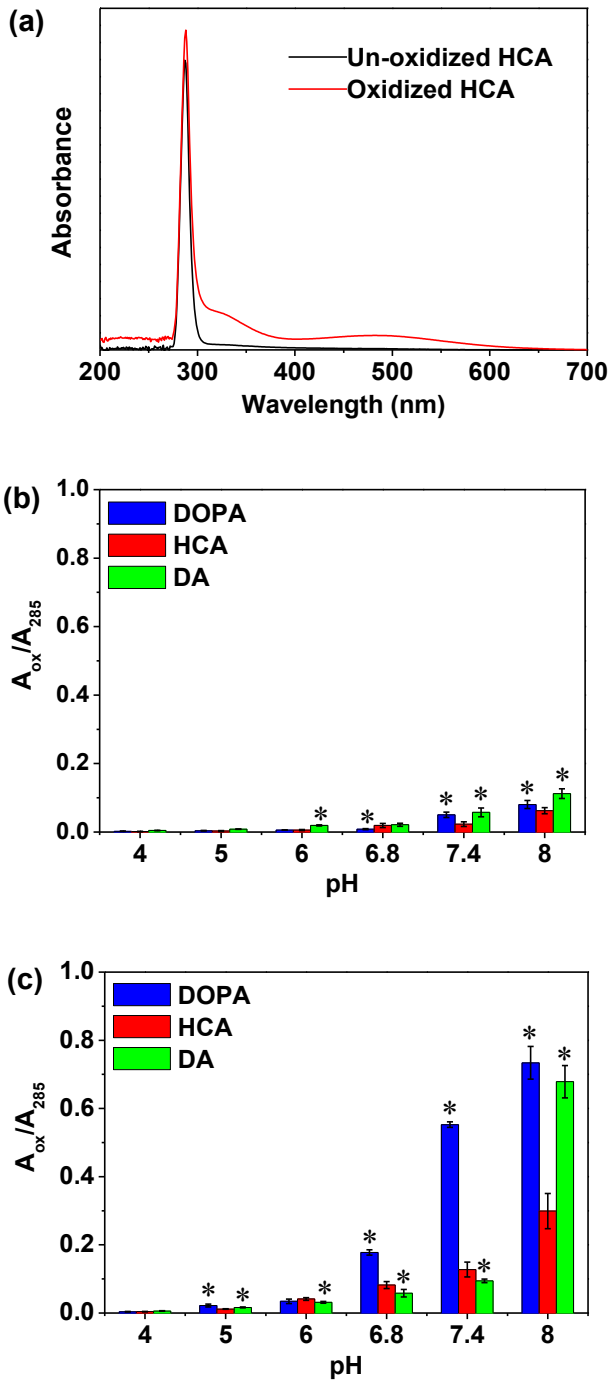

Figure 3.3. Catechol oxidation analysis. (a) Representative UV-vis spectra of non-oxidized and oxidized HCA. (b) Oxidation extent of DOPA, HCA and DA at different pH values after 2 h in PBS. (c) Oxidation extent of DOPA, HCA and DA at different pH values after 48 h in PBS. *$p \leq$ 0.05 compared to HCA with the same oxidation time and pH.

3.4.4 Mucoadhesion tensile tests

Tensile tests are commonly used methods to evaluate mucoadhesion strength [264-266]. In a typical tensile strength test, the mucoadhesive material is brought in contact with mucosal tissue and the force-displacement curve is recorded. The maximum detachment force (MDF) (i.e., the peak of the force-displacement curve) is taken to represent the adhesion of the material on mucosa. Figure 3.4 shows the MDFs of 2 h water-swollen CS, DOPA/CS, HCA/CS and DA/CS hydrogels from rabbit small intestine, after contact times of 10 sec and 3 min. Significant differences were detected between the mucoadhesion of pure CS films and films containing DOPA or HCA compounds when the initial contact time was 10 sec. Longer contact times increased the MDFs for all hydrogels – this trend is consistent with results found in other studies [264-266], since longer contact times increase the interpenetration of polymers chains with mucin, thus increasing mucoadhesion [267]. The MDF measured for HCA/CS hydrogel (0.076±0.011 N/cm^2) was approximately double of that measured for CS hydrogel (0.035±0.005 N/cm^2) (Figure 3.4). DOPA and DA also showed higher MDFs compared to CS alone, but not as high as HCA; most likely this was due to their rapid release from the hydrogels. It is noteworthy here that mucoadhesion tests were done after 2 h in pH 5.5 water where HCA oxidation was minimal. This confirms that the improved mucoadhesion is due to intact HCA and not its oxidation products. The increased adhesion measured on HCA/CS hydrogels indicates the presence of catechol groups at the interface between this hydrogel and the mucosa; catechol groups may in fact act as “bridges” between CS and mucin, as previously proposed by Catron et al. [35].

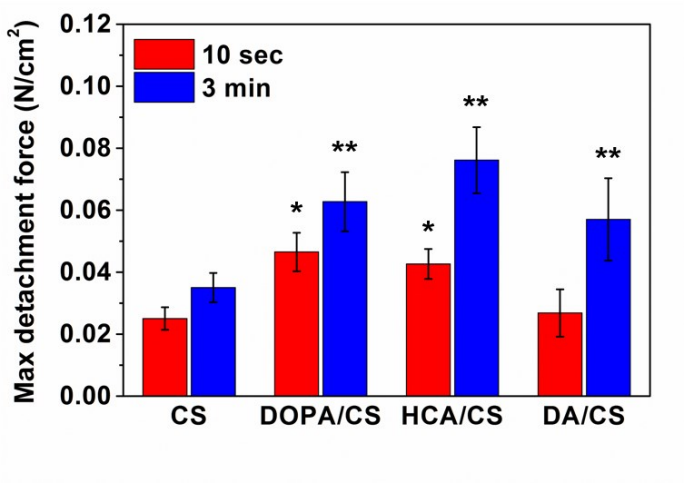

Figure 3.4. MDFs of CS, DOPA/CS, HCA/CS and DA/CS measured upon 10 sec and 3 min contact with mucosal tissue. * $p \leq 0.05$ compared to the CS with 10 sec contact time. ** $p \leq 0.05$ compared to the CS with 3 min contact time.

In order to test the effect of catechol oxidation on mucoadhesion, we measured the adhesion strength of the hydrogels upon oxidation with $NaIO_4$. When $NaIO_4$ was applied on the 2h-swollen hydrogels, DOPA/CS, HCA/CS, and DA/CS changed color to dark brown, thus confirming the presence of unreleased catechol compounds in them (Figure 3.5).

In a first set of samples, we oxidized the hydrogels for 10 min, and then we put them in contact with the mucosal tissue for 3 min. The MDF for HCA/CS decreased to 0.056±0.009 N/cm^2, indicating that the enhanced mucoadhesion effect decreased after the oxidation of HCA (Figure 3.6a). The loss of wet adhesion after catechol oxidation has been reported by previous researchers [190], and can be attributed to formation of crosslinks between oxidized catechols and amino groups from CS, leading to a decrease in the flexibility and thus mucoadhesion of the HCA/CS hydrogel. Yamada et al. reported an increased viscosity of chitosan solution in the presence of enzymatically oxidized DA, due to the covalent reaction between *o*-quinone and chitosan amino groups. Their findings support our explanation that the consumption of catechol with chitosan led to a decrease in mucoadhesion in the first test group [206, 268]. Conversely, the MDF for pure CS

films increased after treatment with $NaIO_4$. $NaIO_4$ is known to react with polysaccharides and form aldehydes [269], however such reaction is not fast, and can take as long as 48 h. Thus we attribute this partial increase in mucoadhesion in an increase in surface roughness observed after the oxidative treatment.

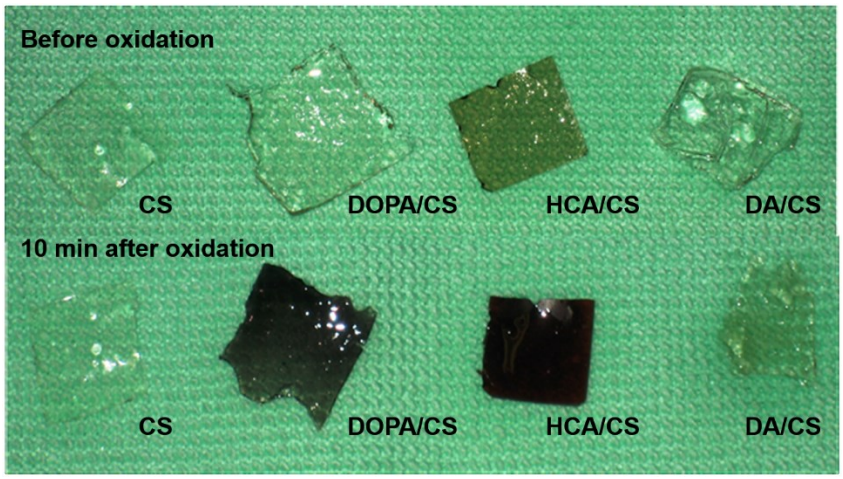

Figure 3.5. Swollen hydrogels before and after oxidation with $NaIO_4$.

In a second group of samples, we contacted the hydrogels with the intestinal mucosa immediately after oxidizing them, and we tested the mucoadhesion after 3 min of contact with the tissue. The results showed a significant increase in the MDF of HCA/CS up to 0.101±0.009 N/cm^2 (Figure 3.6b). This increase may be due to the formation of covalent bonds between oxidized catechols and cysteine-rich domains of glycoprotein in the mucus layer. The catechol forms quinone quickly upon oxidation by $NaIO_4$, which can further react with amino groups by Michael addition and Schiff base reaction, or react with thiol groups by Michael addition [35]. In the first test group, oxidation happened in the absence of mucus, thus consuming the oxidized catechols in the hydrogel itself without contributing to mucoadhesion enhancement. Instead, in the second group oxidation happened at the contact interface, and quinone groups were able to react with glycoproteins in the mucus layer thus inducing enhanced adhesion. Besides the formation of

covalent bonds, physical association via complex formation may contribute to the enhancement of mucoadhesion. Hong et al. proposed the formation of (dopamine)$_2$/5,6-dihydroxyindole complex during dopamine polymerization [258]. This finding raises the possibility that a similar type of molecular association may occur also between catechols and mucin, when catechols are oxidized during the contact with mucus. Neither DOPA nor DA showed an increase in MDF, which might be due to the lower amounts of these compounds remaining in the gels.

Barthelmes et al. reported a 14-fold enhancement of mucoadhesion using CS-thioglycolic acid nanoparticulate drug delivery system [236]. This increase is higher than what achieved in this work, possibly due to the higher surface area of nanoparticles than hydrogels and the more effective thiol-mucin interaction. Ryu et al. were able to increase adhesion on subcutaneous tissue about 7 times using mixed catechol-chitosan and thiolated Pluronic F127 [29]. Though their tests did not involve mucus, the significant enhancement may be attributed to the stable covalent binding of catechol to chitosan and possibly the presence of thiols as well.

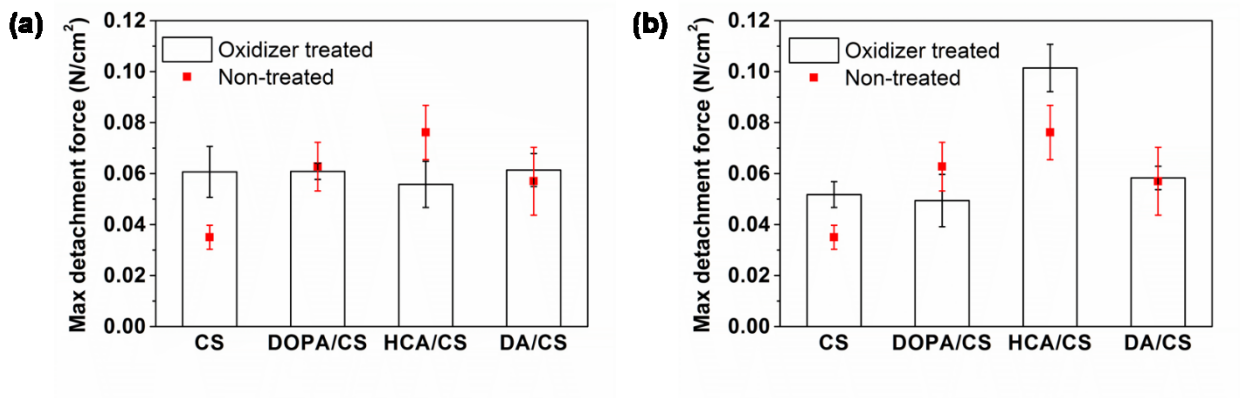

Figure 3.6. MDFs for CS, DOPA/CS, HCA/CS and DA/CS (a) after 10 min oxidation by $NaIO_4$ followed by 3 min contact with tissue; (b) oxidized with $NaIO_4$ and immediately contacted with tissue for 3 min. The "non-oxidized" points in both graphs refer to the MDFs measured after 3 min contact with mucosal tissue using non-oxidized gels (same values as those shown in Figure 3.4, repeated here to facilitate the comparison). * $p \leq 0.05$ compared to CS.

The results of these experiments conclusively show that oxidation can have very different effects on the mucoadhesion of catechol-containing CS gels depending on when it happens: while oxidation before contact with mucus is detrimental, "*in-situ*" oxidation can lead to an increase in mucoadhesion strength. These results suggest an intriguing application for these gels: they could be used in the treatment of diseases such as ulcerative colitis and colon cancer, where reactive oxygen species (ROS) are produced in abnormally high concentrations [270]. Topical drug delivery could be achieved thanks to the enhanced mucoadhesion selectively achieved in the areas producing more ROS.

3.5 Conclusions

We have developed a simple and bioinspired approach to enhance the mucoadhesion of CS in wet conditions by preparing hydrogels containing CS and different catechol compounds. Our results show that the presence of catechol compounds significantly affected the properties of the hydrogels, both in terms of swelling and mucoadhesion. Among the compounds tested, only HCA was able to reduce CS gel swelling and enhanced its mucoadhesion. This underscores the importance of the selection of the correct catechol compound/polymer pair to achieve optimal bioadhesion performance. Our study also shows that oxidation should be prevented before contact with mucus in order to retain enhanced mucoadhesion. However, if the oxidation happens during the contact, a further increase in mucoadhesion occurs for the HCA-containing gel, most likely because the oxidized catechol groups can covalently bind with the cysteine groups in mucin, thus enhancing mucoadhesion even more than in non-oxidized gels.

The hydrogels presented in this study are fabricated by simply mixing catechols and chitosan. The diffusion of catechols from the hydrogels might be the main factor that prevents the achievement of even larger mucoadhesion enhancements. We are currently evaluating new

hydrogels where minimal catechol diffusion is achieved by covalently binding the catechol compounds to chitosan.

3.6 Acknowledgements

The authors acknowledge the support of the Canada Research Chair program, Canada Foundation for Innovation, the Natural Sciences and Engineering Research Council of Canada, and the Advanced Foods & Materials Network.

CHAPTER 4. GENIPIN-CROSSLINKED CATECHOL-CHITOSAN MUCOADHESIVE HYDROGELS FOR BUCCAL DRUG DELIVERY

In the previous chapter, physical mixing of HCA in CS hydrogels showed an enhanced mucoadhesion in vitro. However, we realized that the release of HCA molecules from the hydrogel limited this enhancement. To prevent the release of catechol molecules, in this chapter we proposed a strategy to immobilize catechol groups via covalent conjugation of HCA to CS, forming Cat-CS.

Buccal drug delivery requires drugs to be retained in the oral cavity long enough to be effective. However, the movement of the mouth, and flash of food and saliva may remove drugs easily. Thus, buccal drug delivery can benefit from the use of mucoadhesive systems, which can stick to the buccal mucosa and prolong the retention time of drugs in the oral cavity. In this chapter, we aimed at developing a mucoadhesive hydrogel for buccal drug delivery using catechol-introduced CS. We prepared Cat-CS hydrogels by genipin crosslinking (Cat-CS/GP), with two degrees of catechol conjugation (9% and 19%, namely Cat9-CS/GP and Cat19-CS/GP). We attempted to answer the following questions:

i. Does the Cat-CS/GP hydrogel have suitable physical properties as a buccal drug delivery system, in terms of rheological parameters and sustained release capability?
ii. How is the mucoadhesion of Cat-CS/GP hydrogels in vitro? Does the degree of catechol conjugation affect their mucoadhesion?
iii. Can the mucoadhesive Cat-CS/GP hydrogel achieve a sustained buccal drug delivery in vivo?

This manuscript has been published in Biomaterials in 2014.

Xu J, Strandman S, Zhu JXX, Barralet J, Cerruti M. Genipin-crosslinked catechol-chitosan mucoadhesive hydrogels for buccal drug delivery. Biomaterials. 2015;37:395-404.

4.1 Abstract

Drug administration via buccal mucosa is an attractive drug delivery strategy due to good patient compliance, prolonged localized drug effect, and avoidance of gastrointestinal drug metabolism and first-pass elimination. Buccal drug delivery systems need to maintain an intimate contact with the mucosa lining in the wet conditions of the oral cavity for long enough to allow drug release and absorption. For decades, mucoadhesive polymers such as chitosan (CS) and its derivatives have been explored to achieve this. In this study, inspired by the excellent wet adhesion of marine mussel adhesive protein, we developed a buccal drug delivery system using a novel catechol-functionalized CS (Cat-CS) hydrogel. We covalently bonded catechol functional groups to the backbone of CS, and crosslinked the polymer with a non-toxic crosslinker genipin (GP). We achieved two degrees of catechol conjugation (9% and 19%), forming Cat9-CS/GP and Cat19-CS/GP hydrogels, respectively. We confirmed covalent bond formation during the catechol functionalization and GP crosslinking during the gel formation. The gelation time and the mechanical properties of Cat-CS hydrogels are similar to those of CS only hydrogels. Catechol groups significantly enhanced mucoadhesion in-vitro (7 out of the 10 Cat19-CS hydrogels were still in contact with porcine mucosal membrane after 6 hours, whereas all of the CS hydrogels lost contact after 1.5 hours). The new hydrogel systems sustained the release of lidocaine for about 3 hours. In-vivo, we compared buccal patches made of Cat19-CS/GP and CS/GP adhered to rabbit buccal mucosa. We were able to detect lidocaine in the rabbit's serum at concentration about 1 ng/ml only from the Cat19-CS patch, most likely due to the intimate contact provided by mucoadhesive Cat19-CS/GP systems. No inflammation was observed on the buccal tissue in contact with any of the patches tested. These results show that the proposed catechol-modified CS

hydrogel is a promising mucoadhesive and biocompatible hydrogel system for buccal drug delivery.

Keywords: chitosan, hydrogel, catechols, mucoadhesion, buccal drug delivery.

4.2 Introduction

Buccal drug delivery is a non-invasive method of drug administration that has gained much interest in recent years [271]. The buccal mucosa environment consists of an epithelium layer about 40-50 cell layers thick, a lamina propria layer, a submucosa layer, and the mucus surrounding the epithelia cells that is secreted by salivary glands [272]. The multilayered, non-keratinized human buccal mucosal membrane is rich of underlying blood vessels and has relatively good drug permeability through both transcellular and paracellular routes [273-275]. Buccal drug delivery is superior to oral drug delivery because it avoids presystemic clearance at the gastrointestinal tract as well as the first-pass elimination in the liver during systemic circulation [275, 276]. This is particularly important for therapeutics that suffer from high first-pass metabolism or low bioavailability when administered orally. Fentanyl citrate tablets [277], insulin spray [278], silymarin liposomes [279], and carvedilol patches [280] are examples of buccal drug delivery for systemic drugs. Buccal drug delivery is also used to prolong localized drug effect in periodontal diseases [168], oral mucositis [281] and oral fungal infection [282].

The main challenge related to buccal drug delivery is drug residence time. During buccal delivery, devices need to stay in contact with the mucosal membrane to allow drugs to act at the site of application, or be absorbed through transmucosal paths. However, flushes of saliva, food ingestion, mouth movement and uncontrolled swallowing can prevent such devices from adhering to the buccal mucosa, leading to reduced or no pharmaceutical efficacy [275]. An ideal buccal drug delivery system should adhere to the buccal mucosa quickly with sufficient stability to effect treatment [283].

Several mucoadhesive materials have been reported during the past decades for buccal drug delivery applications [275, 284]. Carbopol (crosslinked polyacrylic acid) and

hydroxypropylmethylcellulose (HPMC) are widely used mucoadhesive materials in buccal film/patch design [159, 163]. Sodium carboxymethyl cellulose (SCMC) is another mucoadhesion enhancer often added to buccal tablets [285, 286]. Buspirone buccal discs based on xanthan gum have been reported recently, and showed enhanced mucoadhesion due to the interaction of mucin with carboxylates and hydroxyl groups in xanthan gum [287].

A well-known mucoadhesive polymer that has been extensively tested for buccal delivery is chitosan (CS) [288-290]. CS is a biocompatible and biodegradable cationic polysaccharide synthesized by partial deacetylation of chitin [291]. At physiological pH, its mucoadhesion is mainly due to electrostatic attraction with negatively charged mucin, combined with contributions of hydrogen bonding and hydrophobic effects [292]. However, the mucoadhesion of CS is limited [25, 126]; thus much research has focused on trying to improve it. N-trimethyl chitosan (TMC), a partially quaternized CS derivative, shows enhanced mucoadhesion at increasing degrees of quaternization [133]. By covalently binding ethylenediaminetetraacetic acid (EDTA) to CS, almost all primary amino groups of CS are replaced by EDTA, and the cationic polymer is transformed to anionogenic. CS-EDTA shows increased mucoadhesion compared to CS, thanks to hydrogen bonds formed between carboxylate groups and mucus [293]. Thiolated CS prepared by CS-thioglycolic acid conjugation (CS-TGA) shows up to a 10.3-fold increase in the total work of adhesion to porcine mucosa compared to plain CS [127], possibly because thiol groups can form covalent disulfide bonds with the cysteine groups that are largely present in mucus glycoproteins [294, 295].

Catechol groups are in part responsible for the underwater adhesion of marine mussels. Catechols can be oxidized at elevated pH, or in the presence of oxidizing agents and catalysts [195, 242]. Many different materials have been modified with catechols [33, 195, 217, 296, 297],

including CS [29]. Lee et al. developed an alginate-catechol hydrogel that exploited catechol oxidation for crosslinking, instead of the conventional calcium ionic crosslinking [297]. This catechol-alginate hydrogel showed not only excellent biocompatibility, but also tunable mechanical properties in contrast to calcium crosslinked alginate hydrogel. Wu et al. prepared a multilayer film by layer-by-layer assembly of catechol-functionalizezd poly(acrylic acid) and poly(allylamine hydrochloride) under mild oxidative conditions [195]. Also in this case, crosslinking was achieved by catechol oxidation, and the final film exhibited great stability against harsh environments. The presence of catechols also increased the stability and viability of stem cells cultured on the films. Fullenkamp et al. developed an antibacterial catechol-polyethylene glycol hydrogel crosslinked by silver nitrate, which could sustain the release of Ag^0 for 2 weeks [217]. Hong et al. showed that human neural stem cells adhered and were viable on catechol-modified hyaluronic acid hydrogels [33]. In another study by Ryu et al., catechol modified CS was crosslinked with thiolated Pluronic, forming a gel that was adhesive to soft tissue [29]. Although part of the catechol groups on the polymer chain participated in crosslinking with –SH by Schiff-base addition, the remaining catechol groups contributed to the enhancement of bioadhesion at tissue surface. More recently, Zhang et al. developed hyperbranched poly (dopamine-co-acrylate) as an adhesive precursor with strong wet tissue adhesion [298]. Our group recently reported increased mucoadhesion when catechols and CS were mixed in a hydrogel, and oxidizing agents were present at the mucosa surface [299].

Most of the studies mentioned above used catechols to crosslink the gels; this implies that some of the catechol groups were not used to induce mucoadhesion, and therefore the full potential of catechols as mucoadhesion enhancers was not exploited. To avoid this, here we crosslink a catechol-modified CS hydrogel using genipin as a natural crosslinker [195, 297], and we test this

gel for buccal drug delivery. The use of genipin as crosslinker instead of oxidized catechols allows for full exploitation of the mucoadhesion properties of catechols, as shown by the high rate of gels adhering to porcine buccal mucosa over the course of 6 hours in-vitro and by the enhanced release of lidocaine hydrochloride (LD), a local anesthesia drug, in vivo in rabbit models.

4.3 Materials and methods

4.3.1 Materials

Low molecular weight chitosan (CS) (MW 50,000 - 190,000 Da, 85% deacetylation), N-(3-Dimethylaminopropyl)-N'-ethylcarbodiimide hydrochloride (EDC) (≥ 98.0%), and lidocaine hydrochloride monohydrate (LD) were purchased from Sigma-Aldrich (USA). Hydrocaffeic acid (≥98%) and procaine hydrochloride (PR) were obtained from Alfa Aesar (USA). Genipin (GP) (≥ 98%) was purchased from Challenge Bioproducts (Taiwan). Lysozyme from human milk (≥ 100,000 units/mg protein) was provided by Sigma-Aldrich (USA). All other reagents used in this study were purchased from Sigma-Aldrich (USA) and used directly without further modification.

4.3.2 Synthesis of catechol-chitosan (Cat-CS)

The protocol of Cat-CS synthesis was modified from previous work [29]. Briefly, 60 ml of 1% (w/v) CS solution was prepared in hydrochloric acid (HCl) at pH 2.5. Then, 0.145 g of hydrocaffeic acid and 0.356 g of EDC and were dissolved in 15 ml ethanol and 15 ml deionized (DI) water respectively. These two solutions were mixed and quickly added to CS solution under intensive stirring, followed by the addition of 1M NaOH to increase the pH to 5.5. The reaction was allowed to continue for 12 hours. After this time, the products were purified by dialysis against a pH 5.0 HCl solution for 3 days using a dialysis membrane tube (MWCO 5,000, Spectrum Laboratories, USA). The final product was freeze dried and stored at -20 °C. To synthesize Cat-CS with a higher

ratio of catechol conjugation, the weights of both hydrocaffeic acid and EDC were doubled (i.e. 0.29 g hydrocaffeic acid and 0.712 g of EDC). The degree of conjugation was determined using a UV-Vis spectrometer (Carry 5000, USA) and measuring the absorbance of aqueous solutions of the two Cat-CS polymers at 280 nm. The results were compared with a standard curve built using hydrocaffeic acid, and showed a catechol content of 9% and 19% (Figure S4.1). The two products are therefore named from here on as Cat9-CS and Cat19-CS, respectively. A schematic of the reaction used to synthesize both Cat-CS polymers is shown in Figure S4.2.

4.3.3 Preparation of capped hydrogels and drug loading

An ethyl cellulose protective cover that prevents drug from diffusing to the lumen of the buccal cavity was prepared by solvent casting. 120 µl of 4% ethyl cellulose ethanol solution was added into a mold and dried at room temperature, forming an open cylindrical cap with diameter of 8.5 mm and height of 1.6 mm (Figure 4.1B). This impenetrable cap provided a protective layer on the back and the sides of the hydrogel, and allowed the drugs loaded in the hydrogels to diffuse only through the side in contact with the mucosa. The cap was used as a mold for curing the hydrogel. To make the hydrogel, a 1.5% (w/v) solution of Cat-CS (Cat9-CS or Cat19-CS) was prepared in 3ml of DI water under stirring. 75 µl of 30 mg/ml GP solution in ethanol was added to the Cat-CS solution at a GP:Cat-CS weight ratio of 1:20. 150 µl of the mixture were transferred to the mold and cured at 37°C for 12 hours. The final hydrogels were named Cat9-CS/GP and Cat19-CS/GP depending on their catechol content.

LD, a local anesthesia drug, was selected as a model drug in this study. To prepare the LD loaded hydrogel, LD was first dissolved in 30 mg/ml GP ethanol solution; 75 µl of this solution was added to 3 ml of Cat9-CS or Cat19-CS solution, followed by curing at 37°C for 12 hours. The final concentration of LD was 1mg/hydrogel.

As control, CS/GP hydrogels were prepared and loaded with LD. CS/GP hydrogels were prepared by first dissolving CS in 1% (v/v) acetic acid, and the same procedures described above for the preparation of Cat-CS/GP capped hydrogels and drug loading were followed afterwards.

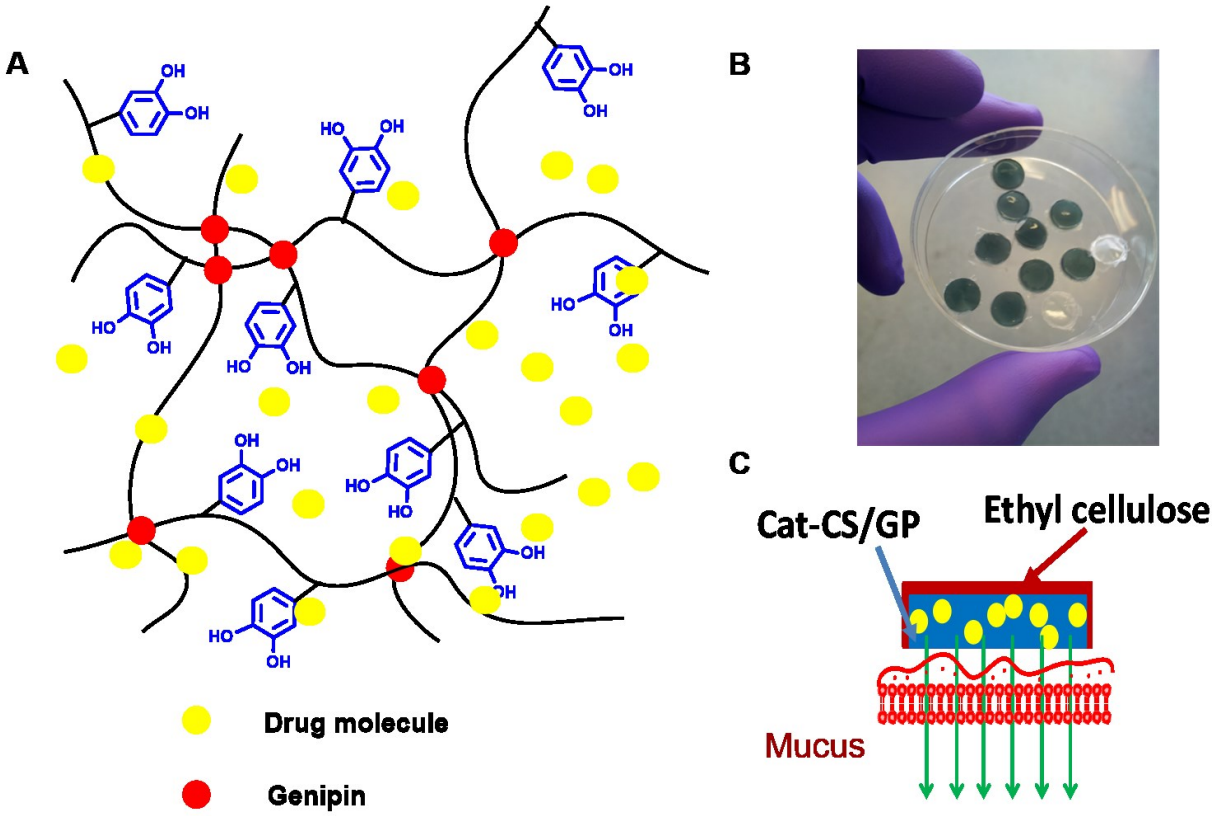

Figure 4.1. Cat-CS/GP Hydrogels. A: Schematic of GP-crosslinked Cat-CS hydrogel network; B: Cat-CS/GP hydrogel with ethyl cellulose protective cap; C: schematic of drug release at the mucosa surface from the capped hydrogel.

4.3.4 Physical characterization of the hydrogel

All hydrogels were freeze-dried before characterization. A Bruker Tensor-27 Fourier transform infrared (FTIR) spectrometer equipped with a DTGS detector and a VariGATR™ grazing angle attenuated total reflectance accessory was used to analyze the functional groups formed on the hydrogels. 256 scans were collected for each sample.

Nuclear magnetic resonance (NMR) spectroscopy was used to confirm the conjugation of catechol functional groups to CS and hydrogel crosslinking. ^{13}C CP-MAS NMR spectra were

obtained at 100 MHz using a 7.5 mm rotor spinning at 5 kHz, a 1.5 ms contact time and recycle time of 2 s for all samples (Agilent/Varian VNMRS-400, USA). Spinning sidebands were eliminated by the TOSS sequence.

The morphology of the freeze dried hydrogels was analyzed on a JEOL JSM7600F scanning electron microscope (SEM). Cross sections of freeze-dried CS/GP, Cat9-CS/GP and Cat19-CS/GP hydrogel disks were observed at an acceleration voltage of 1kV.

4.3.5 Hydrogel erosion in vitro

Freeze-dried hydrogels were immersed at 37°C in PBS (pH 6.8) containing 5 μg/ml of lysozyme (erosion solution). Samples were weighed before being put into the erosion solution (W_0). After specific times, samples were taken out, freeze-dried, and weighed again (W_t). Three replicates were performed for each experiment. The weight loss percent (W_L %) was calculated as in Equation 4.1:

$$W_L\% = (W_0 - W_t) / W_0 \times 100 \quad \text{(Equation 4.1)}$$

4.3.6 Cumulative drug release in vitro

Hydrogels containing 1 mg of LD were immersed in 10 ml of 10 μM phosphate buffer saline (PBS, pH 6.8) at 37°C. At each time point, 1 ml of the solution was taken out to quantify the release, and meanwhile 1 ml of fresh PBS was added. Time points were selected as 15, 30, 45, 60, 90,120, 150 and 180 minutes. Each test was replicated for three times.

The released LD concentration in PBS medium was quantified using a Thermo Finnigan LCQ Duo Spectrometer System equipped with a UV detector. We used a mobile phase made of acetonitrile/water (30/70, v/v) and 0.1% (v/v) trifluoroacetic acid (TFA). 10 μl of sample were injected into the instrument and passed through a C18 Supelco Discovery column (15 cm × 3 mm,

particle size 5 μm), at a flow rate of 0.5 ml/min. Peaks relative to LD were detected at a wavelength of 210 nm, which appeared 2.5 minutes after injection. A standard curve was measured by plotting the areas under the curve (AUC) of the 210 nm peak in a series of samples with known concentrations. Each sample was repeated three times.

4.3.7 Rheological tests

Rheological measurements were conducted to evaluate the gel formation process and the viscoelastic properties of the final hydrogels on a TA Instruments AR2000 stress-controlled rheometer (USA) equipped with a Peltier plate for temperature control. A cone steel geometry (Φ 40 mm, 2°) was used for all experiments. Oscillatory measurements were conducted at a constant frequency (f = 1 Hz) and strain (σ = 0.1%) in the linear viscoelastic regime (LVR), which was established by initial stress sweep tests. The polymer and crosslinker were mixed quickly and placed in the rheometer. The gelation process at 37 °C was followed through the evolution of storage and loss moduli (G', G'', respectively) as a function of time. A solvent trap was used to prevent the dehydration of the hydrogels. We performed time sweeps for a total of 12 hours at 37 °C; longer test times would lead to significant gel dehydration. After 12 hours of gelation and equilibration of the samples, stress sweeps were measured with stress ranging from 0.1 to 10000 Pa to evaluate the structural integrity of the hydrogel network. Each test was replicated three times.

4.3.8 Mucoadhesion test in vitro

Fresh porcine buccal tissue was glued to a microscope glass slide (mucosal membrane facing up) and placed into a beaker vertically (Figure S4.3). The hydrogels were pressed to adhere on the mucosal surface. Both the tissue and the hydrogels were immersed in 30 ml PBS (pH 6.8) at 37°C. A magnetic stirring bar rotating at a speed of 1000 rpm was used to generate flow. Every 15

minutes, the number of hydrogels that still adhered to the mucosa was recorded. The data were evaluated using Kaplan-Meier estimate plots of survival. Ten samples from each hydrogel group were tested.

4.3.9 Mucoadhesion and drug release test in vivo

CS/GP and Cat19-CS/GP capped hydrogels were prepared as previously described, each containing 1 mg of LD. Four male New Zealand rabbits (adults, weight 3.5 kg) were used to study mucoadhesion and drug release in vivo. Animals were received and allowed to acclimatize for a minimum of 72 hours. Each rabbit was pre-anesthetized using Ketamine-Xylazine-Acepromazine injected subcutaneously. After that, the maintenance of anesthesia was guaranteed by intubation through the mouth using a regulated flow of isoflurane (concentration 1.5 – 2 vol%). A catheter was placed into the marginal ear vein of each rabbit to collect blood samples. The mouth of the rabbit was opened, and the mucosal lining of the cheek was exposed. CS/GP hydrogels were applied to two rabbits (R1 and R2) used as control group, and Cat19-CS/GP hydrogels to the other two rabbits (R3 and R4) used as test group. Each hydrogel was pressed against the mucosal lining of the rabbit cheek. Hydrogels were allowed to stay in place for a total of 3 hours. Then, animals were euthanized by intravenous injection of overdosed barbiturate. Blood samples (1 ml at each time point) were collected after 15, 30, 60, 90, 120, 150, and 180 minutes since application of the hydrogels. The blood samples were placed at room temperature for 20 minutes for coagulation, followed by centrifugation at 3000 rpm for 15 minutes. The serum was collected and kept frozen until quantification.

To extract the drug from the serum, serum samples were thawed to room temperature, and a method modified from a previous study was used [300]. Briefly, 600 µl of serum were added to a centrifuge tube containing 100 µl of a 1 M Na_2CO_3 solution, followed by the addition of 10 ml

of ethyl acetate. 5 µl of 5 ppm procaine hydrochloride (PR) water solution was added at the same time as an internal standard. The mixture was vortexed for 2 minutes, and then centrifuged at 4000 rpm for 5 minutes. 7 ml of the supernatant organic layer was transferred to another centrifuge tube with 200 µl of 0.0025 M H_2SO_4. Again, the mixture was vortexed for 2 minutes and centrifuged at 4000 rpm for 5 minutes. The supernatant ethyl acetate was removed, and the remaining solution was neutralized by adding 100 µl of 0.01 M NaOH. The final solution was freeze dried and re-dissolved in 200 µl of DI water and analyzed with liquid chromatography–mass spectrometry (LC-MS).

LC-MS was performed on a Thermo Scientific Exactive Plus Benchtop Full-Scan Orbitrap™ Mass Spectrometer equipped with an electrospray ionization source. Mobile phase flowing at the rate of 300 µl/min consisted of methanol/water (50/50, v/v) and 0.1% TFA. A Thermo Scientific Hypersil GOLD column (50mm × 2.1 mm) with particle size of 1.9 µm was used for compound separation. Serum solutions were loaded in an auto-sampler, and 8 µl were injected by the auto-sampler into the column. The peaks of LD and of the internal standard PR were identified at mass-to-charge values of 285.18049 and 287.15975, respectively. A standard curve based on AUC ratios of LD to PR at known concentration ratios was used to calculate the LD concentration in serum samples.

After the animal was sacrificed, the hydrogel was removed, and the buccal tissue in contact with the hydrogel was extracted for histological examination. The harvested tissue was fixed in 2% paraformaldehyde, dissected longitudinally, and embedded in paraffin. 5 µm thick tissue sections from the mucosa side were stained with haematoxylin and eosin (H&E) to detect inflammation, following literature protocols [301, 302]. Tissue from the cheek that was not in contact with the

hydrogel was also extracted and examined as control. Stained samples were examined under microscope at magnification of 400X.

4.3.10 Statistical analysis

Statistical analysis for all tests (except for the mucoadhesion in vitro study) was carried out using Student's t test. Error bars in the figures represent the standard deviation (SD). For the muoadhesion in vitro study, the Kaplan-Meier estimate statistical analysis was used [303]. Chi-square values were calculated based on log-rank test statistic, and were converted to p values. A value of $p \leq 0.05$ was considered significant in all tests.

4.4 Results

4.4.1 Physical characterization of the hydrogel

Figure 4.2A shows the FTIR spectra of catechol functionalized CS (Cat9-CS and Cat19-CS) and the corresponding hydrogels (Cat9-CS/GP and Cat19-CS/GP). In all spectra, peaks at 905 cm^{-1} and 1159 cm^{-1} are attributed to vibrational modes of the saccharide units [304], while the peak at 1074 cm^{-1} is related to C-O stretching and/or C-N stretching [305]. The main differences among all spectra are found in the 1450-1700 cm^{-1} region. A peak at 1562 cm^{-1} is present in the CS spectrum, and is related to protonated amino groups due to the presence of acetic acid as solvent [306] (Figure 4.2A, a). After GP crosslinking, the primary amino groups in CS decrease in number, and secondary amides are formed [307]. Indeed, the peak at 1562 cm^{-1} decreases in intensity in the spectrum of CS/GP (Figure 4.2A, b), while the intensity of a peak at 1640 cm^{-1} (amide type II [308]) increases. The spectra of the catechol modified CS samples (Figures 4.2A, c - f) show a drastic increase in intensity in the region around 1620 cm^{-1}, which corresponds to the aromatic C=C stretching vibrations [309], thus confirming the presence of catechol groups in the Cat-CS

samples. Since amide bonds are found in this region too [308], crosslinking might have contributed to these peaks for Cat9-CS/GP and Cat19-CS/GP (Figures 4.2A, d and f). A small peak at 1730 cm^{-1} is present in the spectra of Cat-CS samples, which can be related to aromatic and aliphatic C=O stretching [309].

^{13}C Solid state NMR was used to further confirm covalent bond formation occurring during catechol conjugation and GP crosslinking. Figure 4.2B (a) shows the spectrum of the original CS powder. We assigned the peaks of C1 to C6 carbons within the glucose structure of CS repeating units (see schematic representation in Figure 4.2B) [310]. The peaks at 175 ppm and 24 ppm are attributed to C=O bonds and CH_3 due to the presence of remaining acetylated glucose structure in CS [310]. In the spectrum of CS/GP (Figure 4.2B, b), we see an increase in the intensity of the CH_3 peak as well as a new peak at 184 ppm, due to acetate groups; these changes are both associated with the presence of acetic acid for dissolving CS. The spectra of both Cat-CS polymers before crosslinking with GP (Figures 4.2B, c and e) show a higher intensity of the peak at 175 ppm compared to unmodified CS. Since this peak is due to C=O bonds, this increase is to be related to the formation of extra secondary amide bonds during EDC conjugation. On all the Cat-CS samples, both before and after crosslinking with GP (Figures 4.2B, c - f), there is an increase in intensity in the aromatic carbon region (150 – 110 ppm) and aliphatic region (50 -20 ppm) [311-313] compared to the spectra of unmodified CS (Figures 4.2B, a and b), thus confirming the presence of catechol groups.

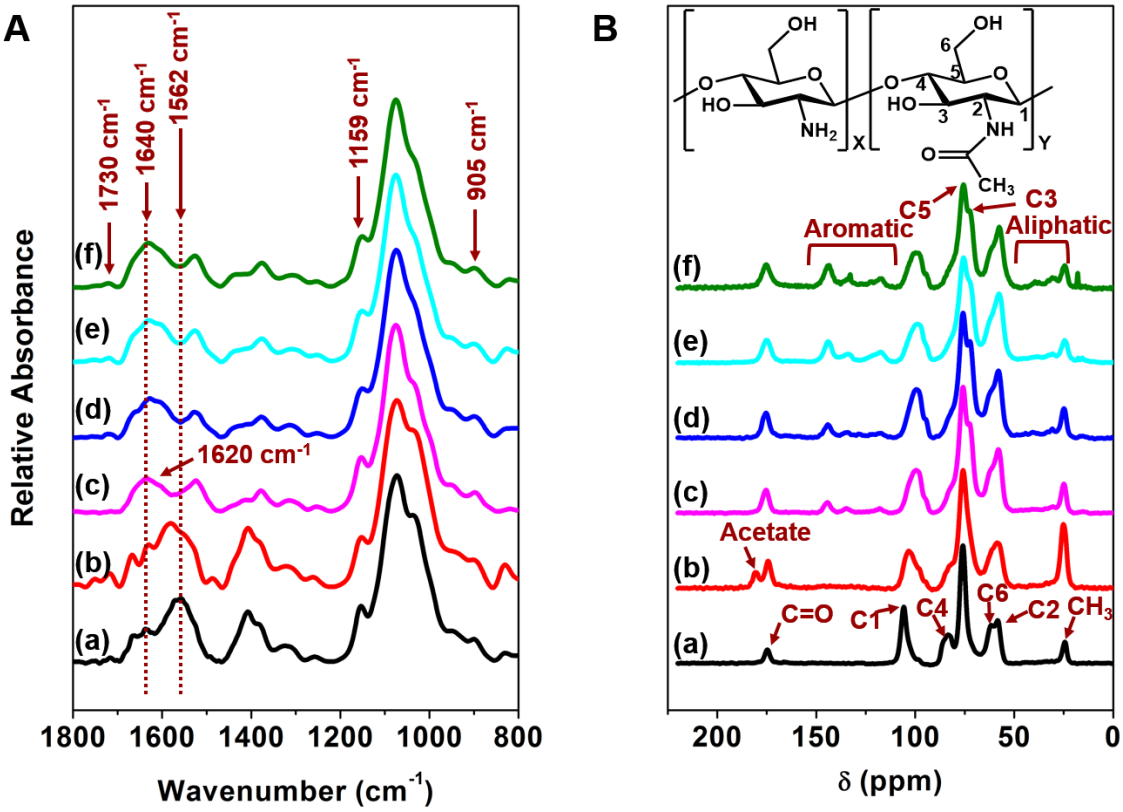

Figure 4.2. FTIR spectra (A) and ^{13}C solid state NMR spectra (B) of (a) CS; (b) CS/GP; (c) Cat9-CS; (d) Cat9-CS/GP; (e) Cat19-CS; (f) Cat19-CS/GP.

Figure 4.3 shows SEM pictures of CS/GP, Cat9-CS/GP and Cat19-CS/GP. Smaller pores can be observed in the order Cat19-CS/GP < Cat9-CS/GP < CS/GP, thus implying that catechol modification leads to the formation of denser hydrogels. This observation suggests that catechol groups may be partially oxidized in Cat-CS hydrogels: when catechols are oxidized, quinones are formed, which can contribute to CS intermolecular crosslinking by forming quinone-quinone or quinone-amino bonds [195]. This leads to a denser structure with smaller pores.

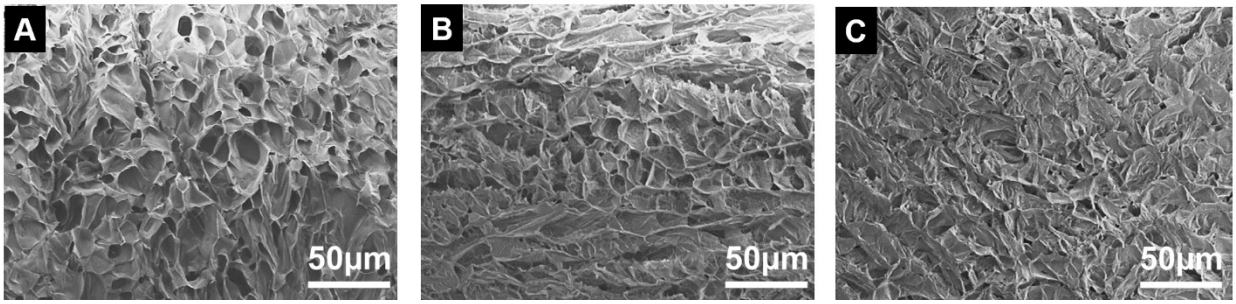

Figure 4.3. SEM images of hydrogel network structure. A: CS/GP; B: Cat9-CS/GP; C: Cat19-CS/GP.

4.4.2 Hydrogel erosion in vitro

Buccal drug delivery systems in forms of tablets, patches, films or gels experience erosion and degradation during the application in the oral cavity [57]. To understand the rate of erosion of the proposed hydrogels, we analyzed their weight loss in PBS buffer solutions with the addition of lysozyme. Figure 4.4A shows that all three GP crosslinked hydrogel systems lost weight during 3 days immersion. Cat-CS/GP hydrogels showed a much slower weight loss than CS/GP hydrogels: after 3 days, CS/GP hydrogels lost 24% of their initial dry weight, while Cat9-CS/GP and Cat19-CS/GP hydrogels lost 17% and 14% respectively. This resistance to erosion in Cat-CS hydrogels may be explained by their higher density (Figure 4.3), which could slow down fluid and lysozyme penetration.

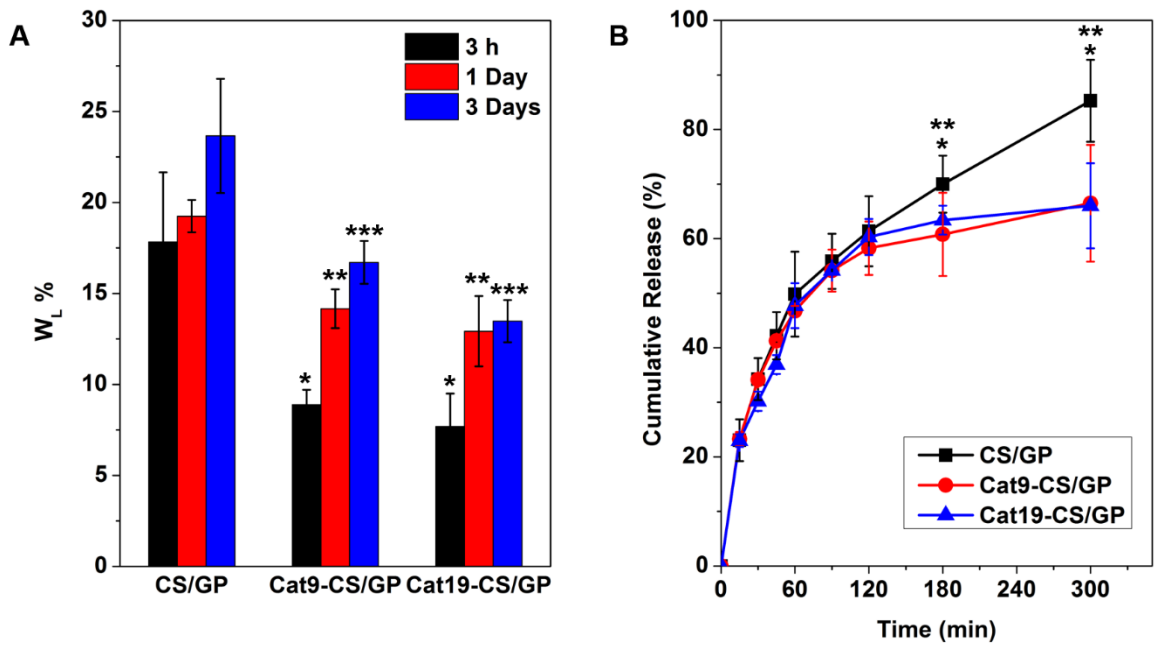

Figure 4.4. In vitro hydrogel erosion and drug release. A: Weight loss percent during CS/GP, Cat9-CS/GP and Cat19-CS/GP erosion in PBS (pH=6.8) with 5 µg/ml of lysozyme. *,**, and *** represent $p \leqslant 0.05$ as compared to CS/GP at 3 hours, 1 day and 3 days, respectively; B: cumulative LD release from the hydrogels in PBS (pH 6.8) at 37° C. * and ** represent $p \leqslant 0.05$ when comparing CS/GP to Cat9-CS/GP and Cat19-CS/GP, respectively.

4.4.3 Cumulative drug release in vitro

We loaded LD as a model drug into CS/GP, Cat9-CS/GP and Cat19-CS/GP hydrogels, and conducted a cumulative drug release study in vitro to understand the rate of drug release. Figure 4.4B shows sustained release of LD from the hydrogels in PBS buffer over 3 hours. The drug was quickly released out of all hydrogels during the first 30 minutes, due to the significant concentration gradient from the hydrogel to the medium. The release then slowed down, and was similar from all hydrogels during the first 3 hours (180 minutes). After 3 hours, the release from Cat9-CS/GP and Cat19-CS/GP almost plateaued, whereas it kept increasing for CS/GP. By the

end of 5 hours, 85±8% of total loaded LD was released from CS/GP, whereas only 67±11% and 66±8% was released from Cat9-CS/GP and Cat19-CS/GP. This result correlates well with the pore size difference observed by SEM (Figure 4.3): the pores in Cat-CS/GP hydrogels are smaller than in unmodified CS/GP hydrogels, and they may trap part of LD.

The data corresponding to the first 60 % of the total amount of drug released can be fitted to the model proposed by Ritger and Peppas (Equation 4.2) to understand drug release kinetics and mechanism [314]:

$M_t / M_\infty = kt^n$ (Equation 4.2),

where M_t and M_∞ represent the amounts of drug released at time t and at equilibrium (the total amount of drug loaded in the hydrogel), and thus M_t / M_∞ represents the fractional release of the drug at time t. The proportionality constant k and the diffusion exponent n were derived based on power fitting of M_t / M_∞ vs. t. k is a constant incorporating characteristics related to the macromolecular network system and the drug, while n reflects the drug release mechanism [253]. For cylindrical sample, when n is within the range of 0.45 to 0.89, the release mechanism is defined as non-Fickian diffusion [314].

Table 4.1 shows that the values of n for CS/GP, Cat9-CS/GP and Cat19-CS/GP are within the range of 0.45 to 0.89, thus they all fit a non-Fickian diffusion model. This indicates that LD was released by both diffusion and erosion. Indeed, hydrogel degradation is significant even within the first 3 hours (Figure 4.4A). CS/GP shows the highest n (0.51), which can be explained by its highest weight loss rate compared to the two catechol-modified systems.

Table 4.1. Summary of diffusional exponent n and correlation coefficient R^2 derived from the fit of the first 60% of the total amount of drug released from CS/GP, Cat9-CS/GP and Cat19-CS/GP according to the Ritger and Peppas model (Equation 4.2).

Hydrogel	Diffusional exponent, n	R^2
CS/GP	0.51	0.99
Cat9-CS/GP	0.47	0.99
Cat19-CS/GP	0.50	0.98

4.4.4 Rheological tests

Mechanical properties are important to consider in the design of a buccal drug delivery system. An ideal buccal delivery system should have sufficient mechanical strength to be applied to the buccal mucosa [283]. We conducted rheological tests to monitor the evolution of G' and G" moduli during gel formation (Figure 4.5A). At the beginning of gelation, G" values were higher than G' for all samples, indicating that they were in liquid-like state and the viscous properties dominated. The initial G' and G" values of both Cat-CS/GP samples were lower than those of CS/GP, indicating that Cat9-CS and Cat19-CS dissolved in water produced a less viscous solution than CS dissolved in acetic acid. After some time, both G' and G" moduli increased, but the G' increased at a higher rate than G". This indicates that the sample solutions transformed into more and more solid samples, and gradually the elastic properties dominated. This transformation is related to the rate and amount of crosslinks formed in the hydrogels. The gelation times, defined as the time at which G' and G'' intersect, were 92 minutes, 136 minutes, and 100 minutes for CS/GP, Cat9-CS/GP and Cat19-CS/GP, respectively (Table 4.2). After 12 hours, all gels almost reached their equilibrium state. The final G' measured was higher for CS than for Cat-CS samples, in the order CS/GP > Cat19-CS/GP > Cat9-CS/GP, which may indicate that catechols interfere with GP crosslinking, and that if there is self-crosslinking among oxidized catechols, this did not increase

the mechanical properties of the Cat-CS gels. In fact, we analyzed self-crosslinking in Cat-CS by performing a similar rheological test on Cat-CS samples without adding GP (Figure 4.5B). The G' and G" moduli of these samples increased gradually with time, and crossed at gelation times of 342 and 345 minutes for Cat9-CS and Cat19-CS, respectively (these values are not statistically significantly different, see Table 4.2). This indicates that self-crosslinking can occur, but much more slowly than the crosslinking achieved in the presence of GP (Figure 4.5A). Figure 4.5B shows rheological tests performed on CS samples without GP for comparison. These samples never gelled (G' and G" lines were horizontal and never crossed), which confirms that in the absence of catechols CS alone is not able to gel by intermolecular interactions. Overall, these results show that Cat-CS samples can self- crosslink into a gel, although at a slower rate than in the presence of GP. This must be related to reaction between oxidized catechols (quinones) and other quinones or amino groups present in Cat-CS [195].

Table 4.2. Summary of rheological tests.

	CS/GP	Cat9-CS	Cat19-CS	Cat9-CS/GP	Cat19-CS/GP
Gelation time (min)	92±3	342±14	345±23	136±8	100±11
Equilibrium G' (Pa)	1403±172	4±1	6±1	282±69	439±59

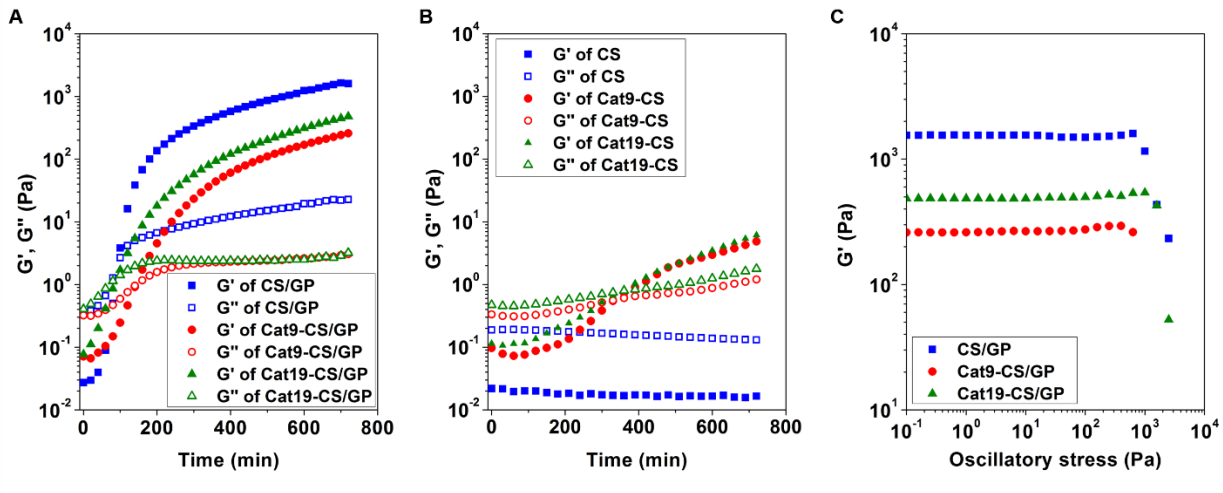

Figure 4.5. Rheological characterization of hydrogels. A: Changes in G' and G'' while curing at 37°C CS and Cat-CS hydrogels in the presence of GP; B: changes in G' and G'' while curing at 37°C CS and Cat-CS hydrogels in the absence of GP; C: changes in G' with increasing oscillatory stress for CS and Cat-CS hydrogels in the presence of GP after 12 hours gelation. For all experiments f = 1 Hz and σ = 0.1 %.

To evaluate the mechanical properties of crosslinked hydrogels, we measured the dependence of G' moduli on oscillatory stress after 12 hours gel equilibration (Figure 4.5C). Within the linear viscoelastic regime (LVR), G' is independent of the applied shear stress while the applied stress is in phase with the strain [315]. Indeed, all three crosslinked hydrogels showed nearly flat G' curves at low stresses. When the stress increased beyond the LVR, G' declined sharply as the network structure of the hydrogels collapsed, and the applied stress was no longer in phase with the strain [315]. The difference of the critical shear stress after which Cat9-CS/GP and Cat19-CS/GP hydrogels broke down compared to CS/GP was not statistically significant. The self-crosslinked hydrogels prepared without GP, Cat9-CS and Cat19-CS, showed a much lower critical shear stress (about 10 Pa), showing that these gels are much weaker (Figure S4.4).

4.4.5 Mucoadhesion in vitro

Buccal drug delivery systems should maintain their adhesion at the buccal mucosa surface for a long time to enhance drug residence time. We evaluated the mucoadhesion of CS/GP, Cat9-CS/GP and Cat19-CS/GP hydrogels in vitro, by recording the number of remaining hydrogels adhered to porcine buccal mucosal membranes in PBS while stirring. Figure 4.6 shows the evolution of this number through Kaplan-Merier estimate survival curves. All unmodified CS/GP hydrogels detached from the mucosal membrane within the first 1.5 hours, thus showing that CS alone provides only weak mucoadhesion to the buccal tissue. In contrast, Cat9-CS/GP and Cat19-CS/GP hydrogels adhered to the tissue for much longer: by the end of 6 hours, two out of ten Cat9-CS/GP hydrogels and seven out of ten Cat19-CS/GP hydrogels were still stuck to the buccal mucosa. This undoubtedly shows that catechols can effectively increase CS mucoadhesion to the buccal tissue, and that such increase is proportional to the amount of catechol groups introduced.

4.4.6 In vivo experiments

Having proved that the Cat-CS/GP hydrogels can induce enhanced mucoadhesion in vitro, we studied in vivo drug delivery on rabbits. We selected unmodified CS/GP hydrogels as control group, and Cat19-CS/GP hydrogels as test group. We loaded the hydrogels with LD as a model drug, and prepared capped hydrogels by casting the hydrogels on an impermeable ethyl cellulose membrane to prevent release in the saliva from the side of the hydrogel that was not in contact with the buccal membrane. After applying the hydrogels inside one of the rabbits' cheeks in contact with the buccal mucosal membrane, we took blood samples at different time points to monitor drug concentration in the serum.

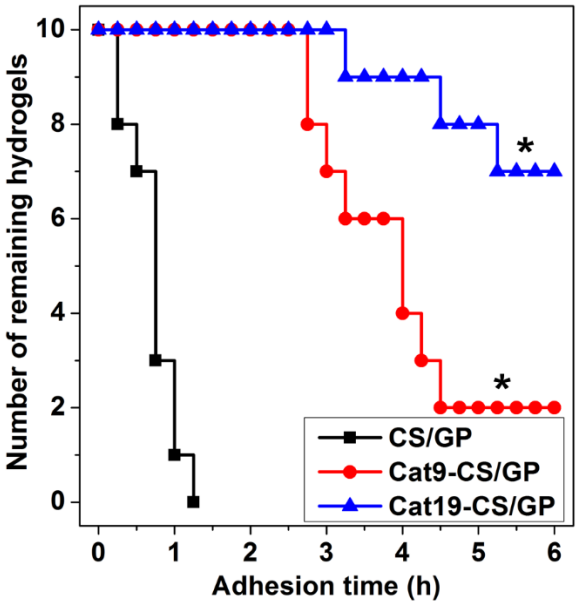

Figure 4.6. Kaplan-Merier estimate survival curves showing adhesion of CS/GP and Cat-CS/GP hydrogels on porcine buccal mucosa in PBS (pH 6.8) at 37° C. * represents $p \leqslant 0.05$ compared to CS/GP.

Figure 4.7 shows that the concentration of LD in serum increased after application of the hydrogels, indicating that LD was absorbed through the buccal mucosal membrane and reached blood circulation. LD serum concentration was much higher if the drug was released from hydrogels made with Cat19-CS (rabbits R3 and R4, test group) as compared to those made with unmodified CS (rabbits R1 and R2, control group). After about 2 hours from the beginning of the application, the concentration of LD measured in the serum of the control group decreased significantly, reaching almost negligible values at the end of the experiment. In contrast, LD concentrations remained relatively high in the test group; about 1 ng of LD per ml of serum could be detected at the end of the experiment, thus showing that Cat19-CS/GP hydrogels can provide sustained LD release in vivo for at least 3 hours.

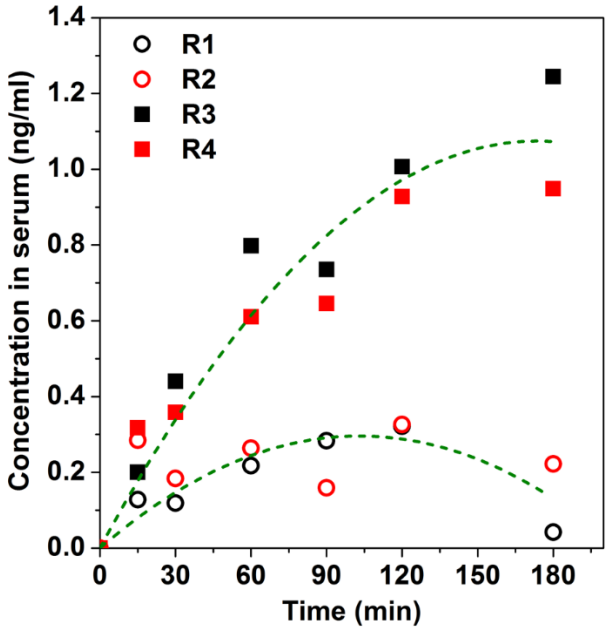

Figure 4.7. LD concentration measured in the serum of rabbits R1-R4 after application of drug-loaded patches on the rabbit buccal mucosa. CS/GP hydrogels are used to make the patches applied on R1 and R2 rabbits (control group); Cat9-CS/GP hydrogels are used for the patches applied on R3 and R4 rabbits (test group).

Figure 4.8 shows histological images of the buccal mucosal tissue collected from the cheek that was not in contact with the hydrogel (Figures 4.8A and B) and from the one that was in contact with Cat19-CS/GP hydrogel for 3 hours (Figures 4.8C and D). The images are very similar. Healthy skeletal muscle fibers (Figures 4.8A and C) and excretory ducts (arrows in Figures 4.8B and D) with no significant inflammation, necrosis, or metaplasia are shown in the tissue in contact with the hydrogels, thus proving that the Cat9-CS/GP hydrogels are highly biocompatible.

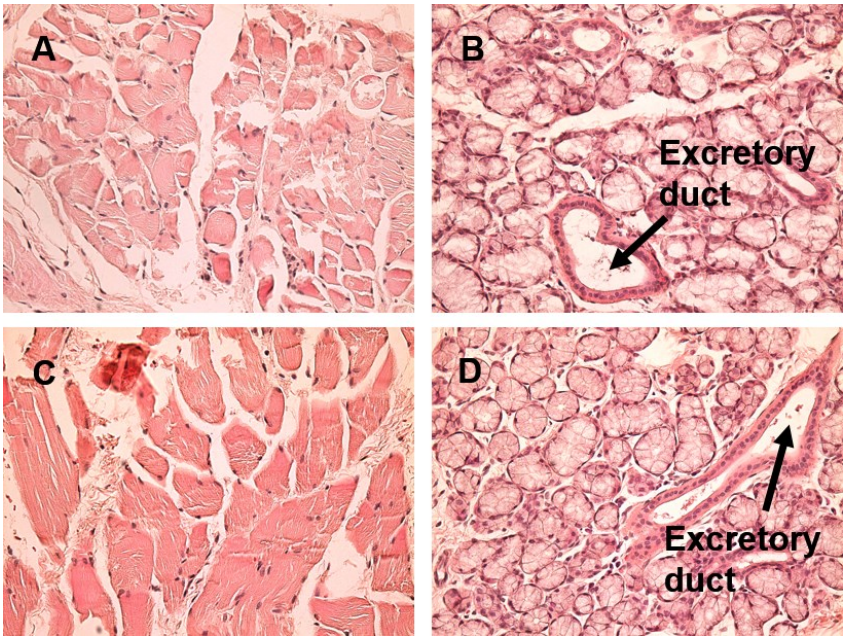

Figure 4.8. H & E staining of rabbit buccal mucosa tissue taken from healthy control tissue from the cheek that was not in contact with a patch (A and B) and from the area in contact with the Cat19-CS/GP patch after 3 hours application (C and D).

4.5 Discussion

We developed a new hydrogel made from GP crosslinked Cat-CS, which shows to be a promising mucoadhesive buccal drug delivery system. Although there are several studies related to catechol-modified hydrogels [29, 33, 195, 217, 296, 297] , this is the first time that such a system is used for mucoadhesive drug delivery. In a previous work, we had shown that by simple mixing catechol compounds and CS, CS mucoadhesion is enhanced [299]. Here we show an even larger mucoadhesion enhancement, probably due to the fact that in this case we covalently bound the catechol groups to CS, and therefore these groups are not released during contact with the mucosa. While CS is normally soluble only at acidic pH, catechol functionalization converts it into a highly water soluble polymer at physiological pH [15]. Indeed, the Cat-CS/GP hydrogels shown in this study are prepared at physiological pH in water. This implies that they could potentially be loaded

with and deliver bioactive compounds or drugs that become unstable at non-physiological conditions.

Differently from previous catechol-containing hydrogels proposed in the literature, gel crosslinking is achieved with GP. In all previous studies, to the best of our knowledge, gelation was achieved either via self-crosslinking of oxidized catechol groups [195, 297], or by interaction of catechols with other groups [29, 217]. Both strategies consume catechol groups; instead, since GP only consumes amino groups for crosslinking, the catechol groups in our gels remain intact. The availability of most catechol groups in the present hydrogels explains the tremendous enhancement in mucoadhesion observed both directly in-vitro and indirectly in-vivo by the drug delivery results. Indeed, the sustained LD release observed from the Cat19-CS/GP hydrogels in vivo has to be related to a more intimate contact between the gel and the mucosa, thus allowing the drug to be absorbed through the mucosa. The lower LD concentrations detected in the control group can be explained by a reduced contact area due to failure of intimate adhesion of the CS/GP patches after application.

The use of GP as crosslinker has the further advantage of its very low cytotoxicity, about 10000 times lower than glutaraldehyde [316]. Indeed, histological analysis did not show any evidence of inflammation or adverse reaction upon contact with the Cat19-CS/GP hydrogel. Finally, GP crosslinking allows for the synthesis of mechanically robust gels: there are no significant differences in the critical shear stress measured on the catechol-modified and CS only hydrogels.

The LD concentration measured in serum after 3 hours release from Cat19-CS/GP patches was around 1.4 ng/ml. This low value is not unexpected. LD has to pass through several barriers before reaching the blood stream, thus the penetration rate is limited. Okamoto et al. reported that

the penetration rate of LD released from lidocaine-hydroxypropylcellulose films for buccal administration was as low as about 5% of the dose loaded per hour, measured in vitro through an excised hamster oral mucosa [317]. Additionally, when LD enter blood circulation, a considerable amount binds to plasma proteins, and between 70% and 90% is rapidly metabolized by the liver [318, 319]. LD half-life (i.e. the time after which half of the LD concentration in the blood is metabolized) is about 1.5 hours [320]. Hersh et al. evaluated LD plasma concentration after applying commercial DentiPatch LD transoral delivery system on human cheeks [321]. They applied 2 cm^2 patches containing 23 mg or 46 mg. After 15 minutes, they were able to detect only about 15 ng/ml or about 20 ng/ml of plasma from the 2 types of patches, respectively. These values correlate well with those found in our study, considering that we put only 1 mg of LD in each hydrogel, and the contact area of our hydrogels was half that of the patches used in [321].

4.6 Conclusions

Buccal drug delivery is an attractive method to administer drugs that can act both systemically and locally. Mucoadhesive materials are crucial for this application, since they increase the retention of the delivery system at the mucosal membrane, thus allowing for an extended drug release. In this study, we developed a mucoadhesive hydrogel made from GP crosslinked Cat-CS. Cat-CS hydrogels are denser than CS hydrogels, thus allowing for a slower degradation and drug release in-vitro. Although less crosslinked than CS/GP hydrogels, the mechanical properties of Cat-CS/GP hydrogels are comparable to those of CS/GP hydrogels.

One unique feature of this hydrogel is that we preserve the functionality of catechol groups, which are responsible for the excellent mucoadhesion enhancement compared to unmodified CS/GP hydrogels. Cat-CS/GP hydrogels are much more adhesive than CS/GP gels to porcine buccal mucosal membrane in vitro. In vivo, Cat19-CS/GP was able to successfully deliver LD

through rabbit buccal mucosal membrane, reaching serum levels that are comparable to those achieved with commercial patches. The hydrogels are biocompatible and do not elicit any tissue inflammation.

Compared to other buccal drug delivery formulations including tablets, films, patches, particulates, semisolids and liquids, Cat-CS/GP hydrogels have the advantage of providing a physiological environment that could be used to deliver nutraceuticals, proteins, or even cells. This, in addition with the good mechanical properties of the hydrogels, makes this system ideal for bioactive pharmaceutics delivery. Besides buccal drug delivery, we envision that these hydrogels could be successfully used as mucoadhesive drug delivery system for other applications, including for example gastrointestinal tract targeting for the treatment of diseases such as ulcerative colitis.

4.7 Acknowledgements

The authors acknowledge the support of the Canada Research Chair program, Canada Foundation for Innovation, the Natural Sciences and Engineering Research Council of Canada, and the Advanced Foods & Materials Network. The authors would like to thank Mr. Nadim Saadeh for the help in experimental procedures and discussion of HPLC and LC-MS analysis, Dr. Frederick Morin for the help in measurement and data interpretation of NMR characterization, and Mr. Sherif Abdalla and Ms. Minh Duong for preparation of the histological samples.

4.8 Supplementary data

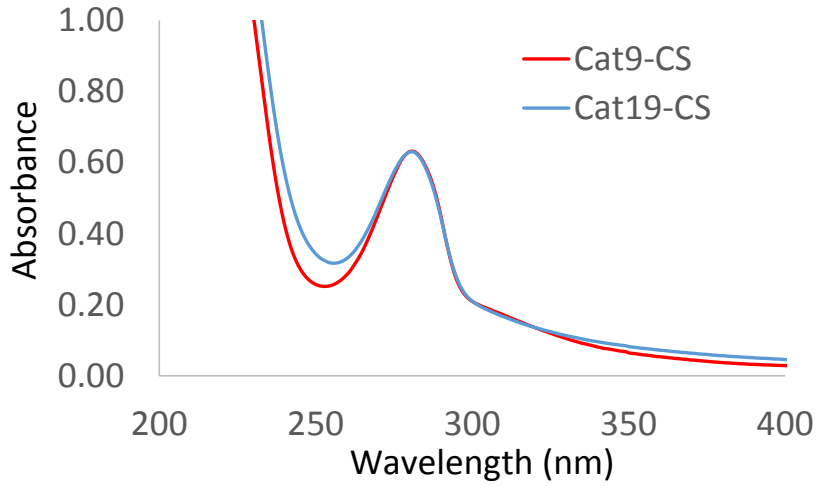

Figure S4.1. UV-vis Spectrum of Cat9-CS (3.2 mg in 5 ml H_2O) and Cat19-CS (3.2 mg in 10 ml H_2O).

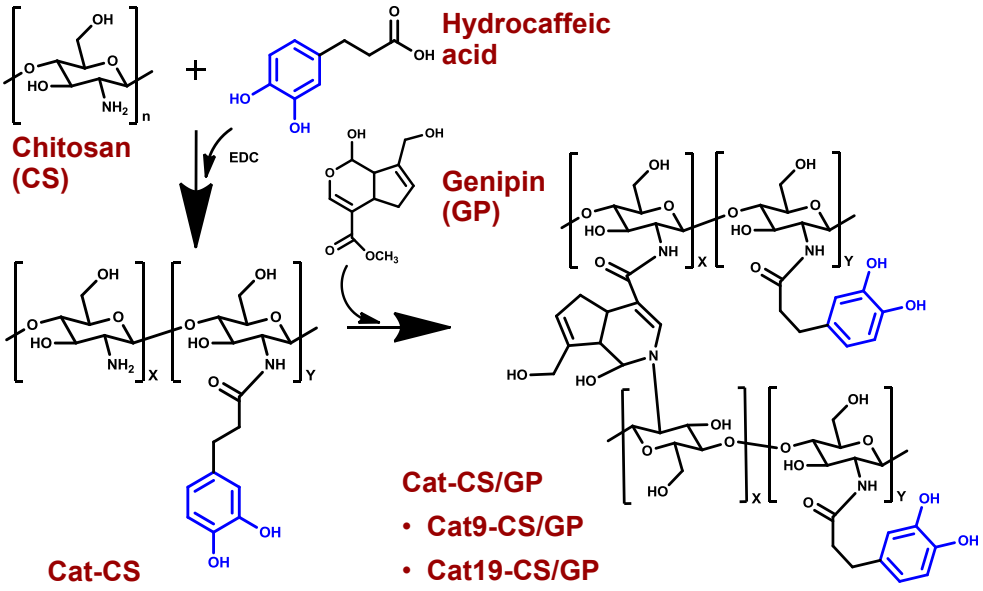

Figure S4.2. Scheme of Cat-CS synthesis and hydrogel formation with GP crosslinking.

Figure S4.3. Experimental set-up for mucoadhesion time measurement in vitro.

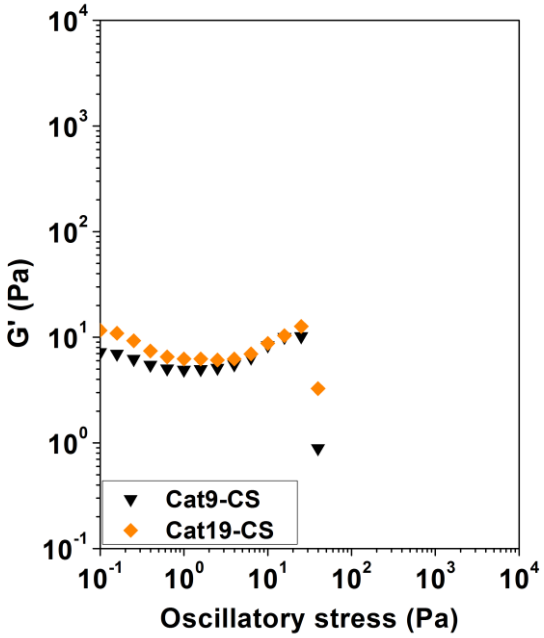

Figure S4.4. Stress sweep of Cat9-CS and Cat19-CS.

CHAPTER 5. RECTAL DRUG DELIVERY OF AN INJECTABLE SULFASALAZINE/CATECHOL-CHITOSAN MUCOADHESIVE FORMULATION TO TREAT ULCERATIVE COLITIS

In the previous chapter, the Cat-CS hydrogels showed promising mucoadhesion both in vitro and in vivo. The lidocaine loaded Cat19-CS/GP hydrogel achieved a sustained delivery of the drug through the rabbit buccal mucosa in vivo, thanks to the intimate contact between the mucoadhesive Cat19-CS/GP hydrogel and the rabbit buccal mucosa.

Based on these encouraging results, we further extended the use of the mucoadhesive Cat-CS hydrogels to the treatment of an inflammatory bowel disease affecting the colon mucosa, ulcerative colitis. SSZ is a conventional drug used to treat mild to moderate ulcerative colitis with both oral and rectal formulations. Oral SSZ formulations are often associated with side effects. Rectal formulations provide topical drug delivery at the inflamed colon mucosa with better therapeutic effects than oral formulations. However, rectal formulations are difficult to retain in the colon. We tried to use our mucoadhesive drug delivery system to overcome this challenge. In this chapter, we developed an SSZ-loaded Cat-CS hydrogel as an injectable mucoadhesive formulation. We attempted to answer the following questions:

i. How does the addition of SSZ affect the mechanical properties and injectability of the SSZ/Cat-CS hydrogel formulation?
ii. How are the therapeutic effects of this mucoadhesive rectal formulation in UC mice?

iii. Can SSZ/Cat-CS hydrogel formulation reduce the side effects associated with oral SSZ?

This chapter is going to be submitted shortly to a peer-reviewed journal.

5.1 Abstract

Ulcerative colitis (UC) is an inflammatory bowel disease characterized by chronic inflammation of the colonic mucosa. UC patients can be treated with various oral and rectal drug formulations. Compared to the oral route, rectal UC drug formulations can provide direct topical effect on the mucosa and avoid the unintended absorption of the drug or its degradation products in the upper gastrointestinal tract. Sulfasalazine (SSZ) is widely used to treat UC. Metabolized by intestinal flora, SSZ releases the therapeutic ingredient 5-aminosalicylic acid (5-ASA) and the toxic sulfapyridine (SP) subproduct, which causes adverse effects. Currently, both oral and rectal SSZ formulations are used, and sometimes both formulations are prescribed together. Rectal formulations such as liquid suppositories and foams are difficult to retain in the colon, thus limiting the therapeutic effect of SSZ. To overcome this challenge, we developed an injectable mucoadhesive SSZ rectal formulation made of catechol modified-chitosan (Cat-CS) crosslinked by genipin. The SSZ/Cat-CS hydrogel showed good injectability and consistency. We evaluated the efficacy of SSZ/Cat-CS hydrogel as a rectal formulation in dextran sulfate sodium (DSS)-induced colitis in mice which provides a model of UC. Compared to oral SSZ treatment, SSZ/Cat-CS achieved better therapeutic effects despite only 50% of the SSZ oral dose was actually delivered via rectal injection. SSZ/Cat-CS treated UC mice had similar histological scores as the mice that received SSZ orally. In addition, SSZ/Cat-CS treated mice showed a lower disease activity index, calculated based on body weight recovery rate, colon length, and TNF-α level. Most importantly, SSZ/Cat-CS treated mice had greatly reduced levels of SP in the plasma, and thus lower side effects caused by SP compared to the mice treated orally. These results overall show SSZ/Cat-CS rectal hydrogels as a more effective and safer formulation for UC treatment than oral SSZ.

5.2 Introduction

Ulcerative colitis (UC) is a chronic idiopathic inflammatory bowel disease caused by various genetic and environmental factors [36]. The disease causes abnormal recurring inflammation and ulcers at the colon mucosa [36]. Yearly, there are 1-20 newly reported UC patients per 100,000 people in the world, thus making the total proportion of UC patients at about 8-246 per 100,000 people [322]. Northern Europe and North America have the highest numbers of reported cases [322, 323]. In general, UC patients may suffer from bloody diarrhea, rectal urgency, tenesmus, lower abdominal pain, fever, weight loss, and risk of colon cancer [322, 324]. Currently, UC patients with mild to moderate symptoms can be treated with medications aiming at inducing and maintaining remission to improve quality of life. Severe cases may receive surgeries that may be as extensive as the removal of the entire colon [324].

Sulfasalazine (SSZ) is a potent oral drug used to treat acute UC or maintain remission. SSZ is very stable in the stomach, but the bacterial flora of the colon metabolizes it to 5-aminosalicylic acid (5-ASA) and sulfapyridine (SP) exploiting the azo-reduction pathway (Figure 5.1) [69].

5-ASA is the effective therapeutic compound in UC therapy. It is a cyclo-oxygenase inhibitor as well as anti-inflammatory [325]. The pharmacological actions of 5-ASA are not fully understood, but studies have shown that its anti-inflammatory action occurs by targeting peroxisome proliferator-activated receptor-γ [326], as well as modulating multiple cellular metabolism activities [327].

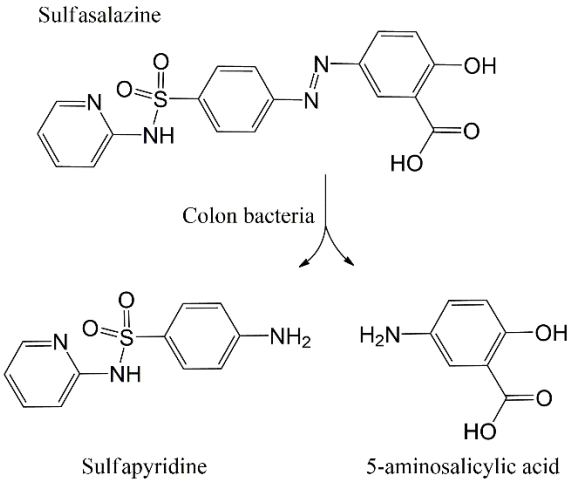

Figure 5.1. SSZ and its metabolites.

Side effects (such as nausea and vomiting) and allergic reactions are often associated with SSZ treatment in patients, due to the intolerance to SSZ's metabolite SP [327, 328]. 5-ASA is better tolerated with minimal side effects, and thus it would be a better drug than SSZ to treat UC. However, when 5-ASA is administrated orally, it is greatly absorbed in the small intestine, leading to little therapeutic effect in the colon [326]. Thus, people developed others forms of oral 5-ASA prodrugs and delayed-release formulations besides SSZ, and have used them as conventional UC treatments for years [326, 329-333].

Clinically, patients receive a regimen of SSZ at a dose of 4-6 g per day, or 5-ASA at a dose of 2-4.8 g per day [331-336]. SSZ and 5-ASA can be administrated either orally or rectally. Sometimes patients receive combined treatment with both oral and rectal formulations [324, 337]. Rectal administration enhances the local effect, and the drug efficacy compared to oral formulations [65, 72, 337]. In addition, it provides faster responses with lower administration frequency and lower systemic absorption [324]. Most rectal formulations deliver 5-ASA, including suppositories, foams, gels, and enemas [71, 73, 338]. A few human studies reported the

use of SSZ in the form of enemas; these formulations eliminated the side effects associated with oral SSZ formulations [37, 38].

The retention time of drugs in the colon affects the efficacy of the rectal therapy approach [72, 324]. For example, suppositories, liquid enemas and foams are usually difficult to retain when frequently administrated at large volumes [338-340]. Mucoadhesive materials can adhere to the mucus layer by forming a number of interactions with mucin, such as electrostatic interactions, hydrogen bonds, hydrophobic interactions, covalent bonds, van de Waals bonds, or physical entanglement of polymeric chains [341]. Since the colon is covered by a mucosal layer, mucoadhesive drug delivery systems used in rectal delivery prolong the drug residence time in the colon and reduce the migration of the drug in the colon lumen, thus sustaining the release of the drug and enhancing its efficacy [24, 123]. Compared to the oral route, rectal mucoadhesive drug delivery systems improve drug absorption and bioavailability [68, 175, 177]. Despite these clear advantages, we found only two studies on mucoadhesive systems for application in UC treatment [342, 343].

Various functionalization methods can enhance the mucoadhesion of polymeric materials. One example is the addition of catechol groups, which are largely present in the sticky marine mussel foot proteins and are responsible for their strong underwater adhesion [186, 187]. Researchers have developed catechol-functionalized polymers showing improved mucoadhesion [34, 35]. Interactions between catechols and the mucin may involve the formation of both covalent and non-covalent bonds [29, 188, 344]. In our previous studies, we developed catechol-modified chitosan (Cat-CS) hydrogels as mucoadhesive drug delivery systems for oral and buccal drug delivery [299, 345]. The presence of catechols enhanced the mucoadhesion of the hydrogels on

the rabbit small intestine mucosa [299] and porcine buccal mucosa in vitro [345], and on the rabbit buccal mucosa in vivo [345].

In this study, we used the mucoadhesive Cat-CS hydrogel as a rectal drug delivery system for UC treatment. We prepared a Cat-CS mucoadhesive hydrogel crosslinked by a non-toxic naturally derived crosslinker, genipin (GP). We injected the SSZ-loaded Cat-CS hydrogel (SSZ/Cat-CS) rectally to treat mice in which UC was induced by dextran sulfate sodium (DSS) administration. This system showed a better therapeutic effect than the conventional oral formulation given by gavage. Specifically, a lower SSZ dose given rectally using the gel provided a similar histological score as a larger oral dose, and a significantly lower disease activity index involving the overall assessment of body weight recovery rate, colon length, and TNF-α level. Most importantly, SSZ/Cat-CS reduced the amount of the drug metabolite SP in the plasma, leading to fewer side effects compared to the conventional oral formulation. Overall these results show the great potential of SSZ/Cat-CS mucoadhesive rectal formulation in UC treatment.

5.3 Materials and methods

5.3.1 Materials

Materials used in this study include: chitosan (CS) with medium molecular weight (MW 190,000-310,000 Da) and 75-85% degree of deacetylation (Sigma-Aldrich, USA); hydrocaffeic acid (3-(3,4-Dihydroxyphenyl)propionic acid, 98+%) (Alfa Aesar, USA); the crosslinker genipin (GP) (≥ 98.0%) (Challenge Bioproducts, Taiwan); dextran sulfate sodium (DSS, MW 36000-50000 Da, MP Biochemicals) to induce UC in the mice; sulfasalazine (SSZ) (Sigma-Aldrich, USA) to treat the disease; N-(3-Dimethylaminopropyl)-N'-ethylcarbodiimide hydrochloride (EDC) (≥ 98.0%)

(Sigma-Aldrich, USA), and lysozyme (from human milk, ≥ 100,000 units/mg protein) (Sigma-Aldrich, USA). All other reagents were from Sigma-Aldrich (USA).

5.3.2 Synthesis of catechol-chitosan (Cat-CS)

We synthesized Cat-CS by a protocol modified from our previous study [345]. Briefly, we first dissolved 0.6 g of medium molecular weight CS in 60 ml of hydrochloric acid (HCl) with final pH adjusted to 2.5. We prepared 0.29 g of hydrocaffeic acid in 15 ml ethanol, and 0.712 g of EDC in 15 ml deionized (DI) water separately, followed by rapid mixing. We added the well-mixed solution to CS solution with constant stirring. We adjusted the final pH of the mixture to 5.5 by addition of 1M NaOH, and brought the reaction to completion under 12 h stirring. To purify Cat-CS, we transferred the mixture to a dialysis membrane tube (MWCO 5,000, Spectrum Laboratories, USA), and conducted the dialysis under 0.01 mM HCl solution (pH 5.0) for 3 days. We freeze-dried the dialysis product and stored it at -20°C. To determine the percentage of catechol content in Cat-CS, we dissolved Cat-CS in DI water under constant stirring, and measured the absorbance of the solution at 280 nm using a UV-Vis spectrometer (Carry 5000, USA) (Figure S5.1). Based on the standard curve of hydrocaffeic acid, we calculated the catechol content as 20%.

5.3.3 Preparation of injectable SSZ/Cat-CS hydrogel system

We homogenized 1% (w/v) solution of Cat-CS in DI water by intensive stirring. We added an ethanol-based GP solution (6 mg/ml) to the Cat-CS solution as a crosslinker, at a volume ratio of GP: Cat-CS = 1: 400. To remove large aggregates which may block the needle during injection, we sieved SSZ powders through a stainless steel screen with a pore size of 50 μm. Then, we homogenized the fine SSZ powders with the mixture of Cat-CS and GP at a concentration of 10 mg/ml by intensive stirring at room temperature for 10 minutes. We loaded this viscous

drug/polymer mixture inside 1 ml Tuberculin syringes (Becton, Dickinson and Company, USA), transferred them to a 37°C incubator, and kept them there for 12 h, which allowed gelation of Cat-CS inside the syringes.

5.3.4 Physical characterization of SSZ/Cat-CS hydrogel system

We removed the syringes from the incubator after 12 h gelation. We conducted two physical characterizations: 1) injection force measurement, and 2) rheological tests of injected hydrogels.

For the injection force measurement, we loaded 0.5 ml as an initial volume of hydrogel in each syringe. Before the test, we mounted the syringe vertically on a BOSE 3220 Pulse System equipped with a load cell (load range ± 200N) pushing on the plunger (Figure S5.2). We applied a pre-load of ~ 0.1 N at the beginning of the injection. The instrument could lower the load cell to push the plunger and measure the force recorded by the load cell. We first did a sequence of 3 injections, during which the load cell pushed the plunger for 4 mm at a rate of 0.8 mm/s, with a pause of 10 seconds in between injections. Due to the limitation of moving distance of the load cell (max 12 mm), we re-located the load cell to its original position, and performed another series of 3 injections with the same syringe. For the control group, we prepared syringes loaded with Cat-CS hydrogels but without SSZ, and evaluated their injectability using the same protocol. We performed 3 repeated measurements for each group.

We collected the injected SSZ/Cat-CS hydrogels for rheology tests to understand their viscoelastic behaviors. We used an Anton Paar MCR 301 Rheometer (Austria) equipped with a cone steel geometry (d = 25mm, angle = 1°) for oscillatory stress sweep tests with constant frequency (f = 1Hz). The instrument recorded the evolution of storage modulus G' as a function of oscillatory stress at room temperature. We used the injected Cat-CS hydrogels without SSZ as control. We performed 3 repeated measurements for each group.

5.3.5 Animals

We obtained 21 C57BL/6 male, littermate mice from a specific pathogen-free breeding colony at the Research Institute of the McGill University Health Centre (RI-MUHC). We housed these mice in conventional care facility for 3 weeks to allow them to acquire the local bacterial flora prior to the experiment. All procedures followed the protocol approved by the McGill University Animal Care Committee (UACC).

5.3.6 In vivo experiment

5.3.6.1 Experimental design and grouping

The total length of the in vivo experiment was 10 days. Day 1 to 5 was the disease development period, and Day 6 to Day 10 was the treatment period. On Day 11, we sacrificed the animals following the UACC-approved procedures to harvest the samples. Figure 5.2 shows the schematic and the timeline of our experiment.

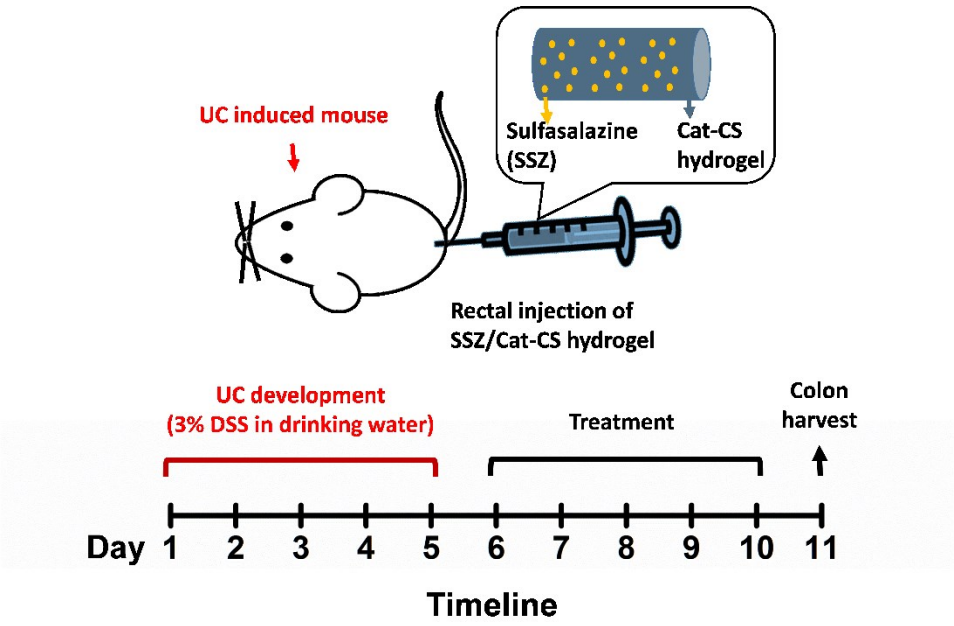

Figure 5.2. Schematic and timeline of the experiment.

We divided the mice into 5 groups. Group 1 was the healthy control group, and mice in this group had access to normal food and water without any treatment. Groups 2-5 were UC groups induced by DSS (procedures described in the following section). Group 2 was the negative control group, and mice received no treatment. Group 3 received 1.5 mg SSZ by oral gavage once daily, which was equivalent to the normal oral dose used in UC patients. Group 4 received rectal injection of 75 μl Cat-CS hydrogel alone, not loaded with SSZ, twice per day. Group 5 received the same volume of SSZ/Cat-CS hydrogel by rectal injection twice per day. Since each injection contained 0.75 mg of SSZ, the total SSZ dose delivered per day to this group equaled the dose given orally to Group 3. The description and number of mice in each group are summarized in Table 5.1.

Table 5.1. Summary of the experimental groups.

Group	Name	DSS	Treatment (Day6-10)	# of mice
1	Healthy control	No	No	4
2	No treatment	Yes	No	5
3	SSZ 1.5 mg oral	Yes	1.5 mg SSZ, oral gavage, once per day	4
4	Cat-CS rectal	Yes	Cat-CS hydrogel alone without SSZ, rectal injection, twice per day	3
5	SSZ/Cat-CS rectal	Yes	SSZ loaded in Cat-CS hydrogel, rectal injection, twice per day	5

5.3.6.2 Induction of UC by DSS

DSS is often used to induce UC in mice to mimic the pathology of the disease [346]. We used the procedure of UC induction by DSS modified from a previous study [347].We grouped and housed the animals in the animal facility for 3 weeks for them to acquire the local bacterial flora prior to DSS treatment. From Day 1 to 5, we added 3% (w/v) DSS to drinking water given to the mice in

Group 2-5. This allowed the disease to develop in the colon. We renewed the DSS water bag of each cage daily.

5.3.6.3 Rectal drug delivery

The DSS treatment was stopped on Day 5, and mice began to receive regular water and the treatment on Day 6. We treated Group 5 with SSZ/Cat-CS gel (10 mg/ml) via rectal injection twice per day. Every time before administering a hydrogel dose, we anesthetized the mice by subcutaneous injection of 0.1 ml of a drug mixture containing ketamine 20 mg/ml and xylazine 5mg/ml. Then, we inserted a gavage needle (26 gauge, with beaded tip) connected to the hydrogel-loaded syringe through rectum for ~2.5 cm. We injected 75 µl of SSZ/Cat-CS gel slowly (at a rate of ~0.8 mm/s), then inserted a cylinder-shaped glycerin plug (d ≈ 2mm, length ≈ 5 mm) to secure the retention of the hydrogel at early stages.

5.3.7 Body weight monitoring and fecal occult blood assessment

We monitored the body weights of all mice daily in the morning. We calculated the weight loss (%) as the percentage of original body weight before DSS induction. We also qualitatively conducted fecal occult blood assessment using a Hemoccult kit.

5.3.8 Quantification of rectal dose

In our preliminary study, we observed that the injected SSZ/Cat-CS hydrogels were expelled by the mice after a few hours. The expelled hydrogels were compressed and dehydrated due to the water absorption mechanism of colon [348], and looked like thin threads containing unabsorbed SSZ (Figure S5.3). To quantify the drug dose delivered in the colon, we collected feces containing visible expelled hydrogels. We immersed each individually expelled hydrogel in 2 ml of lysozyme solution (5 mg/ml) and stirred for 3 days, allowing Cat-CS to be completely degraded and expose

the undelivered SSZ in the hydrogel structure. Then, we added 1 ml of 1M NaOH to solubilize the SSZ particles, which turned the solution to an orange color. We measured the absorbance of the solution at 458 nm using a UV-vis spectrometer (Cary 5000, USA). We calculated the drug content by comparing these results with a pre-established standard curve of SSZ.

5.3.9 Blood sample collection

We collected the plasma from all the sacrificed mice on Day 11 to measure the levels of SSZ and its metabolites 5-ASA and SP. We collected approximately 1 ml of blood from each mouse via cardiac puncture into an anti-coagulation tube, followed by centrifuging at 10000 rpm for 15 min. Then, we transferred the clarified plasma to a new tube and stored the samples at -80°C for HPLC-MS analysis.

5.3.10 Colon length measurement

We dissected the colon (from the start of cecum till the end of rectum) of each mouse and cleaned the tissue by phosphate buffer saline (PBS) with care. We carefully removed the fecal content inside the colon. Then, we aligned the cleaned and straightened colons on a piece of wet filter paper to measure the length of each colon (from the beginning of colon till the end of rectum).

5.3.11 Histology

We removed the distal part of each of the colon samples (1 cm in total) and fixed the tissue in buffered formalin. We made two 5 μm-thick sections on each colon sample: one is in the middle of each sample, i.e., 0.5 cm from the end of the rectum; the other one is the top of the each colon sample, i.e., 1 cm from the end of the rectum. We named these two sections as “distal” and “proximal” respectively. The slides were stained with hematoxylin and eosin (H&E).

We examined the stained slides using a Leica microscope at magnification of 50x and images of the colon cross sections taken using the Bioquant Nova Prime software. Since the shapes of the colon cross sections were close to elliptical, we measured the largest distance d_L and the smallest distance d_w across the ellipse. We compared the sum of these two distances of each group. In addition, we also measured the thickness of the colon wall containing the submucosa and muscle layers.

5.3.12 Tumor necrosis factor alpha (TNF-α) ELISA assay

We immersed the remaining tissue in each harvested colon sample in 1 ml of PBS, and homogenized the tissue on ice using a Polytron homogenizer at 3000 rpm for 1 min. We transferred the homogenate to an Eppendorf tube, followed by centrifugation at 10000 rpm for 15 min. Then, we transferred the supernatant to a new tube and stored the samples at -80°C for TNF-α ELISA assay. We performed the TNF-α ELISA using anti-mouse TNF- α paired antibody set (R&D Systems Inc.) using a standard sandwich ELISA protocol.

5.3.13 Histological score and disease activity index assessment

We developed two grading systems to evaluate the therapeutic efficacy of our treatments: the histological score system and the disease activity index system. The detailed grading criteria are shown in Table 5.2 and Table 5.3.

We scored the histology based on four parameters analyzed from the distal H&E microscopy images: crypt damage, neutrophil infiltration, colon wall enlargement ($d_L + d_w$), and colon wall thickening. The final histological score refers to the sum of the grades of these four parameters. Since we did not perform H&E staining on all individual mice in each group, the

histological score of a specific group represents the average of the scores of all the stained slides in that group. A higher histology score means a more severe tissue damage.

We scored the disease activity index based on three parameters: body weight recovery rate, colon length, and TNF-α level. The final disease activity index score refers to the sum of the grades of these three parameters. To calculate the disease activity index, we averaged the scores of all the mice in a specific group. Higher score indicates a more serious disease condition, while lower score indicates a healthier condition.

5.3.14 Cumulative plasma concentrations of SSZ and its metabolites

After the frozen plasma samples were thawed at room temperature, we mixed 40 µl of sample with 100 µl of 0.5 µM atenolol (internal standard, solution made from acetonitrile/methanol at volume ratio of 40/60) in an Eppendorf tube. We intensively vortexed the mixture, and then centrifuged it at 13000 rpm for 5 min. We diluted 25 µl of the supernatant with 50 µl of water containing 0.1% formic acid for the analysis of SSZ and SP. We transferred another 25 µl of supernatant to 50 µl of water containing 0.5% formic acid for the analysis of 5-ASA. We used an Agilent 1100 series HPLC LC/MS/MS AB/SCIEX 4000 QTRAP system. For SSZ and SP analysis, we used a Luna C8 column (30 × 2 mm, size 5 µm). For 5-ASA analysis, we used a Betasil Silica column (50 × 3 mm, size 5 µm). The mobile phase was acetonitrile with 0.1 formic acid. We injected 3 µl of sample into the column at a flow rate of 0.7 ml/min for SSZ and SP, and 0.85 ml/min for 5-ASA. We analyzed the area under the curve of each peak, and calculated the concentration of the chemicals based on the previously developed standard curve.

Table 5.2. Grading criteria to determine histological score.

Parameter	Grade	Description
Crypt damage	0	None
	1	Loss < 1/3
	2	Loss 1/3 – 2/3
	3	Loss > 2/3
Neutrophil infiltration	0	None
	1	Superficial
	2	Involving submucosa
	3	Involving muscle layer
Colon wall enlargement ($d_L + d_w$)	0	< 6 mm
	1	6 – 7 mm
	2	7 – 8 mm
	3	> 8 mm
Colon wall thickness	0	< 0.2 mm
	1	0.2 – 0.4 mm
	2	0.4 – 0.6 mm
	3	> 0.6 mm

Table 5.3. Grading criteria to determine disease activity index.

Parameter	Grade	Description
Body weight recovery rate	0	> 2% per day
	1	1 – 2 % per day
	2	0 – 1 % per day
	3	Negative recovery rate
Colon length (compared to the average of the healthy group)	0	Same or longer
	1	Up to 8 mm shorter
	2	8 – 16 mm shorter
	3	> 16 mm shorter
TNF-α level	0	< 150 pg/ml
	1	150 – 200 pg/ml
	2	200 – 250 pg/ml
	3	> 250 pg/ml

5.3.15 Statistical analysis

We performed statistical analysis for the injection force measurement using an unpaired t-Test. All other tests used ordinary one-way ANOVA with multiple comparisons (GraphPad Prism 6). Error bars in the figures represented the standard error of the mean (SEM), except for the standard deviation (SD) in Figure 5.5, as indicated in the graph caption. We considered a value of $p \leq 0.05$ as significant in all tests.

5.4 Results

5.4.1 Physical characterization of the SSZ/Cat-CS hydrogel system

The SSZ/Cat-CS hydrogel was formed in a syringe after 12 h at 37 °C. After gelation, the hydrogel turned to green due to the crosslinking by GP. Fine SSZ powders were distributed in the 3D hydrogel network homogeneously. We evaluated the injection force required to push the syringe plunger using an injection force measurement apparatus (Figure S5.2). Figure S5.5 shows the force-displacement curves measured during a continuous sequence of 3 injections of the Cat-CS gel both with and without SSZ. When the injection of SSZ/Cat-CS started, there was a sharp increase in the force required to push the plunger, followed by a gradual increase until equilibrium was reached. For the Cat-CS gel without SSZ, instead, the force measured went back to equilibrium rapidly after injection, and stayed at this level until the load cell stopped pushing. The injection force, defined as the max load during the injection [349, 350], was analyzed through multiple replicates. The average injection force of SSZ/Cat-CS gel was 2.76 ± 0.05 N (mean ± SEM, n=16), which was almost half of the value measured for Cat-CS gel without SSZ (4.44 ± 0.22 N, mean ± SEM, n=12) (Figure 5.3a).

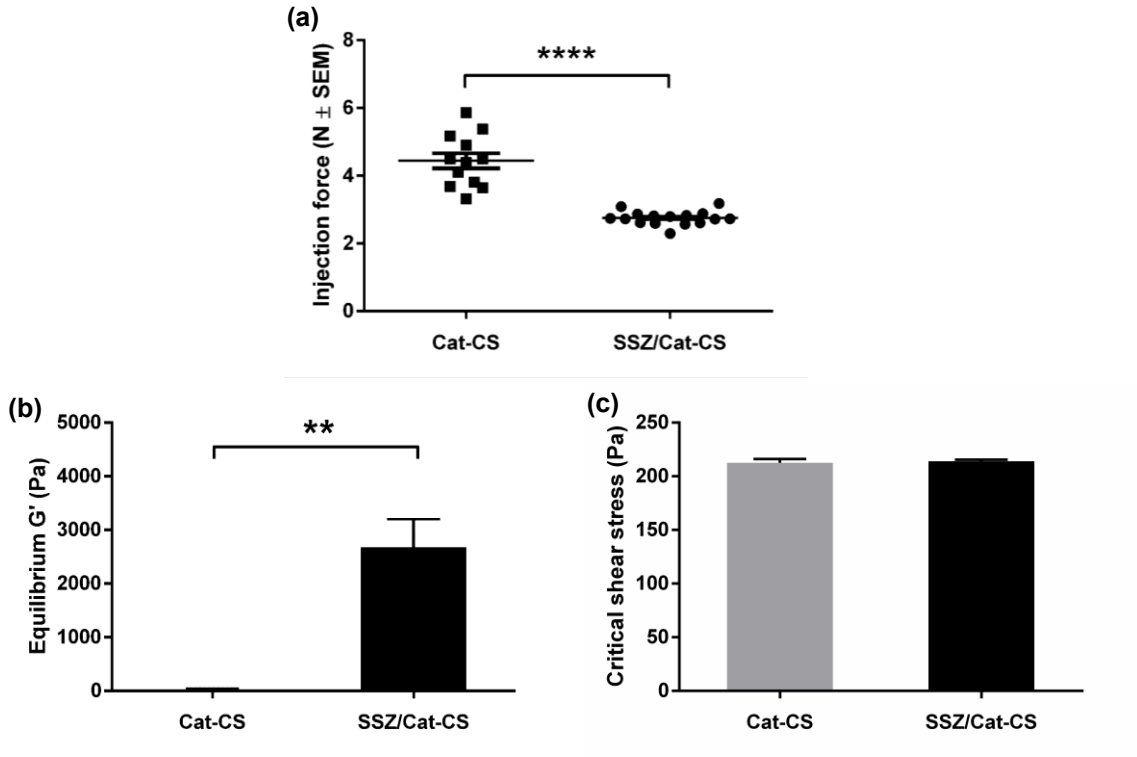

Figure 5.3. Physical characterization of the Cat-CS and SSZ/Cat-CS hydrogel systems: (a) the average injection force; (b) average equilibrium G' during the oscillatory stress sweep tests; and (c) critical shear stress. For all oscillatory stress sweep, f = 1 Hz. ** and **** represent $p < 0.01$ and $p < 0.0001$ respectively. Error bars represent SEM.

We performed a stress sweep rheological test on the crosslinked hydrogel after passing through the needle. The equilibrium G' of both systems remained constant within the linear viscoelastic regime (LVR) (Figure S5.6). However, with increasing oscillatory stress, the hydrogel network started breaking down. When the stress exceeded the LVR, we observed a sudden drop in G' (Figure S5.6); this point was defined as the critical shear stress. The SSZ-loaded hydrogel showed much higher equilibrium G' than the Cat-CS gel without SSZ (Figure 5.3b). Both systems showed critical shear stresses of around 200 Pa with no significant differences, which implies that the addition of SSZ did not significantly alter the gel strength.

5.4.2 Quantification of rectal dose

After collecting a total of 15 fecal pellets, we measured an average delivered dose of 51.1% ± 4.0% (mean ± SEM, n=15) of the normal SSZ oral dose (Figure S5.4). This result indicates that about half of the SSZ dose loaded in the rectal hydrogel retained in the colon, while the other half was expelled. The effectiveness of the rectal formulation on UC thus correlates with this delivered dose.

5.4.3 Body weight and fecal occult blood

Body weight loss is a key indicator of colitis development in DSS treated mice [346]. Weight loss often starts on Day 3 of the DSS induction, and reaches a maximum by Day 7 [346]. Indeed, we observed a clear weight loss of the mice in the DSS treated groups starting from Day 3 (Figure S5.7). After 5 days of DSS induction, the mice lost about 15% of their original weight. Beginning on Day 6, the mice started receiving different treatments. The weight kept decreasing for an additional 1-2 days, even after DSS administration was stopped on Day 6. From Day 8 to Day 10, all groups showed an increase in body weight, including the mice in the group that received no treatment. This indicates that the mice were able to self-heal from this specific disease symptom after stopping DSS administration.

We compared the body weight recovery rate of each group. We performed a 3-point linear regression on weight loss percentages of Day 8, 9, and 10. The weight recovery rates of the SSZ 1.5 mg oral group and the SSZ/Cat-CS gel group were close and much higher than the other three groups (Table 5.4). Thus, the mice that recovered their weight fastest were those that received an oral dose of 1.5 mg SSZ and those that were treated with the drug loaded in the Cat-CS gel.

Table 5.4. Summary of the 3-point linear regression based on individual weight loss percentages of Day 8, 9 and 10.

Groups	Slope (weight increase rate, % per day)	R^2
No treatment	0.61	0.99
SSZ 1.5 mg oral	1.77	0.84
Cat-CS rectal	0.12	0.7
SSZ/Cat-CS rectal	1.57	0.99

Another common symptom associated with UC is the presence of loose and bloody stool. We assessed fecal occult blood qualitatively using a Hemoccult kit. We observed rectal redness on all DSS-treated mice after 5 days. All mice had loose stool with visible rectal blooding. After 2 days of treatment (Day 8), the bloody stool symptom in groups treated with SSZ 1.5 mg oral, and SSZ/Cat-CS rectal hydrogel was greatly improved. We did not detect occult blood from the stools in these groups. In comparison, the no-treatment group continued to have black stool containing occult blood without much improvement till the end of the experiment.

5.4.4 Colon length

In DSS-induced UC mice, the colon usually shortens compared to healthy animals [347]. Colon length shortening is an indicator of colitis development and disease severity [351, 352]. We dissected the entire large intestines on Day 11, and compared the colon lengths of all groups.

Figure 5.4a presents the colons after removal of fecal content. The cecums (above the red line) of the healthy control group were clearly larger than all other groups, thus confirming a previous study showing that DSS can cause colitis in the cecum and the upper colon [353]. The reduced size of the cecum for DSS-treated mice might be related to inflammation developed in this region.

We measured the colon length from the end of the cecum (red line in Figure 5.4a) to the end of the rectum. Figure 5.4b shows the colon length results of all groups. The healthy control group had the highest average colon length (87 mm ± 1 mm, mean ± SEM, n=4), which was

significantly higher than the length of the group that received no treatment (73 mm ± 1 mm, mean ± SEM, n=5). This result confirmed our expectation that untreated UC would cause colon shorthening. The average colon length of the SSZ 1.5 mg oral group was 81 mm ± 4 mm (mean ± SEM, n=4). This value is higher than the average colon length of the no treatment group; however, it is not statistically significant. In fact, even the group treated with the empty Cat-CS hydrogel showed a higher, but not statistically significant, colon length than the no-treatment group.

The group treated with the SSZ/Cat-CS hydrogel had an average colon length of 84 mm ± 2 mm (mean ± SEM, n=5), which was significantly higher than that of the group that received no treatment. This result indicates that rectal SSZ/Cat-CS hydrogel treatment helped recover the colon length from the damage of UC. In addition, this value was also higher than SSZ 1.5 mg oral group and Cat-CS rectal group, although not statistically significant. Thus, the therapeutic effect of SSZ related to preventing shortening of the colon was more pronounced when the drug was delivered rectally in our SSZ/Cat-CS hydrogel than when it was delivered orally.

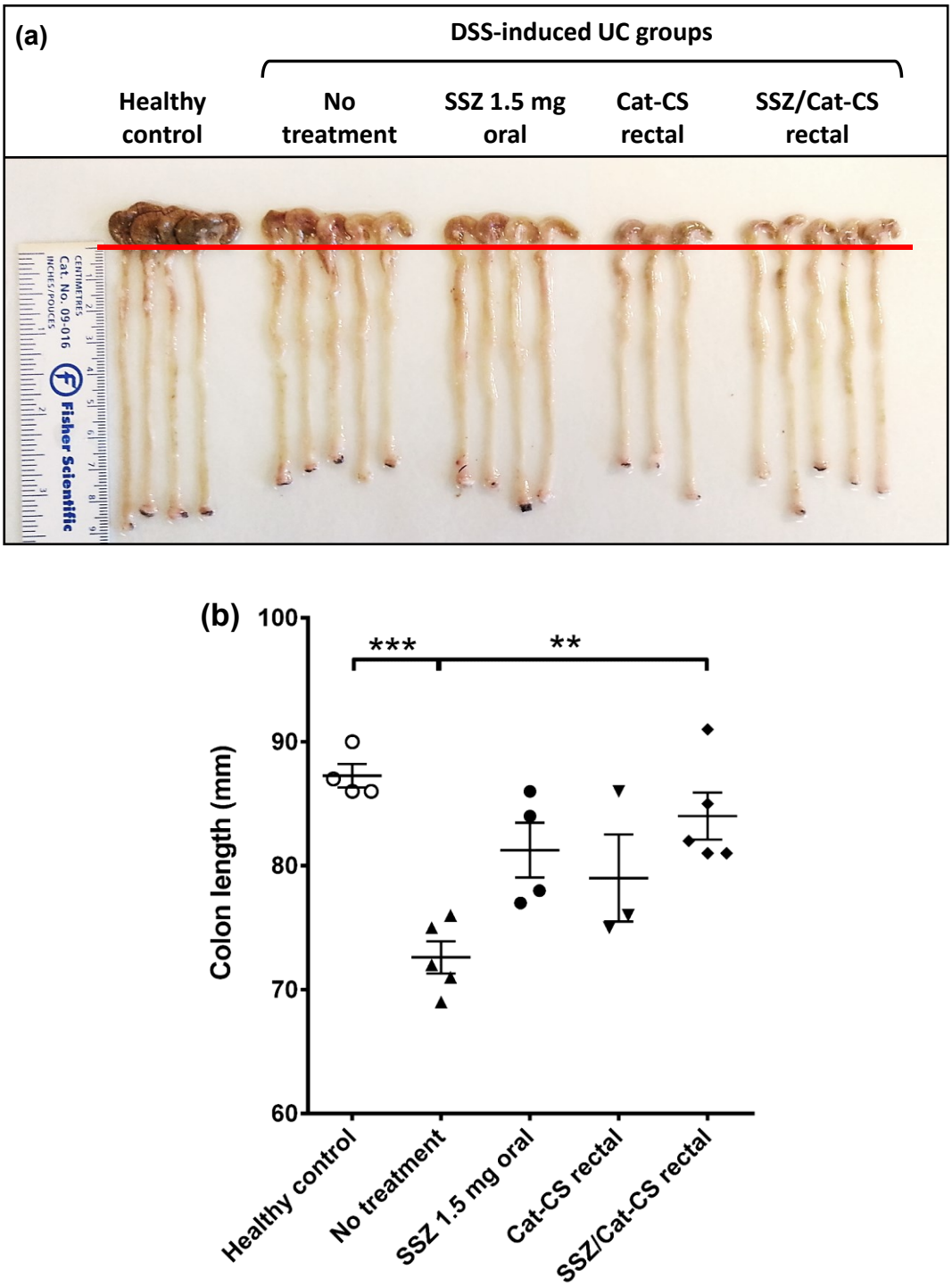

Figure 5.4. Colon length measurements: (a) harvested colon tissues of each group on Day 11 (cecums are above the red line); (b) colon length comparison. Error bars represent SEM. ** and *** represent $p < 0.01$ and $p < 0.001$, respectively.

5.4.5 Histology

Figure 5.5a shows the H&E stained colon sections of all groups harvested on Day 11. We acquired the images of both distal sections (0.5 cm to the end of the rectum) and proximal sections (1 cm to the end of the rectum). Compared to the healthy control group, all the DSS treated mice showed crypt damage and epithelial erosion, due to the induction of UC. In addition, we observed inflammatory cells in all the DSS treated mice. The distal sections showed more severe tissue damage than the proximal sections, in terms of their high loss of the epithelium. This result is expected, since DSS, with a molecular weight of around 40 kDa, induces more severe colitis in the middle and distal third of the colon [353]. We also observed the presence of lymphocytes in some sections (see red arrows in Figure 5.5a).

The no-treatment group showed the most severe tissue damage among all the DSS treated mice. Nearly half of the epithelium was completely lost in the distal section, and the epithelial surface showed intensive ulceration. We found a high level of inflammatory neutrophil infiltration in the lamina propria, which further extended to the mucosa and submucosa (see black arrows in Figure 5.5a). The SSZ 1.5 mg oral group showed less inflammatory infiltration, although we observed a few lymphocytes, such as those shown in the image presented in Figure 5.5a. About half of the crypts were damaged. The SSZ/Cat-CS rectal group showed less severe tissue damage. Neutrophil infiltration in the mucosal and submucosal area was less extensive compared to the no-treatment group.

Severe UC in the colon is often associated with tissue enlargement and thickening [354]. We summed the largest distance (d_L) and the shortest distance (d_W) across the elliptical colon sections (Figures 5.5b and 5.5c) and used this value to evaluate the enlargement of the colon tissue after UC induction and the treatment. For the distal colon sections, d_L+d_w of the no-treatment group

was significantly higher than in all of the treated groups, as well as the healthy control group (Figure 5.5b). This is obvious also just from Figure 5.5a, where the no-treatment group showed a much thicker distal colon section than all other groups. This result indicates that the UC caused a serious enlargement in the distal colon tissue of the mice that received no treatment. In contrast, SSZ 1.5 mg oral, Cat-CS rectal and SSZ/Cat-CS rectal groups did not show an obvious enlargement effect in the distal colon, since they had similar d_L+d_w values as the healthy group. For the proximal colon sections, similarly, the no-treatment group showed significantly higher d_L+d_w value than the SSZ 1.5 mg oral and Cat-CS rectal groups. The proximal colon d_L+d_w value for the SSZ 1.5 mg oral was lower than the SSZ/Cat-CS rectal. This result seems to indicate that oral formulation might have somewhat better therapeutic effects at the proximal colon region compared to the rectal formulation.

We evaluated the thickening of the colon wall by measuring the total thickness of the submucosa and muscle layers. In the no-treatment group, the thickening of the distal colon submucosal membrane and muscle layers was much higher than all the other groups (Figure 5.5d). However, after the treatment, there were no significant differences in this parameter compared to the healthy group, except for the group treated with Cat-CS hydrogel alone, which was the only one showing somewhat thicker walls of the distal colon. For the proximal colon sections, we could not detect significant differences in the thicknesses of the colon walls in any of the groups, with the notable exception of the group treated with SSZ/Cat-CS hydrogel, which showed thinner walls than the no-treatment group.

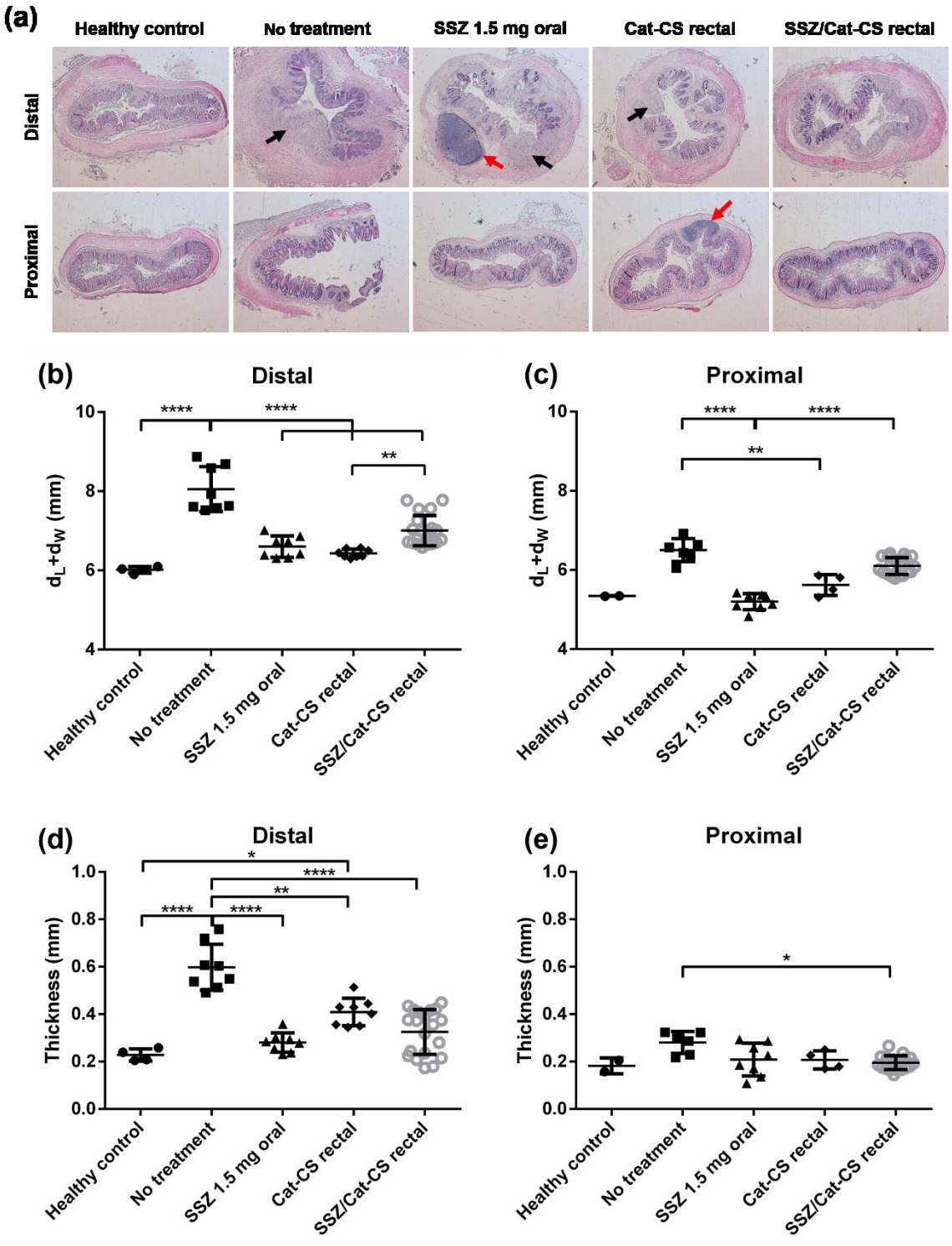

Figure 5.5. Histological assessment of the colon tissue: (a) H&E staining of the distal (0.5 cm toward the end of the rectum) and proximal (1 cm toward the end of the rectum) colon sections after Day 10; red arrows represent lymphocytes, black arrows represent the inflammatory neutrophil infiltration; (b) d_L+d_w values of the distal colon sections; (c) d_L+d_w values of the

proximal colon sections; (d) the thickness of the distal colon wall containing the submucosal and muscle layer; (e) the thickness of the proximal colon wall containing the submucosal and muscle layer. Error bars represent SD. *, **, and **** represent $p < 0.05$, $p < 0.01$, and $p < 0.0001$, respectively.

5.4.6 TNF-α assay

TNF-α is a cytokine involved in systemic inflammation. The expression of the TNF- α increases in DSS induced UC mice [346]. Thus, the TNF- α level is an indicator of the severity of the disease. Figure 5.6 shows the average levels of TNF-α of all groups. The average levels of TNF-α of all groups were in the range of 100-300 pg/ml. The healthy group had the lowest average TNF-α level, as expected. The only group that showed a significantly lower level of TNF-α than the non-treated group, along with the healthy group, was the group treated with SSZ/Cat-CS. This result indicates that this treatment was the most effective at reducing local inflammation. Contrary to expectations, only the group treated with SSZ 1.5 mg administrated by oral gavage showed a significantly higher average TNF- α level. This result seems to indicate that although the oral SSZ 1.5 mg dose was effective at restoring colon length and colon wall thickness, it was not able to decrease local inflammation.

5.4.7 Histological score and disease activity index assessment

Taking into consideration all the parameters we previously evaluated, we conducted an overall assessment of the therapeutic effects of the treatments by calculating a histological score and a disease activity index. The histological score assessed the tissue damage and recovery condition in all groups based on the histological H&E images. The healthy group showed a significantly lower histological score than all the UC-induced groups (Figure 5.7a), thus setting a baseline for our comparison. The no-treatment group showed a significantly higher histological score than all

of the treated groups (Figure 5.7a). This result indicates that both the oral and rectal SSZ formulation and also the empty Cat-CS hydrogel injected rectally helped the recovery of the colon tissue in the UC-induced mice. The scores achieved in these three groups were not statistically significantly different.

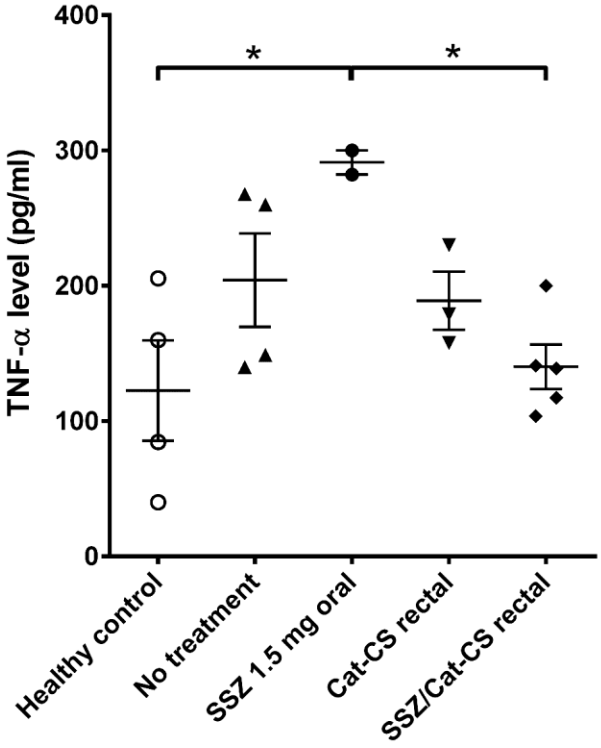

Figure 5.6. TNF- α level in the colon tissue homogenates. Error bars represent SEM. * represents $p < 0.05$.

The disease activity index assessed the general degree of disease development and recovery. The healthy control group showed a significantly lower disease activity index compared to all other groups except for the SSZ/Cat-CS rectal group, with which there were no significant differences (Figure 5.7b). This result clearly shows that the SSZ/Cat-CS rectal treatment was the most effective at lowering the disease activity index, thus showing an excellent therapeutic effect in UC-induced mice.

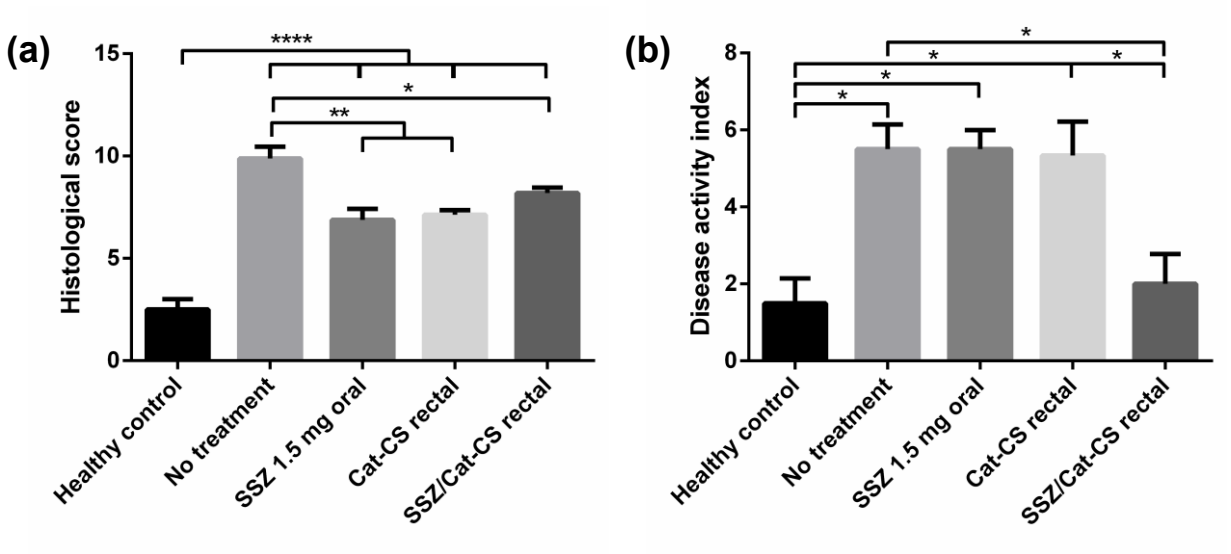

Figure 5.7. Histological score (a) and disease activity index (b).

5.4.8 Cumulative plasma concentrations of SSZ and its metabolites

We quantified the plasma concentrations of SSZ and its two metabolites, SP and 5-ASA. The plasma samples were collected on Day 11, thus these results represent the cumulative amount of these compounds present in the mice blood. Figure 5.8 shows the summary of the plasma concentrations of SSZ, SP and 5-ASA in the treated groups.

In the SSZ 1.5 mg oral group, the level of SSZ in plasma was close to zero (i.e., reached the detection limit of the instrument). We measured a higher level of SSZ in the SSZ/Cat-CS rectal group. Although the difference between the groups was not statistically significant, the trend indicates that rectal delivery of SSZ using the SSZ/Cat-CS hydrogels may help SSZ absorption through the colon.

The average concentration of SP for the SSZ 1.5 mg oral group was higher than that for the SSZ/Cat-CS rectal group (statistically significant at $p=0.067$), which indicates that the rectal SSZ/Cat-CS gel treatment reduced the presence of the undesirable SP metabolite in plasma.

The concentration of 5-ASA for the SSZ 1.5 mg oral group was significantly higher than the SSZ/Cat-CS rectal group. This indicates that more 5-ASA was absorbed in the GI tract for the SSZ 1.5 mg oral group. The low presence of 5-ASA in the serum of the mice treated with the SSZ/Cat-CS gel is in agreement with previous findings showing that 5-ASA is barely absorbed in the colon, partially due to the low permeability of hydrophilic molecules through the lipid membranes of the colon mucosa [326, 355].

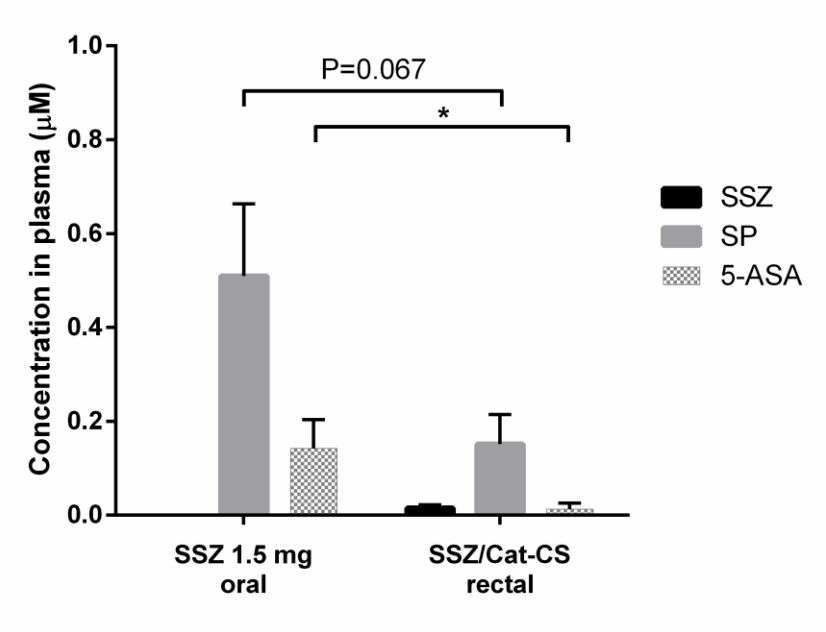

Figure 5.8. Cumulative plasma concentrations of SSZ, SP and 5-ASA in SSZ 1.5 mg oral and SSZ/Cat-CS rectal groups. Error bars represent SEM. * represents $p < 0.05$.

5.5 Discussion

We developed an SSZ-loaded, catechol-modified CS hydrogel (SSZ/Cat-CS) as a rectal formulation to treat UC. The presence of SSZ particles did not hinder gel injectability (Figure 5.3a), and actually decreased the force necessary to perform the injections compared to unloaded Cat-CS

gels. Probably, the presence of solid SSZ particles destroyed the overall hydrogel integrity, and divided the hydrogel network into discrete micro gel clusters around the drug particles. In fact, such a structure may benefit our rectal formulation, since each SSZ particle is coated with the mucoadhesive hydrogel, and thus has more chance to stick to the colon mucosa.

To evaluate the efficacy of the proposed formulation compared to standard oral gavage, we first evaluated how much drug was effectively delivered rectally. We measured that only about 50% of the loaded SSZ in the rectal Cat-CS hydrogels was retained in the colon, and the rest was eliminated with the expelled hydrogels. This implies that the therapeutic effects observed with the rectal formulation are related to only about half of the dose delivered orally.

We then tested several parameters. Weight changes are an indication of disease development and recovery. In fact, all groups treated with DSS showed a drastic weight decrease during the administration of DSS (Figure S5.7). After stopping DSS administration and beginning the treatments, though, the mice that received no treatment showed an overall higher relative body weight compared to all the mice that received treatments. This result shows that the manipulations that the treated mice had to withstand in order to receive the treatment (gavage, rectal hydrogel insertion), affected their body weight recovery, leading to an overall larger weight loss than the mice that received no treatment. This is why we decided to assess the body weight recovery rate based on the last three days of the experiment, rather than the absolute weight change. The SSZ 1.5 mg oral group and the SSZ/Cat-CS rectal group showed the fastest body weight recovery rates.

A better indication of disease recovery is the colon length. We measured a significantly shorter colon length for the group that received no treatment compared to the healthy group. Among the three treated groups, only the group treated with our rectal SSZ/Cat-CS gel showed a

significantly higher colon length than the no-treatment group. Thus, the positive therapeutic effect of SSZ/Cat-CS was very obvious for what concerned this parameter.

In the histological assessment, we noted that even without SSZ, the Cat-CS rectal hydrogel alone contributed to the healing of the disease to some extent. This result may be related to the fact that catechols can donate electrons and be transformed into oxidized quinones in the presence of oxidizing agents [195]. UC is associated with an abnormally high level of reactive oxygen species (ROS) in the inflamed colon mucosa [270]. The rectal injection of Cat-CS hydrogel alone might have reduced the level of ROS locally in the inflamed tissue, due to the reduction induced by catechols. This effect would be somewhat similar to that of 5-ASA itself: 5-ASA too is a hydroxyl radical scavenger, and the decrease in oxidative stress induced by this action may contribute to its therapeutic effect against UC [356, 357]. Further investigation of the effect of Cat-CS in UC treatment is going to be necessary in order to confirm this hypothesis, for example by comparing with the effect of gels made of CS alone.

Another indication of the inflammation-reducing effect of Cat-CS is the level of TNF-α, which represents the degree of inflammation in the colon. The SSZ 1.5 mg oral group showed a significantly higher TNF-α level than the SSZ/Cat-CS rectal group and the healthy control group. Thus, the oral formulation did not show good anti-inflammatory effects in our study. The low level of TNF-α measured for the groups treated with Cat-CS hydrogels, and especially with the SSZ/Cat-CS hydrogel, may be explained by two factors: 1) the mucoadhesive Cat-CS rectal hydrogel improved SSZ efficacy, and 2) the Cat-CS hydrogel itself reduced the local inflammation in the colon. As we discussed in the previous section, the effect of Cat-CS hydrogels needs further investigation.

To evaluate the overall therapeutic effect of the treatments, we combined the histology results in a histological score, and all other parameters in a disease activity index. Low scores in both parameters indicated a better treatment. The SSZ/Cat-CS group clearly showed low scores in both grading systems. Based on the histological score assessment, all treatments (oral SSZ, SSZ/Cat-CS, and Cat-CS rectal) showed a clear improvement in tissue recovery compared to the no-treatment group. However, based on the disease activity index, only the treatment with SSZ/Cat-CS caused a significant improvement.

These results alone indicate the tremendous potential of the SSZ/Cat-CS rectal treatment for UC treatment. However, another set of findings from this study makes this formulation even more appealing: the cumulative plasma concentrations measured for SSZ and its metabolites.

We measured a notably high concentration of 5-ASA in the plasma of the mice treated with SSZ 1.5 orally (Figure 5.8). Theoretically, SSZ only releases 5-ASA in the colon; since 5-ASA is hydrophilic, it is not easily absorbed by the lipid membranes present in the colon mucosa [326, 355]. Thus, if 5-ASA was only present in the colon, its plasma concentration should be very low. Indeed, the 5-ASA plasma levels measured in the mice treated by SSZ/Cat-CS rectally were very low (Figure 5.8). Thus, the presence of 5-ASA in the plasma of the mice treated by SSZ orally has to be related to its absorption through the small intestine, which can be very high [326]. This result indicates that in the SSZ 1.5 mg oral group, SSZ released 5-ASA before reaching the colon. This is a clear shortcoming of the oral treatment, since the therapeutic effect of 5-ASA is attributed to its topical action on the colon mucosa, rather than systemic action [338, 343]. The early released 5-ASA absorbed in the blood did not contribute to its therapeutic effect, which may explain why the oral treatment gave an overall higher disease activity index than the rectal treatment. Also, this result is likely correlated to the level of TNF-α discussed in the previous section. The early release

of 5-ASA from the oral SSZ formulation reduced the anti-inflammatory efficacy of the drug in the colon, thus leading to a high TNF-α level for the SSZ 1.5 mg oral group.

The most exciting result in the cumulative plasma concentrations of SSZ and its metabolites was the reduced level of plasma SP measured in the SSZ/Cat-CS treatment group. SP is the molecule that has been linked to many of the side effects of SSZ in patients, especially when SP circulates within the blood stream [327, 328]. The presence of less SP in the plasma of the mice treated with the SSZ/Cat-CS hydrogel thus implies that this treatment is safer than orally delivered SSZ. In fact, this result is in accordance with some clinical results in UC patients: SSZ enemas treated patients showed no side effect, including the patients previously intolerant to oral SSZ [37, 38].

SSZ release from SSZ/Cat-CS hydrogels might correlate to multiple factors. The colon and cecum contain a large amount of microflora [358]. CS can be degraded in the colon, possibly due to the enzymes secreted by these bacteria [328, 358]. When we injected the SSZ/Cat-CS hydrogel into the mice rectally, the Cat-CS hydrogel might have degraded via a similar action in the colon, thus speeding up the drug release. In addition, the colon absorbed the water content from the hydrogel intensively, reducing the gels to thin threads (Figure S5.3). This action too may have helped SSZ release. Once exposed to the colon microorganism environment, SSZ further released 5-ASA, which performed its expected therapeutic action locally on the inflamed colon mucosa. Overall, thus, these results show that we the proposed rectal formulation is both more effective and safer than the standard oral formulation.

5.6 Conclusion

We presented an SSZ-loaded Cat-CS hydrogel as an injectable mucoadhesive formulation to treat UC. This new system showed better therapeutic effects in DSS induced UC mice than SSZ given by oral gavage, although the amount of drug actually delivered via the rectal formulation corresponded to only 50% of the dose administered orally. Most importantly, this approach reduced the risk of side effects associated with oral SSZ formulation, thus showing that SSZ-loaded Cat-CS hydrogels are not only more effective, but safer than oral delivery.

The tests were performed in mice, which caused additional challenges for the rectal formulation: the small colon size makes it easier for the gel to be detached during bowel movements; additionally, the mice may intentionally expel the injected hydrogels, thus reducing the retention time of the drug and its efficacy. It is difficult to control such factors in an animal model, and it is possible that even better therapeutic effects would be found in human trials.

This study was performed as a preliminary test on a limited number of animals. Adding more animals in each group may reduce some of the variability. In addition, adding more control groups (such as CS rectal hydrogels without catechol modification, and SSZ-loaded CS rectal hydrogels) will be necessary in further studies, in order to better understand the mechanism of action of the gel, such as its increased mucoadhesion and its efficacy in ROS reduction.

5.7 Acknowledgements

We acknowledge the support of the Canada Research Chair program, Canada Foundation for Innovation, and the Natural Sciences and Engineering Research Council of Canada. We also thank the Platform of Biopharmacy (Faculté de Pharmacie, Université de Montréal) for the help with the

HPLC LC/MS/MS analysis, and Ms. Fatemeh Zehtabi for the help with the injectability and rheological measurements.

5.8 Supplementary data

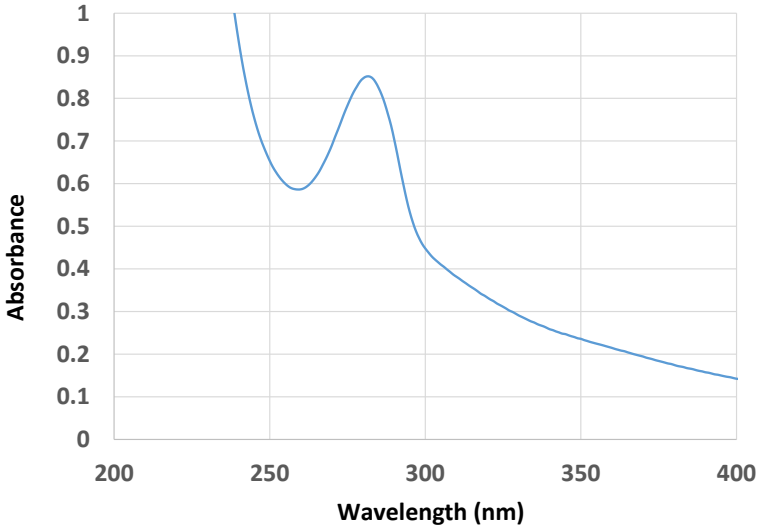

Figure S5.1. UV-vis spectrum of Cat-CS, 0.4 mg/ml in water.

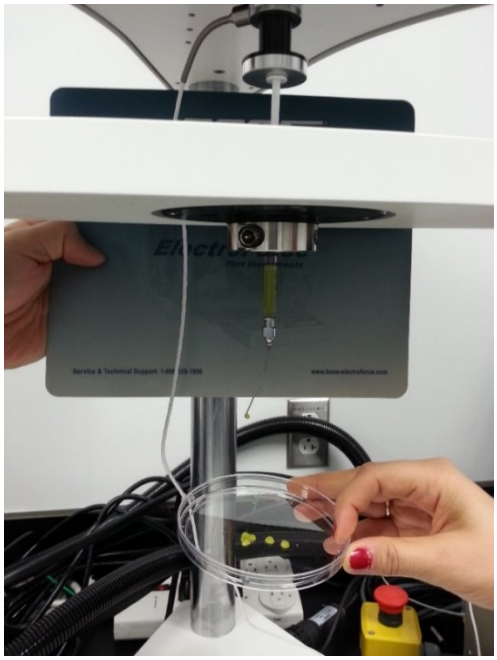

Figure S5.2. Apparatus used to measure injectability.

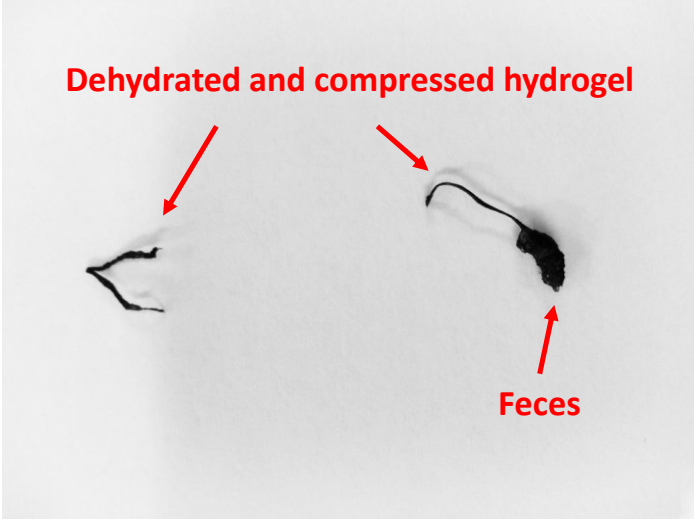

Figure S5.3. Expelled Cat-CS in fecal content.

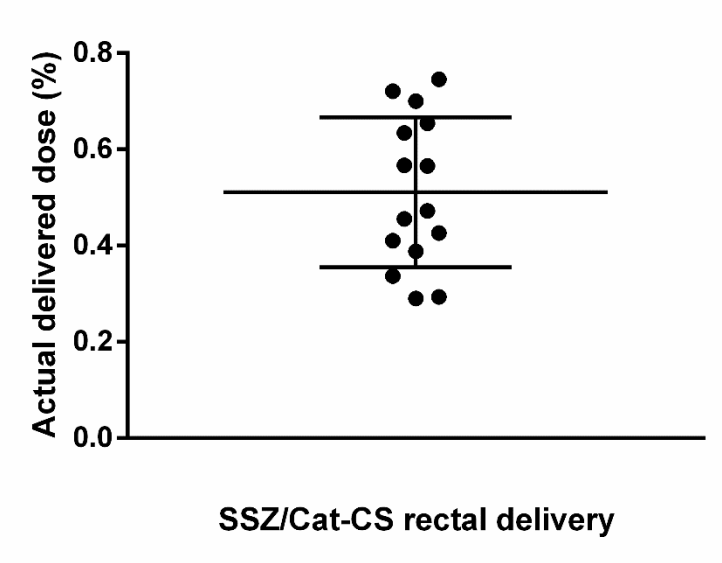

Figure S5.4. Actual delivered dose, percent of the normal SSZ oral dose.

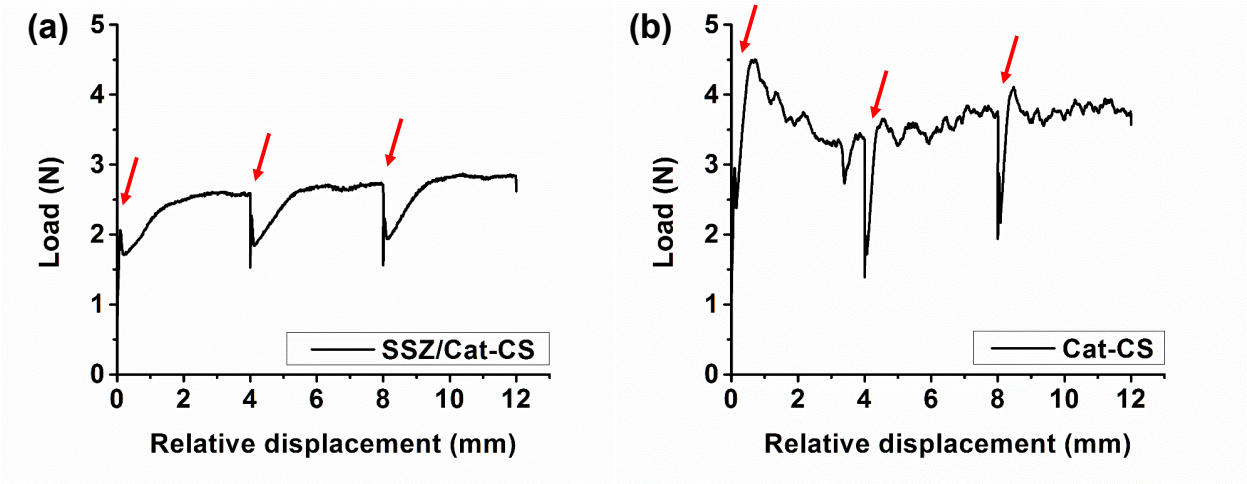

Figure S5.5. Injection force measurement: force-displacement curve showing the sequence of 3 injections of (a) SSZ/Cat-CS gel and (b) Cat-CS gel. Red arrows represent the beginning of each injection. Between each injection there was a 10 sec pause.

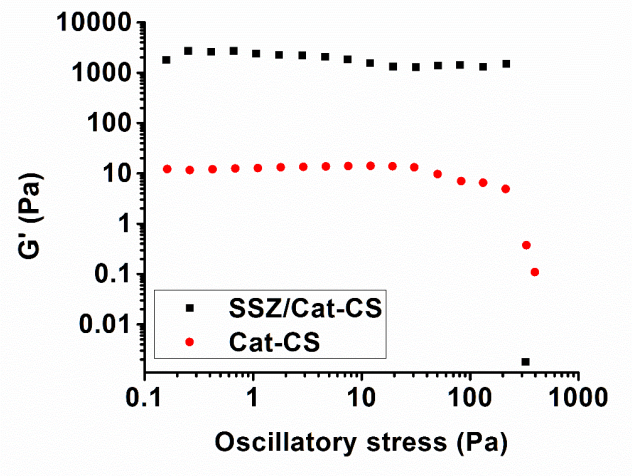

Figure S5.6. Evolution of G' with increasing oscillatory stress from 0.1 – 1000 Pa, for SSZ/Cat-CS gel (black squares) and Cat-CS gel without SSZ (red dots).

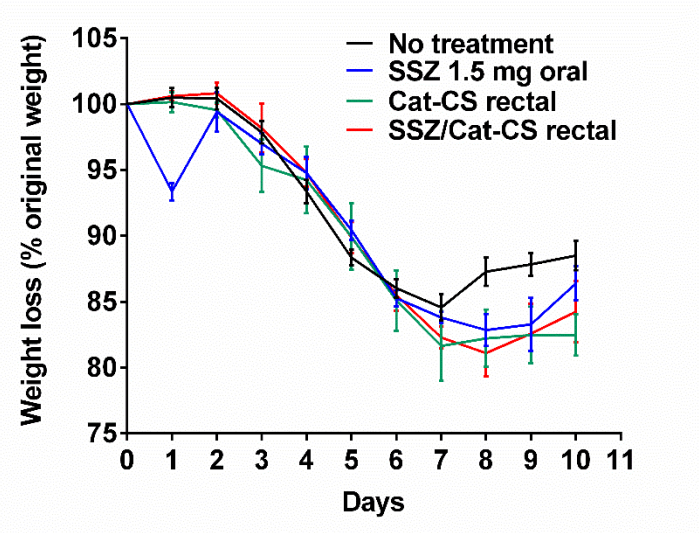

Figure S5.7. Weight loss calculated as percentage of original weight prior to DSS treatment. Error bars represent SEM. There are no statistically significant difference among the weight loss of different groups on each day.

CHAPTER 6. CONCLUSIONS AND PERSPECTIVES

6.1 Contributions to original knowledge

Inspired by marine mussel adhesion, we enhanced the mucoadhesion of CS hydrogels by the addition of catechol groups, and improved the drug efficacy and therapeutic effects using such systems in drug delivery. The mucoadhesive catechol-containing CS hydrogels showed good biocompatibility in animal models, tunable mechanical properties suitable for different drug delivery applications, and sustained release of various drugs.

This thesis provides several contributions that were presented to the scientific community for the first time:

I. *We proved that introducing catechols into CS hydrogels enhance their mucoadhesion.*

   Catechol functionalization has enhanced the adhesion of polymers on many different surfaces, including biological surfaces such as skin and mucin. People have developed catechol-containing surgical glue and hemostatic showing excellent adhesion to biological tissues. Despite the evidence of catechol-mucin interaction, before our work there were no examples of exploiting the mucoadhesion of catechol modified systems. Our study proved that introducing catechols into CS hydrogels enhance the mucoadhesion of CS, thus providing an intimate and prolonged contact on mucus.

II. *We proved that catechol-containing CS hydrogels loaded with drugs improve drug efficacy and therapeutic effects compared to CS hydrogels without catechols.*

Before our work, there were no examples of exploiting the drug delivery applications of catechol modified systems. We showed the sustained release of loaded drugs from catechol-containing CS hydrogels both in vitro and in vivo. Due to the prolonged retention on the mucosa surface, the catechol-containing hydrogels achieve a sustained drug delivery to the mucosa. We were able to show this in rabbit buccal mucosa and mouse rectal mucosa in vivo.

III. *We showed that buccal and rectal delivery can benefit from a mucoadhesive hydrogel-based formulation compared to conventional formulations.*

In buccal drug delivery, most mucoadhesive systems are tablets, films, or patches. These systems in general have lower biocompatibility than a hydrogel formulation, which contains a large amount of water similar to biological tissue. Our catechol-containing hydrogels can be used to deliver bioactive therapeutics that could not be delivered through conventional buccal drug formulations.

In rectal drug delivery, most of the current formulations are non-mucoadhesive liquid suppositories or enemas. These formulations are difficult to retain in the colon, and are uncomfortable for patients. Our catechol-containing hydrogels are semi-solid formulations, which is likely to be more comfortable and improve patient compliance. In addition, our hydrogels are mucoadhesive so that they reduce the migration of loaded drugs in the colon, thus providing a better local treatment.

IV. We found a correlation between catechol-induced mucoadhesion and oxidation time in vitro.

Previous studies indicated that oxidation can affect the interaction between catechols and mucin. However, no one had directly correlated the oxidation time with the catechol-induced mucoadhesion. In this study, we proved the importance of oxidation time on the mucoadhesion of HCA/CS hydrogels. We found that oxidation happening during the contact between HCA/CS hydrogel and mucus enhances the gel mucoadhesion, while oxidation happening before the contact eliminates the catechol-induced mucoadhesion. These findings provide important insights for future studies; for example, catechol-containing mucoadhesive drug delivery systems could be explored to treat diseases involving high levels of ROS locally produced.

V. We proved the possibility of using a simple physical mixing technique to introduce catechols into CS for mucoadhesion enhancement.

In order to enhance the adhesion on biological surfaces, most studies used chemical methods to covalently conjugate catechol groups to polymers. Our study was the first one showing mucoadhesion enhancement by simply mixing catechol molecules with CS. We also clarified the importance of introducing the right catechol molecules into CS. DOPA and DA suffered from fast release from CS hydrogels due to lack of electrostatic interactions with CS, and thus could not enhance its mucoadhesion.

VI. *We showed that using GP as crosslinker is an ideal strategy to form catechol-containing hydrogels, since it preserves the catechol groups instead of sacrificing them to build the crosslinking.*

Many studies formed catechol-containing hydrogels by adding enzymes or oxidizing agents to trigger catechol crosslinking. Or, they added polymers containing functional groups that could form covalent bonds with the catechols, such as –SH groups. These strategies sacrificed catechols during the crosslinking, thus limiting their capability of inducing mucoadhesion. Our study used GP as a crosslinker to form catechol-containing hydrogels. Since GP only crosslinks the amino groups in CS, the catechol groups are preserved, and contribute to the mucoadhesion enhancement to the greatest possible extent.

The mucoadhesive catechol-containing CS hydrogels have shown several advantages in comparison with previously reported systems.

I. *They can achieve both local and systemic drug delivery.*

Since the catechol-containing CS hydrogel can be immobilized on the mucosa, the drug released from the system can either act locally at the site of application, or act on other tissues via systemic circulation. Thus, they are suitable for both local and systemic drug delivery. In contrast, many previously reported systems, such as nanoparticle drug delivery systems, are only suitable for one type of drug delivery [359].

II. *They can deliver bioactive therapeutics such as genes.*

The catechol-containing CS hydrogels contain a large amount of water similar to the body environment. Thus, they are suitable to deliver bioactive therapeutics without affecting their bioactivity before applications. Conventional drug delivery systems such as patches and dried macro/nano particle systems cannot achieve this [360].

III. *They have tunable mechanical properties.*

The catechol-containing CS hydrogels showed tunable mechanical properties: from injectable liquid to strong solid disk. This feature allows us to adjust the mechanical properties of the mucoadhesive hydrogels to fit different drug delivery applications, such as subcutaneous, intraperitoneal, vaginal drug delivery. Many previous reported hydrogel drug delivery systems lack such tunable mechanical properties, thus limiting their applications [361].

IV. *They provide stable mucoadhesion for long time.*

Previous studies showed that the addition of thiol groups to drug delivery systems is a very effective approach to enhance their mucoadhesion. Thiol-induced mucoadhesion relies on the formation of disulfide bonds between the thiol groups in the polymeric systems and cysteine domains in the mucin [22, 27]. Disulfide bonds are reversible when hydrolysis occurs. Therefore, although some thiolated polymeric mucoadhesive drug delivery systems showed strong mucoadhesion in the short term, their long term mucoadhesion may not be as good [362]. Catechol-induced mucoadhesion, however, involves multiple interactions between catechol groups and mucin, including H-bonding, π-π stacking interactions, and

various non-reversible covalent bonds. Thus, catechol-containing CS hydrogels are likely to provide a stable mucoadhesion for longer time than thiolated mucoadhesive polymers.

6.2 Future directions

Although this study has succeeded in using catechol-containing hydrogels as mucoadhesive drug delivery systems, there are still several research directions worth exploring in the future:

I. In this work, we explored the use of our mucoadhesive hydrogels in three drug delivery routes: oral, buccal and rectal routes. The use of catechol-containing mucoadhesive materials can be explored in other drug delivery routes involving mucus coverage, such as ocular, nasal, and vaginal drug delivery.

II. We showed that the mucoadhesion of CS hydrogels was enhanced by the addition of catechols. Besides CS hydrogels, future work should explore the possibility of introducing catechols into other hydrogels to enhance their mucoadhesion. One potential direction is to improve the mucoadhesion of "smart" hydrogels with stimuli-responsive properties, such as thermosensitive hydrogels. It is possible that these "smart" hydrogels may become mucoadhesive in addition to their original properties; an example could be a thermosensitive mucoadhesive hydrogel for vaginal drug delivery to heal diseases in the vaginal tract. The liquid-state drug formulation at room temperature would gel rapidly when exposed to the body temperature in the vaginal tract, due to its thermosensitivity. If it was also mucoadhesive, this formulation would stick to the vaginal mucosa, and thus extend the drug retention in the vaginal tract and improve drug efficacy.

III. We used GP as the crosslinker to form the catechol-containing CS hydrogels for buccal and rectal drug delivery. Although GP was a good choice compared to other commonly used aldehyde-based crosslinkers due to its low toxicity, it has a strong limitation: GP interacts with amino groups, which implies that GP will crosslink to CS any drugs containing amino groups. Thus, using GP as a crosslinker in our system limited the type of drugs that can be delivered. Future work can focus on exploring other crosslinkers or crosslinking methods (such as an anionic copolymer to form physical crosslinking); this would increase the range of drugs that could be delivered from the gels, including proteins and peptides.

IV. We showed that the mucoadhesion of catechol-containing CS hydrogels was enhanced if they were oxidized during the contact with mucus in vitro, and based on this we hypothesized that the gels would show a greater mucoadhesion in presence of ROS. This hypothesis needs to be confirmed in vivo.

V. We showed that rectal catechol-containing CS hydrogels without SSZ had some therapeutic effects in UC mice, and hypothesized that this was due to the anti-inflammatory effect of the hydrogels. However, we do not have a solid evidence for this yet. The anti-inflammatory effect of catechol-containing CS hydrogels needs to be studied in vitro and in vivo.

VI. The gelation time of our hydrogels was 12 h. This slow gelation may be a limitation for certain applications. For example, for intraperitoneal drug delivery, the injected solution should gel rapidly in the peritoneal cavity to maintain the integrity of the drug delivery system. A mucoadhesive hydrogel can avoid the migration of the system within the peritoneal cavity. Thus, a fast-gelling mucoadhesive hydrogel that gels within seconds after injection could greatly benefit these applications. Future studies need to explore the method to make a fast-gelling catechol-containing CS hydrogel.

VII. This thesis proved that catechol-containing CS hydrogels stick to mucus and establish an intimate contact. However, the mechanism of catechol-mucin interactions is still not clear. Fundamental studies need to focus on understanding the mechanism of catechol-mucin interactions. Isothermal Titration Calorimetry could be a good candidate for these studies, since it measures the heat of interaction developed during the mixing of two reactants. The heat of interaction evolved during the mixing of catechols, catechol-CS and mucin may be analyzed to get information about the bonds formed between the molecules.

APPENDIX – SUMMARY OF METHODOLOGY

Chapter 3

A1. CS hydrogel film preparation

CS powder (0.4 g) was dissolved in 20 ml of 1% v/v aqueous solution of acetic acid. DOPA, HCA, and DA were added to the CS solution under stirring so that the catechol/CS repeating unit molar ratio was 0.5:1. The homogeneous solution was cast into a mold (opening area 25 cm^2) and stored in refrigerator at 4 ˚C overnight to remove air bubbles. The samples were then dried in vacuum at 55 ˚C for 24 h. The films so obtained (namely CS, DOPA/CS, HCA/CS, and DA/CS) were removed from the mold for further testing.

A2. CS hydrogel swelling

Dry films were cut into 1 × 1 cm^2 pieces and were immersed in 20 ml water with pH of 1, 5.5, 6.8 and 7.4 adjusted by 1 M HCl or 1 M NaOH, respectively. The three dimensional sizes of the swollen hydrogel films were measured by a digital caliper at time points of 0, 5, 10, 15, 20, 25, 30, 60 and 120 min. Total volumes were calculated and the swelling ratio (degree of swelling) was taken as the ratio of the volume in the swollen state to the volume in the dry state. Each experiment was repeated three times.

A3. Catechol compound release

Release of catechol compounds from the hydrogels was tested by immersing small pieces of dry films (1 × 1 cm^2, containing ~3.2 mg/cm^2 of catechol compounds) into 40 ml deionized water of pH 5.5 maintained at 37 ˚C. At different time intervals, 3 ml samples were collected and replaced by 3 ml fresh medium. The concentrations of the catechol compounds were quantified by Cary

5000 UV-Vis-NIR Spectrophotometer (Agilent Technologies) by measuring the absorbance at 285 nm and using a calibration curve. The cumulative release percentage was calculated for each catechol compound and plotted as a function of the release time. Each experiment was repeated three times.

A4. Catechol oxidation studies

We studied oxidation of HCA, DOPA and DA as a function of solution pH and exposure time using UV-vis spectroscopy. However, due to the multiple pathways of catechol oxidation and the formation of various intermediate products [246, 247], quantitative analysis is difficult. Indeed, most studies only qualitatively compared the UV-vis spectra evolution representative of catechol oxidation [215, 243, 248]. In this study, we compared the absorbance ratio of the oxidation peak A_{OX} (465 nm, 500 nm and 465 nm for DOPA, HCA and DA respectively) to the non-oxidized catechol peak at 285 nm (A_{285}) as a semi-quantitative measurement of catechol oxidation. DOPA, HCA and DA solutions (1 mM) were first prepared in phosphate buffered saline (PBS) (pH 7.4, buffer strength 50 mM) and their pH values were adjusted to 4, 5, 6, 6.8, 7.4 and 8 using 1 M HCl or 1 M NaOH. Aliquots of solutions were incubated at room temperature for 48 h and were scanned at different time intervals by UV-vis spectrophotometer from 200 to 700 nm. Each experiment was repeated three times.

A5. Mucoadhesion test

The mucoadhesion of different CS hydrogels (CS, DOPA/CS, HCA/CS, and DA/CS) was evaluated by measuring the maximum detachment force (MDF) between the surface of the swollen hydrogel and intestinal mucosa using a tensile tester with a load cell of ±100N (Instron 5569, USA). Hydrogels used for all mucoadhesion tests were prepared by swelling the dry films in deionized

water for 2h. This allowed complete swelling of all four types of hydrogels, thus allowing us to evaluate mucoadhesion in the absence of morphological and physico-chemical changes of the gels. A piece of rabbit small intestine (1 × 1 cm^2) was fixed to the probe using tissue glue (Vetbond, 3M, USA), and the hydrogel was placed on the sample holder. An initial contact force of 0.1 N was applied, and held for either 10 s or 3 min. The probe was elevated at a speed of 0.1 mm/s until completely detached from the hydrogel surface. The force-displacement curve was recorded and the peak force was noted as the MDF. The effect of oxidation on mucoadhesion was tested on two groups: in the first group, four hydrogels were oxidized by immersing them in $NaIO_4$ (0.01 mol/L) for 10 min, and mucoadhesion was tested after this treatment; in the second group, four hydrogels were put in contact with a droplet of $NaIO_4$ (0.01 mol/L), and mucoadhesion was measured right after. In both groups, the contact force of 0.1 N was held for 3 min before detaching the probe to measure the MDF. Each experiment was repeated four times.

A6. Statistical analysis

The statistical analysis was carried out using Student's t-Test. Error bars in the figures represent the standard deviation (SD). A value of $p \leq 0.05$ was considered significant in all tests.

Chapter 4

A7. Synthesis of catechol-chitosan (Cat-CS)

The protocol of Cat-CS synthesis was modified from previous work [29]. Briefly, 60 ml of 1% (w/v) CS solution was prepared in hydrochloric acid (HCl) at pH 2.5. Then, 0.145 g of hydrocaffeic acid and 0.356 g of EDC and were dissolved in 15 ml ethanol and 15 ml deionized (DI) water respectively. These two solutions were mixed and quickly added to CS solution under intensive

stirring, followed by the addition of 1M NaOH to increase the pH to 5.5. The reaction was allowed to continue for 12 hours. After this time, the products were purified by dialysis against a pH 5.0 HCl solution for 3 days using a dialysis membrane tube (MWCO 5,000, Spectrum Laboratories, USA). The final product was freeze dried and stored at -20 °C. To synthesize Cat-CS with a higher ratio of catechol conjugation, the weights of both hydrocaffeic acid and EDC were doubled (i.e. 0.29 g hydrocaffeic acid and 0.712 g of EDC). The degree of conjugation was determined using a UV-Vis spectrometer (Carry 5000, USA) and measuring the absorbance of aqueous solutions of the two Cat-CS polymers at 280 nm. The results were compared with a standard curve built using hydrocaffeic acid, and showed a catechol content of 9% and 19% (Figure S4.1). The two products are therefore named from here on as Cat9-CS and Cat19-CS, respectively. A schematic of the reaction used to synthesize both Cat-CS polymers is shown in Figure S4.2.

A8. Preparation of capped hydrogels and drug loading

An ethyl cellulose protective cover that prevents drug from diffusing to the lumen of the buccal cavity was prepared by solvent casting. 120 µl of 4% ethyl cellulose ethanol solution was added into a mold and dried at room temperature, forming an open cylindrical cap with diameter of 8.5 mm and height of 1.6 mm (Figure 4.1B). This impenetrable cap provided a protective layer on the back and the sides of the hydrogel, and allowed the drugs loaded in the hydrogels to diffuse only through the side in contact with the mucosa. The cap was used as a mold for curing the hydrogel. To make the hydrogel, a 1.5% (w/v) solution of Cat-CS (Cat9-CS or Cat19-CS) was prepared in 3ml of DI water under stirring. 75 µl of 30 mg/ml GP solution in ethanol was added to the Cat-CS solution at a GP:Cat-CS weight ratio of 1:20. 150 µl of the mixture were transferred to the mold and cured at 37°C for 12 hours. The final hydrogels were named Cat9-CS/GP and Cat19-CS/GP depending on their catechol content.

LD, a local anesthesia drug, was selected as a model drug in this study. To prepare the LD loaded hydrogel, LD was first dissolved in 30 mg/ml GP ethanol solution; 75 μl of this solution was added to 3 ml of Cat9-CS or Cat19-CS solution, followed by curing at 37°C for 12 hours. The final concentration of LD was 1mg/hydrogel.

As control, CS/GP hydrogels were prepared and loaded with LD. CS/GP hydrogels were prepared by first dissolving CS in 1% (v/v) acetic acid, and the same procedures described above for the preparation of Cat-CS/GP capped hydrogels and drug loading were followed afterwards.

A9. Physical characterization of the hydrogel

All hydrogels were freeze-dried before characterization. A Bruker Tensor-27 Fourier transform infrared (FTIR) spectrometer equipped with a DTGS detector and a VariGATR™ grazing angle attenuated total reflectance accessory was used to analyze the functional groups formed on the hydrogels. 256 scans were collected for each sample.

Nuclear magnetic resonance (NMR) spectroscopy was used to confirm the conjugation of catechol functional groups to CS and hydrogel crosslinking. ^{13}C CP-MAS NMR spectra were obtained at 100 MHz using a 7.5 mm rotor spinning at 5 kHz, a 1.5 ms contact time and recycle time of 2 s for all samples (Agilent/Varian VNMRS-400, USA). Spinning sidebands were eliminated by the TOSS sequence.

The morphology of the freeze dried hydrogels was analyzed on a JEOL JSM7600F scanning electron microscope (SEM). Cross sections of freeze-dried CS/GP, Cat9-CS/GP and Cat19-CS/GP hydrogel disks were observed at an acceleration voltage of 1kV.

A10. Hydrogel erosion in vitro

Freeze-dried hydrogels were immersed at 37°C in PBS (pH 6.8) containing 5 μg/ml of lysozyme (erosion solution). Samples were weighed before being put into the erosion solution (W_0). After specific times, samples were taken out, freeze-dried, and weighed again (W_t). Three replicates were performed for each experiment. The weight loss percent (W_L %) was calculated as in Equation 4.1:

$$W_L\% = (W_0 - W_t) / W_0 \times 100 \quad \text{(Equation 4.1)}$$

A11. Cumulative drug release in vitro

Hydrogels containing 1 mg of LD were immersed in 10 ml of 10 μM phosphate buffer saline (PBS, pH 6.8) at 37°C. At each time point, 1 ml of the solution was taken out to quantify the release, and meanwhile 1 ml of fresh PBS was added. Time points were selected as 15, 30, 45, 60, 90,120, 150 and 180 minutes. Each test was replicated for three times.

The released LD concentration in PBS medium was quantified using a Thermo Finnigan LCQ Duo Spectrometer System equipped with a UV detector. We used a mobile phase made of acetonitrile/water (30/70, v/v) and 0.1% (v/v) trifluoroacetic acid (TFA). 10 μl of sample were injected into the instrument and passed through a C18 Supelco Discovery column (15 cm × 3 mm, particle size 5 μm), at a flow rate of 0.5 ml/min. Peaks relative to LD were detected at a wavelength of 210 nm, which appeared 2.5 minutes after injection. A standard curve was measured by plotting the areas under the curve (AUC) of the 210 nm peak in a series of samples with known concentrations. Each sample was repeated three times.

A12. Rheological tests

Rheological measurements were conducted to evaluate the gel formation process and the viscoelastic properties of the final hydrogels on a TA Instruments AR2000 stress-controlled rheometer (USA) equipped with a Peltier plate for temperature control. A cone steel geometry (Φ 40 mm, 2°) was used for all experiments. Oscillatory measurements were conducted at a constant frequency (f = 1 Hz) and strain (σ = 0.1%) in the linear viscoelastic regime (LVR), which was established by initial stress sweep tests. The polymer and crosslinker were mixed quickly and placed in the rheometer. The gelation process at 37 °C was followed through the evolution of storage and loss moduli (G', G'', respectively) as a function of time. A solvent trap was used to prevent the dehydration of the hydrogels. We performed time sweeps for a total of 12 hours at 37 °C; longer test times would lead to significant gel dehydration. After 12 hours of gelation and equilibration of the samples, stress sweeps were measured with stress ranging from 0.1 to 10000 Pa to evaluate the structural integrity of the hydrogel network. Each test was replicated three times.

A13. Mucoadhesion test in vitro

Fresh porcine buccal tissue was glued to a microscope glass slide (mucosal membrane facing up) and placed into a beaker vertically (Figure S4.3). The hydrogels were pressed to adhere on the mucosal surface. Both the tissue and the hydrogels were immersed in 30 ml PBS (pH 6.8) at 37°C. A magnetic stirring bar rotating at a speed of 1000 rpm was used to generate flow. Every 15 minutes, the number of hydrogels that still adhered to the mucosa was recorded. The data were evaluated using Kaplan-Meier estimate plots of survival. Ten samples from each hydrogel group were tested.

A14. Mucoadhesion and drug release test in vivo

CS/GP and Cat19-CS/GP capped hydrogels were prepared as previously described, each containing 1 mg of LD. Four male New Zealand rabbits (adults, weight 3.5 kg) were used to study mucoadhesion and drug release in vivo. Animals were received and allowed to acclimatize for a minimum of 72 hours. Each rabbit was pre-anesthetized using Ketamine-Xylazine-Acepromazine injected subcutaneously. After that, the maintenance of anesthesia was guaranteed by intubation through the mouth using a regulated flow of isoflurane (concentration 1.5 – 2 vol%). A catheter was placed into the marginal ear vein of each rabbit to collect blood samples. The mouth of the rabbit was opened, and the mucosal lining of the cheek was exposed. CS/GP hydrogels were applied to two rabbits (R1 and R2) used as control group, and Cat19-CS/GP hydrogels to the other two rabbits (R3 and R4) used as test group. Each hydrogel was pressed against the mucosal lining of the rabbit cheek. Hydrogels were allowed to stay in place for a total of 3 hours. Then, animals were euthanized by intravenous injection of overdosed barbiturate. Blood samples (1 ml at each time point) were collected after 15, 30, 60, 90, 120, 150, and 180 minutes since application of the hydrogels. The blood samples were placed at room temperature for 20 minutes for coagulation, followed by centrifugation at 3000 rpm for 15 minutes. The serum was collected and kept frozen until quantification.

To extract the drug from the serum, serum samples were thawed to room temperature, and a method modified from a previous study was used [300]. Briefly, 600 µl of serum were added to a centrifuge tube containing 100 µl of a 1 M Na_2CO_3 solution, followed by the addition of 10 ml of ethyl acetate. 5 µl of 5 ppm procaine hydrochloride (PR) water solution was added at the same time as an internal standard. The mixture was vortexed for 2 minutes, and then centrifuged at 4000 rpm for 5 minutes. 7 ml of the supernatant organic layer was transferred to another centrifuge tube

with 200 µl of 0.0025 M H_2SO_4. Again, the mixture was vortexed for 2 minutes and centrifuged at 4000 rpm for 5 minutes. The supernatant ethyl acetate was removed, and the remaining solution was neutralized by adding 100 µl of 0.01 M NaOH. The final solution was freeze dried and re-dissolved in 200 µl of DI water and analyzed with liquid chromatography–mass spectrometry (LC-MS).

LC-MS was performed on a Thermo Scientific Exactive Plus Benchtop Full-Scan Orbitrap™ Mass Spectrometer equipped with an electrospray ionization source. Mobile phase flowing at the rate of 300 µl/min consisted of methanol/water (50/50, v/v) and 0.1% TFA. A Thermo Scientific Hypersil GOLD column (50mm × 2.1 mm) with particle size of 1.9 µm was used for compound separation. Serum solutions were loaded in an auto-sampler, and 8 µl were injected by the auto-sampler into the column. The peaks of LD and of the internal standard PR were identified at mass-to-charge values of 285.18049 and 287.15975, respectively. A standard curve based on AUC ratios of LD to PR at known concentration ratios was used to calculate the LD concentration in serum samples.

After the animal was sacrificed, the hydrogel was removed, and the buccal tissue in contact with the hydrogel was extracted for histological examination. The harvested tissue was fixed in 2% paraformaldehyde, dissected longitudinally, and embedded in paraffin. 5 µm thick tissue sections from the mucosa side were stained with haematoxylin and eosin (H&E) to detect inflammation, following literature protocols [301, 302]. Tissue from the cheek that was not in contact with the hydrogel was also extracted and examined as control. Stained samples were examined under microscope at magnification of 400X.

A15. Statistical analysis

Statistical analysis for all tests (except for the mucoadhesion in vitro study) was carried out using Student's t test. Error bars in the figures represent the standard deviation (SD). For the muoadhesion in vitro study, the Kaplan-Meier estimate statistical analysis was used [303]. Chi-square values were calculated based on log-rank test statistic, and were converted to p values. A value of $p \leq 0.05$ was considered significant in all tests.

Chapter 5

A16. Synthesis of catechol-chitosan (Cat-CS)

We synthesized Cat-CS by a protocol modified from our previous study [345]. Briefly, we first dissolved 0.6 g of medium molecular weight CS in 60 ml of hydrochloric acid (HCl) with final pH adjusted to 2.5. We prepared 0.29 g of hydrocaffeic acid in 15 ml ethanol, and 0.712 g of EDC in 15 ml deionized (DI) water separately, followed by rapid mixing. We added the well-mixed solution to CS solution with constant stirring. We adjusted the final pH of the mixture to 5.5 by addition of 1M NaOH, and brought the reaction to completion under 12 h stirring. To purify Cat-CS, we transferred the mixture to a dialysis membrane tube (MWCO 5,000, Spectrum Laboratories, USA), and conducted the dialysis under 0.01 mM HCl solution (pH 5.0) for 3 days. We freeze-dried the dialysis product and stored it at -20°C. To determine the percentage of catechol content in Cat-CS, we dissolved Cat-CS in DI water under constant stirring, and measured the absorbance of the solution at 280 nm using a UV-Vis spectrometer (Carry 5000, USA) (Figure S5.1). Based on the standard curve of hydrocaffeic acid, we calculated the catechol content as 20%.

A17. Preparation of injectable SSZ/Cat-CS hydrogel system

We homogenized 1% (w/v) solution of Cat-CS in DI water by intensive stirring. We added an ethanol-based GP solution (6 mg/ml) to the Cat-CS solution as a crosslinker, at a volume ratio of GP: Cat-CS = 1: 400. To remove large aggregates which may block the needle during injection, we sieved SSZ powders through a stainless steel screen with a pore size of 50 μm. Then, we homogenized the fine SSZ powders with the mixture of Cat-CS and GP at a concentration of 10 mg/ml by intensive stirring at room temperature for 10 minutes. We loaded this viscous drug/polymer mixture inside 1 ml Tuberculin syringes (Becton, Dickinson and Company, USA), transferred them to a 37°C incubator, and kept them there for 12 h, which allowed gelation of Cat-CS inside the syringes.

A18. Physical characterization of SSZ/Cat-CS hydrogel system

We removed the syringes from the incubator after 12 h gelation. We conducted two physical characterizations: 1) injection force measurement, and 2) rheological tests of injected hydrogels.

For the injection force measurement, we loaded 0.5 ml as an initial volume of hydrogel in each syringe. Before the test, we mounted the syringe vertically on a BOSE 3220 Pulse System equipped with a load cell (load range ± 200N) pushing on the plunger (Figure S5.2). We applied a pre-load of ~ 0.1 N at the beginning of the injection. The instrument could lower the load cell to push the plunger and measure the force recorded by the load cell. We first did a sequence of 3 injections, during which the load cell pushed the plunger for 4 mm at a rate of 0.8 mm/s, with a pause of 10 seconds in between injections. Due to the limitation of moving distance of the load cell (max 12 mm), we re-located the load cell to its original position, and performed another series of 3 injections with the same syringe. For the control group, we prepared syringes loaded with Cat-

CS hydrogels but without SSZ, and evaluated their injectability using the same protocol. We performed 3 repeated measurements for each group.

We collected the injected SSZ/Cat-CS hydrogels for rheology tests to understand their viscoelastic behaviors. We used an Anton Paar MCR 301 Rheometer (Austria) equipped with a cone steel geometry (d = 25mm, angle = 1°) for oscillatory stress sweep tests with constant frequency (f = 1Hz). The instrument recorded the evolution of storage modulus G' as a function of oscillatory stress at room temperature. We used the injected Cat-CS hydrogels without SSZ as control. We performed 3 repeated measurements for each group.

A19. Animals

We obtained 21 C57BL/6 male, littermate mice from a specific pathogen-free breeding colony at the Research Institute of the McGill University Health Centre (RI-MUHC). We housed these mice in conventional care facility for 3 weeks to allow them to acquire the local bacterial flora prior to the experiment. All procedures followed the protocol approved by the McGill University Animal Care Committee (UACC).

A20. In vivo experiment

Experimental design and grouping

The total length of the in vivo experiment was 10 days. Day 1 to 5 was the disease development period, and Day 6 to Day 10 was the treatment period. On Day 11, we sacrificed the animals following the UACC-approved procedures to harvest the samples. Figure 5.2 shows the schematic and the timeline of our experiment.

We divided the mice into 5 groups. Group 1 was the healthy control group, and mice in this group had access to normal food and water without any treatment. Groups 2-5 were UC groups

induced by DSS (procedures described in the following section). Group 2 was the negative control group, and mice received no treatment. Group 3 received 1.5 mg SSZ by oral gavage once daily, which was equivalent to the normal oral dose used in UC patients. Group 4 received rectal injection of 75 µl Cat-CS hydrogel alone, not loaded with SSZ, twice per day. Group 5 received the same volume of SSZ/Cat-CS hydrogel by rectal injection twice per day. Since each injection contained 0.75 mg of SSZ, the total SSZ dose delivered per day to this group equaled the dose given orally to Group 3. The description and number of mice in each group are summarized in Table 5.1.

Induction of UC by DSS

DSS is often used to induce UC in mice to mimic the pathology of the disease [346]. We used the procedure of UC induction by DSS modified from a previous study [347].We grouped and housed the animals in the animal facility for 3 weeks for them to acquire the local bacterial flora prior to DSS treatment. From Day 1 to 5, we added 3% (w/v) DSS to drinking water given to the mice in Group 2-5. This allowed the disease to develop in the colon. We renewed the DSS water bag of each cage daily.

Rectal drug delivery

The DSS treatment was stopped on Day 5, and mice began to receive regular water and the treatment on Day 6. We treated Group 5 with SSZ/Cat-CS gel (10 mg/ml) via rectal injection twice per day. Every time before administering a hydrogel dose, we anesthetized the mice by subcutaneous injection of 0.1 ml of a drug mixture containing ketamine 20 mg/ml and xylazine 5mg/ml. Then, we inserted a gavage needle (26 gauge, with beaded tip) connected to the hydrogel-loaded syringe through rectum for ~2.5 cm. We injected 75 µl of SSZ/Cat-CS gel slowly (at a rate of ~0.8 mm/s), then inserted a cylinder-shaped glycerin plug (d ≈ 2mm, length ≈ 5 mm) to secure the retention of the hydrogel at early stages.

A21. Body weight monitoring and fecal occult blood assessment

We monitored the body weights of all mice daily in the morning. We calculated the weight loss (%) as the percentage of original body weight before DSS induction. We also qualitatively conducted fecal occult blood assessment using a Hemoccult kit.

A22. Quantification of rectal dose

In our preliminary study, we observed that the injected SSZ/Cat-CS hydrogels were expelled by the mice after a few hours. The expelled hydrogels were compressed and dehydrated due to the water absorption mechanism of colon [348], and looked like thin threads containing unabsorbed SSZ (Figure S5.3). To quantify the drug dose delivered in the colon, we collected feces containing visible expelled hydrogels. We immersed each individually expelled hydrogel in 2 ml of lysozyme solution (5 mg/ml) and stirred for 3 days, allowing Cat-CS to be completely degraded and expose the undelivered SSZ in the hydrogel structure. Then, we added 1 ml of 1M NaOH to solubilize the SSZ particles, which turned the solution to an orange color. We measured the absorbance of the solution at 458 nm using a UV-vis spectrometer (Cary 5000, USA). We calculated the drug content by comparing these results with a pre-established standard curve of SSZ.

A23. Blood sample collection

We collected the plasma from all the sacrificed mice on Day 11 to measure the levels of SSZ and its metabolites 5-ASA and SP. We collected approximately 1 ml of blood from each mouse via cardiac puncture into an anti-coagulation tube, followed by centrifuging at 10000 rpm for 15 min. Then, we transferred the clarified plasma to a new tube and stored the samples at -80°C for HPLC-MS analysis.

A24. Colon length measurement

We dissected the colon (from the start of cecum till the end of rectum) of each mouse and cleaned the tissue by phosphate buffer saline (PBS) with care. We carefully removed the fecal content inside the colon. Then, we aligned the cleaned and straightened colons on a piece of wet filter paper to measure the length of each colon (from the beginning of colon till the end of rectum).

A25. Histology

We removed the distal part of each of the colon samples (1 cm in total) and fixed the tissue in buffered formalin. We made two 5 μm-thick sections on each colon sample: one is in the middle of each sample, i.e., 0.5 cm from the end of the rectum; the other one is the top of the each colon sample, i.e., 1 cm from the end of the rectum. We named these two sections as "distal" and "proximal" respectively. The slides were stained with hematoxylin and eosin (H&E).

We examined the stained slides using a Leica microscope at magnification of 50x and images of the colon cross sections taken using the Bioquant Nova Prime software. Since the shapes of the colon cross sections were close to elliptical, we measured the largest distance d_L and the smallest distance d_w across the ellipse. We compared the sum of these two distances of each group. In addition, we also measured the thickness of the colon wall containing the submucosa and muscle layers.

A26. Tumor necrosis factor alpha (TNF-α) ELISA assay

We immersed the remaining tissue in each harvested colon sample in 1 ml of PBS, and homogenized the tissue on ice using a Polytron homogenizer at 3000 rpm for 1 min. We transferred the homogenate to an Eppendorf tube, followed by centrifugation at 10000 rpm for 15 min. Then, we transferred the supernatant to a new tube and stored the samples at -80°C for TNF-α ELISA

assay. We performed the TNF-α ELISA using anti-mouse TNF- α paired antibody set (R&D Systems Inc.) using a standard sandwich ELISA protocol.

A27. Histological score and disease activity index assessment

We developed two grading systems to evaluate the therapeutic efficacy of our treatments: the histological score system and the disease activity index system. The detailed grading criteria are shown in Table 5.2 and Table 5.3.

We scored the histology based on four parameters analyzed from the distal H&E microscopy images: crypt damage, neutrophil infiltration, colon wall enlargement ($d_L + d_w$), and colon wall thickening. The final histological score refers to the sum of the grades of these four parameters. Since we did not perform H&E staining on all individual mice in each group, the histological score of a specific group represents the average of the scores of all the stained slides in that group. A higher histology score means a more severe tissue damage.

We scored the disease activity index based on three parameters: body weight recovery rate, colon length, and TNF-α level. The final disease activity index score refers to the sum of the grades of these three parameters. To calculate the disease activity index, we averaged the scores of all the mice in a specific group. Higher score indicates a more serious disease condition, while lower score indicates a healthier condition.

A28. Cumulative plasma concentrations of SSZ and its metabolites

After the frozen plasma samples were thawed at room temperature, we mixed 40 µl of sample with 100 µl of 0.5 µM atenolol (internal standard, solution made from acetonitrile/methanol at volume ratio of 40/60) in an Eppendorf tube. We intensively vortexed the mixture, and then centrifuged it at 13000 rpm for 5 min. We diluted 25 µl of the supernatant with 50 µl of water containing 0.1%

formic acid for the analysis of SSZ and SP. We transferred another 25 µl of supernatant to 50 µl of water containing 0.5% formic acid for the analysis of 5-ASA. We used an Agilent 1100 series HPLC LC/MS/MS AB/SCIEX 4000 QTRAP system. For SSZ and SP analysis, we used a Luna C8 column (30 × 2 mm, size 5 µm). For 5-ASA analysis, we used a Betasil Silica column (50 × 3 mm, size 5 µm). The mobile phase was acetonitrile with 0.1 formic acid. We injected 3 µl of sample into the column at a flow rate of 0.7 ml/min for SSZ and SP, and 0.85 ml/min for 5-ASA. We analyzed the area under the curve of each peak, and calculated the concentration of the chemicals based on the previously developed standard curve.

A29. Statistical analysis

We performed statistical analysis for the injection force measurement using an unpaired t-Test. All other tests used ordinary one-way ANOVA with multiple comparisons (GraphPad Prism 6). Error bars in the figures represented the standard error of the mean (SEM), except for the standard deviation (SD) in Figure 5.5, as indicated in the graph caption. We considered a value of $p \leq 0.05$ as significant in all tests.

REFERENCES

1. Paolino, D., et al., *Drug Delivery Systems*, in *Encyclopedia of Medical Devices and Instrumentation*. 2006, John Wiley & Sons, Inc.
2. Gardner, C.R., *Potential and limitations of drug targeting: an overview.* Biomaterials, 1985. **6**(3): p. 153-60.
3. Tomlinson, E., *Theory and practice of site-specific drug delivery.* Advanced Drug Delivery Reviews, 1988. **1**(3): p. 271-272.
4. Meng, E. and T. Hoang, *Micro- and nano-fabricated implantable drug-delivery systems.* Therapeutic delivery, 2012. **3**(12): p. 1457-1467.
5. Dash, A. and G. Cudworth Ii, *Therapeutic applications of implantable drug delivery systems.* Journal of Pharmacological and Toxicological Methods, 1998. **40**(1): p. 1-12.
6. Chen, M.C., et al., *A review of the prospects for polymeric nanoparticle platforms in oral insulin delivery.* Biomaterials, 2011. **32**(36): p. 9826-38.
7. Torchilin, V.P., *Multifunctional, stimuli-sensitive nanoparticulate systems for drug delivery.* Nat Rev Drug Discov, 2014. **13**(11): p. 813-827.
8. Martin, L., et al., *Sustained buccal delivery of the hydrophobic drug denbufylline using physically cross-linked palmitoyl glycol chitosan hydrogels.* European Journal of Pharmaceutics and Biopharmaceutics, 2003. **55**(1): p. 35-45.
9. Cui, F., et al., *Preparation and evaluation of chitosan-ethylenediaminetetraacetic acid hydrogel films for the mucoadhesive transbuccal delivery of insulin.* Journal of Biomedical Materials Research Part A, 2009. **89A**(4): p. 1063-1071.
10. Chen, S.-C., et al., *A novel pH-sensitive hydrogel composed of N,O-carboxymethyl chitosan and alginate cross-linked by genipin for protein drug delivery.* Journal of Controlled Release, 2004. **96**(2): p. 285-300.
11. Muzzarelli, R.A.A., *Genipin-crosslinked chitosan hydrogels as biomedical and pharmaceutical aids.* Carbohydrate Polymers, 2009. **77**(1): p. 1-9.
12. Liu, T.-Y. and Y.-L. Lin, *Novel pH-sensitive chitosan-based hydrogel for encapsulating poorly water-soluble drugs.* Acta Biomaterialia, 2010. **6**(4): p. 1423-1429.
13. Bhattarai, N., et al., *PEG-grafted chitosan as an injectable thermosensitive hydrogel for sustained protein release.* Journal of Controlled Release, 2005. **103**(3): p. 609-624.
14. Giri, T.K., et al., *Modified chitosan hydrogels as drug delivery and tissue engineering systems: present status and applications.* Acta Pharmaceutica Sinica B, 2012. **2**(5): p. 439-449.
15. Bhattarai, N., J. Gunn, and M. Zhang, *Chitosan-based hydrogels for controlled, localized drug delivery.* Advanced Drug Delivery Reviews, 2010. **62**(1): p. 83-99.
16. Gisbert, J.P., et al., *Clinical trial evaluating amoxicillin and clarithromycin hydrogels (Chitosan-polyacrylic acid polyionic complex) for H. pylori eradication.* J Clin Gastroenterol, 2006. **40**(7): p. 618-22.
17. Yang, J., et al., *pH-sensitive interpenetrating network hydrogels based on chitosan derivatives and alginate for oral drug delivery.* Carbohydrate Polymers, 2013. **92**(1): p. 719-725.

18. Munjeri, O., J.H. Collett, and J.T. Fell, *Hydrogel beads based on amidated pectins for colon-specific drug delivery: the role of chitosan in modifying drug release.* Journal of Controlled Release, 1997. **46**(3): p. 273-278.
19. Xu, Y., et al., *Preparation of dual crosslinked alginate–chitosan blend gel beads and in vitro controlled release in oral site-specific drug delivery system.* International Journal of Pharmaceutics, 2007. **336**(2): p. 329-337.
20. Huang, Y., et al., *Molecular aspects of muco- and bioadhesion:: Tethered structures and site-specific surfaces.* Journal of Controlled Release, 2000. **65**(1–2): p. 63-71.
21. Khutoryanskiy, V.V., *Advances in Mucoadhesion and Mucoadhesive Polymers.* Macromolecular Bioscience, 2011. **11**(6): p. 748-764.
22. Smart, J.D., *The basics and underlying mechanisms of mucoadhesion.* Advanced Drug Delivery Reviews, 2005. **57**(11): p. 1556-1568.
23. Ducheˇne, D., F. Touchard, and N.A. Peppas, *Pharmaceutical and Medical Aspects of Bioadhesive Systems for Drug Administration.* Drug Development and Industrial Pharmacy, 1988. **14**(2-3): p. 283-318.
24. Peppas, N.A. and J.J. Sahlin, *Hydrogels as mucoadhesive and bioadhesive materials: a review.* Biomaterials, 1996. **17**(16): p. 1553-1561.
25. Lehr, C.-M., et al., *In vitro evaluation of mucoadhesive properties of chitosan and some other natural polymers.* International Journal of Pharmaceutics, 1992. **78**(1–3): p. 43-48.
26. Bernkop-Schnürch, A. and S. Dünnhaupt, *Chitosan-based drug delivery systems.* European Journal of Pharmaceutics and Biopharmaceutics, In Press(0).
27. Werle, M. and A. Bernkop-Schnürch, *Thiolated chitosans: useful excipients for oral drug delivery.* Journal of Pharmacy and Pharmacology, 2008. **60**(3): p. 273-281.
28. Ninan, L., et al., *Adhesive strength of marine mussel extracts on porcine skin.* Biomaterials, 2003. **24**(22): p. 4091-9.
29. Ryu, J.H., et al., *Catechol-Functionalized Chitosan/Pluronic Hydrogels for Tissue Adhesives and Hemostatic Materials.* Biomacromolecules, 2011. **12**(7): p. 2653-2659.
30. Lee, Y., et al., *Thermo-sensitive, injectable, and tissue adhesive sol-gel transition hyaluronic acid/pluronic composite hydrogels prepared from bio-inspired catechol-thiol reaction.* Soft Matter, 2010. **6**(5).
31. Burke, S.A., et al., *Thermal gelation and tissue adhesion of biomimetic hydrogels.* Biomed Mater, 2007. **2**(4): p. 203-10.
32. Mehdizadeh, M., et al., *Injectable citrate-based mussel-inspired tissue bioadhesives with high wet strength for sutureless wound closure.* Biomaterials, 2012. **33**(32): p. 7972-7983.
33. Hong, S., et al., *Hyaluronic Acid Catechol: A Biopolymer Exhibiting a pH-Dependent Adhesive or Cohesive Property for Human Neural Stem Cell Engineering.* Advanced Functional Materials, 2012: p. n/a-n/a.
34. Huang, K., et al., *Synthesis and Characterization of Self-Assembling Block Copolymers Containing Bioadhesive End Groups.* Biomacromolecules, 2002. **3**(2): p. 397-406.
35. Catron, N., H. Lee, and P. Messersmith, *Enhancement of poly (ethylene glycol) mucoadsorption by biomimetic end group functionalization.* Biointerphases, 2006. **1**(4): p. 134-141.
36. Abraham, C. and J.H. Cho, *Inflammatory Bowel Disease.* The New England journal of medicine, 2009. **361**(21): p. 2066-2078.
37. Gallone, L., L. Olmi, and V. Marchetti, *Use of topical rectal therapy to preserve the rectum in surgery of ulcerative colitis.* World Journal of Surgery, 1980. **4**(5): p. 609-613.

38. Palmer, K.R., J.R. Goepel, and C.D. Holdsworth, *Sulphasalazine retention enemas in ulcerative colitis: a double-blind trial.* British Medical Journal (Clinical research ed.), 1981. **282**(6276): p. 1571-1573.
39. Ng, R., *Appendix 1: History of Drug Discovery and Development*, in *Drugs*. 2008, John Wiley & Sons, Inc. p. 391-397.
40. Pina, A.S., A. Hussain, and A.C. Roque, *An historical overview of drug discovery.* Methods Mol Biol, 2009. **572**: p. 3-12.
41. Drews, J., *Drug Discovery: A Historical Perspective.* Science, 2000. **287**(5460): p. 1960-1964.
42. Hoffman, A.S., *The origins and evolution of "controlled" drug delivery systems.* Journal of Controlled Release, 2008. **132**(3): p. 153-163.
43. Folkman, J. and D.M. Long, *The use of silicone rubber as a carrier for prolonged drug therapy.* Journal of Surgical Research, 1964. **4**(3): p. 139-142.
44. Ranade, V. and M. Hollinger, *Site-Specific Drug Delivery Using Liposomes and Emulsions as Carriers*, in *Drug Delivery Systems, Third Edition*. 2011, CRC Press. p. 1-46.
45. Damgé, C., C.P. Reis, and P. Maincent, *Nanoparticle strategies for the oral delivery of insulin.* Expert Opinion on Drug Delivery, 2008. **5**(1): p. 45-68.
46. Ranade, V.V. and M.A. Hollinger, *Drug Delivery System (2nd Edition), CRC Press LLC.* 2004.
47. Pamies, P. and A. Stoddart, *Materials for drug delivery.* Nat Mater, 2013. **12**(11): p. 957-957.
48. Peterfreund, R.A. and J.H. Philip, *Critical parameters in drug delivery by intravenous infusion.* Expert Opinion on Drug Delivery, 2013. **10**(8): p. 1095-1108.
49. Peppas, N.A. and P.A. Buri, *Surface, interfacial and molecular aspects of polymer bioadhesion on soft tissues.* Journal of Controlled Release, 1985. **2**(0): p. 257-275.
50. Gum, J.R., *Human mucin glycoproteins: varied structures predict diverse properties and specific functions.* Biochemical Society transactions, 1995. **23**(4): p. 795-799.
51. Wang, B., T. Siahaan, and R.A. Soltero, *Drug Delivery: Principles and Applications.* 2005.
52. Harding, S.E., et al., *Biopolymer Mucoadhesives.* Biotechnology and Genetic Engineering Reviews, 1999. **16**(1): p. 41-86.
53. Shishu, N. Gupta, and N. Aggarwal, *Stomach-specific drug delivery of 5-fluorouracil using floating alginate beads.* AAPS PharmSciTech, 2007. **8**(2): p. E143-E149.
54. Philip, A.K. and B. Philip, *Colon Targeted Drug Delivery Systems: A Review on Primary and Novel Approaches.* Oman Medical Journal, 2010. **25**(2): p. 79-87.
55. Chourasia, M.K. and S.K. Jain, *Pharmaceutical approaches to colon targeted drug delivery systems.* J Pharm Pharm Sci, 2003. **6**(1): p. 33-66.
56. Squier, C.A., N.W. Johnson, and R.M. Hopps, *Human Oral Mucosa, Development, Structure and Function*. The organization of oral mucosa. 1976, Oxford: Blackwell Scientific Publications.
57. Salamat-Miller, N., M. Chittchang, and T.P. Johnston, *The use of mucoadhesive polymers in buccal drug delivery.* Advanced Drug Delivery Reviews, 2005. **57**(11): p. 1666-1691.
58. Harris, D. and J.R. Robinson, *Drug delivery via the mucous membranes of the oral cavity.* J Pharm Sci, 1992. **81**(1): p. 1-10.
59. Asane, G.S., et al., *Polymers for mucoadhesive drug delivery system: a current status.* Drug Dev Ind Pharm, 2008. **34**(11): p. 1246-66.

60. Woolfson, A.D., D.F. McCafferty, and G.P. Moss, *Development and characterisation of a moisture-activated bioadhesive drug delivery system for percutaneous local anaesthesia.* International Journal of Pharmaceutics, 1998. **169**(1): p. 83-94.
61. Paderni, C., et al., *Oral local drug delivery and new perspectives in oral drug formulation.* Oral Surgery, Oral Medicine, Oral Pathology and Oral Radiology, 2012. **114**(3): p. e25-e34.
62. Sankar, V., et al., *Local drug delivery for oral mucosal diseases: challenges and opportunities.* Oral Diseases, 2011. **17**: p. 73-84.
63. Hearnden, V., et al., *New developments and opportunities in oral mucosal drug delivery for local and systemic disease.* Advanced Drug Delivery Reviews, 2012. **64**(1): p. 16-28.
64. Shaikh, R., et al., *Mucoadhesive drug delivery systems.* Journal of Pharmacy and Bioallied Sciences, 2011. **3**(1): p. 89-100.
65. Lakshmi, P.J., B. Deepthi, and R.N. Rama, *Rectal drug delivery: A promising route for enhancing drug absorption.* Asian J. Res. Pharm. Sci., 2012. **2**(4): p. 143-149.
66. Ofokansi, K.C., M.U. Adikwu, and V.C. Okore, *Preparation and Evaluation of Mucin-Gelatin Mucoadhesive Microspheres for Rectal Delivery of Ceftriaxone Sodium.* Drug Development and Industrial Pharmacy, 2007. **33**(6): p. 691-700.
67. El-Leithy, E.S., et al., *Evaluation of Mucoadhesive Hydrogels Loaded with Diclofenac Sodium–Chitosan Microspheres for Rectal Administration.* AAPS PharmSciTech, 2010. **11**(4): p. 1695-1702.
68. Kim, C.-K., et al., *Trials of in situ-gelling and mucoadhesive acetaminophen liquid suppository in human subjects.* International Journal of Pharmaceutics, 1998. **174**(1–2): p. 201-207.
69. Das, K.M. and R. Dubin, *Clinical pharmacokinetics of sulphasalazine.* Clin Pharmacokinet, 1976. **1**(6): p. 406-25.
70. Travis, S.P.L., *Which 5-ASA?* Gut, 2002. **51**(4): p. 548-549.
71. Ramadass, S.K., et al., *Preparation and evaluation of mesalamine collagen in situ rectal gel: A novel therapeutic approach for treating ulcerative colitis.* European Journal of Pharmaceutical Sciences, 2013. **48**(1–2): p. 104-110.
72. Marshall, J.K. and E.J. Irvine, *Putting rectal 5-aminosalicylic acid in its place: the role in distal ulcerative colitis.* Am J Gastroenterol, 2000. **95**(7): p. 1628-1636.
73. Marshall, J.K., et al., *Rectal 5-aminosalicylic acid for induction of remission in ulcerative colitis.* Cochrane Database Syst Rev, 2010(1): p. CD004115.
74. Campieri, M., et al., *Mesalazine (5-Aminosalicylic Acid) Suppositories in the Treatment of Ulcerative Proctitis or Distal Proctosigmoiditis: A Randomized Controlled Trial.* Scandinavian Journal of Gastroenterology, 1990. **25**(7): p. 663-668.
75. Thassu, D., Y. Pathak, and M. Deleers, *Naoparticulate Drug-Delivery Systems: An Overview*. Nanoparticulate Drug Delivery Systems. 2007, New York, London.: Informa Healthcare.
76. Kalepu, S., M. Manthina, and V. Padavala, *Oral lipid-based drug delivery systems – an overview.* Acta Pharmaceutica Sinica B, 2013. **3**(6): p. 361-372.
77. Henry, S., et al., *Microfabricated microneedles: a novel approach to transdermal drug delivery.* J Pharm Sci, 1998. **87**(8): p. 922-5.
78. Prausnitz, M.R., *Microneedles for transdermal drug delivery.* Advanced Drug Delivery Reviews, 2004. **56**(5): p. 581-587.

79. Norman, J.J., et al., *Microneedle patches: Usability and acceptability for self-vaccination against influenza.* Vaccine, 2014. **32**(16): p. 1856-1862.
80. DeMuth, P.C., et al., *Vaccine delivery with microneedle skin patches in nonhuman primates.* Nat Biotech, 2013. **31**(12): p. 1082-1085.
81. Sullivan, S.P., et al., *Dissolving polymer microneedle patches for influenza vaccination.* Nat Med, 2010. **16**(8): p. 915-920.
82. Hoffman, A.S., *Hydrogels for biomedical applications.* Advanced Drug Delivery Reviews, 2002. **54**(1): p. 3-12.
83. Peppas, N.A., et al., *Hydrogels in pharmaceutical formulations.* European Journal of Pharmaceutics and Biopharmaceutics, 2000. **50**(1): p. 27-46.
84. Gibas, I. and H. Janik, *Review: synthetic polymer hydrogels for biomedical applications.* Chemistry & Chemical Technology, 2010. **4**: p. 297-304.
85. Deligkaris, K., et al., *Hydrogel-based devices for biomedical applications.* Sensors and Actuators B: Chemical, 2010. **147**(2): p. 765-774.
86. Gulrez, S.K.H., S. Al-Assaf, and G.O. Philips, *Hydrogels: Methods of Preparation. Characterisation and Applications*, in *Progress in Molecular and Environmental Bioengineering- From Analysis and Modeling to Technology Applications*, A. Carpi, Editor. 2011, InTech.
87. Van Vlierberghe, S., P. Dubruel, and E. Schacht, *Biopolymer-Based Hydrogels As Scaffolds for Tissue Engineering Applications: A Review.* Biomacromolecules, 2011. **12**(5): p. 1387-1408.
88. van der Linden, H.J., et al., *Stimulus-sensitive hydrogels and their applications in chemical (micro)analysis.* Analyst, 2003. **128**(4): p. 325-331.
89. Qiu, Y. and K. Park, *Environment-sensitive hydrogels for drug delivery.* Advanced Drug Delivery Reviews, 2001. **53**(3): p. 321-339.
90. Park, S.-E., et al., *Preparation of pH-sensitive poly(vinyl alcohol-g-methacrylic acid) and poly(vinyl alcohol-g-acrylic acid) hydrogels by gamma ray irradiation and their insulin release behavior.* Journal of Applied Polymer Science, 2004. **91**(1): p. 636-643.
91. Berger, J., et al., *Structure and interactions in covalently and ionically crosslinked chitosan hydrogels for biomedical applications.* European Journal of Pharmaceutics and Biopharmaceutics, 2004. **57**(1): p. 19-34.
92. Ravi Kumar, M.N.V., *A review of chitin and chitosan applications.* Reactive and Functional Polymers, 2000. **46**(1): p. 1-27.
93. Prabaharan, M., *Review Paper: Chitosan Derivatives as Promising Materials for Controlled Drug Delivery.* Journal of Biomaterials Applications, 2008. **23**(1): p. 5-36.
94. Denkbas, E.B. and R.M. Ottenbrite, *Perspectives on: Chitosan Drug Delivery Systems Based on their Geometries.* Journal of Bioactive and Compatible Polymers, 2006. **21**(4): p. 351-368.
95. Duarte, A.R.C., J.F. Mano, and R.L. Reis, *Preparation of chitosan scaffolds loaded with dexamethasone for tissue engineering applications using supercritical fluid technology.* European Polymer Journal, 2009. **45**(1): p. 141-148.
96. Berth, G., H. Dautzenberg, and M.G. Peter, *Physico-chemical characterization of chitosans varying in degree of acetylation.* Carbohydrate Polymers, 1998. **36**(2–3): p. 205-216.
97. Chenite, A., et al., *Rheological characterisation of thermogelling chitosan/glycerol-phosphate solutions.* Carbohydrate Polymers, 2001. **46**(1): p. 39-47.

98. Cheng, Y.-H., et al., *Thermosensitive Chitosan–Gelatin–Glycerol Phosphate Hydrogels as a Cell Carrier for Nucleus Pulposus Regeneration: An In Vitro Study.* Tissue Engineering Part A, 2010. **16**(2): p. 695-703.
99. Chenite, A., et al., *Novel injectable neutral solutions of chitosan form biodegradable gels in situ.* Biomaterials, 2000. **21**(21): p. 2155-2161.
100. Berger, J., et al., *Structure and interactions in chitosan hydrogels formed by complexation or aggregation for biomedical applications.* European Journal of Pharmaceutics and Biopharmaceutics, 2004. **57**(1): p. 35-52.
101. Brack, H.P., S.A. Tirmizi, and W.M. Risen Jr, *A spectroscopic and viscometric study of the metal ion-induced gelation of the biopolymer chitosan.* Polymer, 1997. **38**(10): p. 2351-2362.
102. Pieróg, M., M. Gierszewska-Drużyńska, and J. Ostrowska-Czubenko, *Effect of ionic crosslinking agents on swelling behaviour of chitosan hydrogel membranes*, in *Progress on chemistry and application of chitin and its derivatives, Volume XIV*, M.M. Jaworska, Editor. 2009, Media-Press: Lodz, Poland.
103. Sæther, H.V., et al., *Polyelectrolyte complex formation using alginate and chitosan.* Carbohydrate Polymers, 2008. **74**(4): p. 813-821.
104. El-Sherbiny, I.M., *Enhanced pH-responsive carrier system based on alginate and chemically modified carboxymethyl chitosan for oral delivery of protein drugs: Preparation and in-vitro assessment.* Carbohydrate Polymers, 2010. **80**(4): p. 1125-1136.
105. Lin, J., et al., *In Vitro and in Vivo characterization of alginate-chitosan-alginate artificial microcapsules for therapeutic oral delivery of live bacterial cells.* Journal of Bioscience and Bioengineering, 2008. **105**(6): p. 660-665.
106. Hamman, J.H., *Chitosan Based Polyelectrolyte Complexes as Potential Carrier Materials in Drug Delivery Systems.* Marine Drugs, 2010. **8**(4): p. 1305-1322.
107. Vrana, N.E., et al., *Characterization of Poly(vinyl alcohol)/Chitosan Hydrogels as Vascular Tissue Engineering Scaffolds.* Macromolecular Symposia, 2008. **269**(1): p. 106-110.
108. Li, Y., et al., *A novel pH-sensitive and freeze-thawed carboxymethyl chitosan/poly(vinyl alcohol) blended hydrogel for protein delivery.* Polymer International, 2009. **58**(10): p. 1120-1125.
109. Liu, Y., et al., *Physically crosslinked composite hydrogels of PVA with natural macromolecules: Structure, mechanical properties, and endothelial cell compatibility.* Journal of Biomedical Materials Research Part B: Applied Biomaterials, 2009. **90B**(2): p. 492-502.
110. Yang, X., et al., *Investigation of PVA/ws-chitosan hydrogels prepared by combined γ-irradiation and freeze-thawing.* Carbohydrate Polymers, 2008. **73**(3): p. 401-408.
111. Qu, X., A. Wirsén, and A.C. Albertsson, *Novel pH-sensitive chitosan hydrogels: swelling behavior and states of water.* Polymer, 2000. **41**(12): p. 4589-4598.
112. Tan, H., et al., *Injectable in situ forming biodegradable chitosan–hyaluronic acid based hydrogels for cartilage tissue engineering.* Biomaterials, 2009. **30**(13): p. 2499-2506.
113. Wu, Z.M., et al., *Disulfide-crosslinked chitosan hydrogel for cell viability and controlled protein release.* European Journal of Pharmaceutical Sciences, 2009. **37**(3–4): p. 198-206.
114. Lee, S.J., S.S. Kim, and Y.M. Lee, *Interpenetrating polymer network hydrogels based on poly(ethylene glycol) macromer and chitosan.* Carbohydrate Polymers, 2000. **41**(2): p. 197-205.

115. Şenel, S., et al., *Enhancing effect of chitosan on peptide drug delivery across buccal mucosa.* Biomaterials, 2000. **21**(20): p. 2067-2071.
116. Bernkop-Schnürch, A., *Mucoadhesive systems in oral drug delivery.* Drug Discovery Today: Technologies, 2005. **2**(1): p. 83-87.
117. Scrivener, C.A. and C.W. Schantz, *Penicillin; new methods for its use in dentistry.* J Am Dent Assoc, 1947. **35**(9): p. 644-647.
118. Nagai, T., *Adhesive topical drug delivery system.* Journal of Controlled Release, 1985. **2**(0): p. 121-134.
119. Lee, J.W., J.H. Park, and J.R. Robinson, *Bioadhesive-based dosage forms: The next generation.* Journal of Pharmaceutical Sciences, 2000. **89**(7): p. 850-866.
120. Voiutskii, S.S., *Autohesion and adhesion of high polymers*. 1963, New York: Wiley.
121. Kinloch, A.J., *The science of adhesion.* Journal of Materials Science, 1980. **15**(9): p. 2141-2166.
122. Ponchel, G., et al., *Bioadhesive analysis of controlled-release systems. I. Fracture and interpenetration analysis in poly(acrylic acid)-containing systems.* Journal of Controlled Release, 1987. **5**(2): p. 129-141.
123. Boddupalli, B.M., et al., *Mucoadhesive drug delivery system: An overview.* Journal of Advanced Pharmaceutical Technology & Research, 2010. **1**(4): p. 381-387.
124. Liu, P. and T.R. Krishnan, *Alginate-Pectin-Poly-L-lysine Particulate as a Potential Controlled Release Formulation.* Journal of Pharmacy and Pharmacology, 1999. **51**(2): p. 141-149.
125. Sadeghi, A.M.M., et al., *Permeation enhancer effect of chitosan and chitosan derivatives: Comparison of formulations as soluble polymers and nanoparticulate systems on insulin absorption in Caco-2 cells.* European Journal of Pharmaceutics and Biopharmaceutics, 2008. **70**(1): p. 270-278.
126. Grabovac, V., D. Guggi, and A. Bernkop-Schnürch, *Comparison of the mucoadhesive properties of various polymers.* Advanced Drug Delivery Reviews, 2005. **57**(11): p. 1713-1723.
127. Kast, C.E. and A. Bernkop-Schnürch, *Thiolated polymers — thiomers: development and in vitro evaluation of chitosan–thioglycolic acid conjugates.* Biomaterials, 2001. **22**(17): p. 2345-2352.
128. Bernkop-Schnürch, A., U.M. Brandt, and A.E. Clausen, *Synthesis and in vitro evaluation of chitosan-cysteine conjugates.* Scientia Pharmaceutica, 1999. **67**: p. 196-208.
129. Kafedjiiski, K., et al., *Synthesis and in Vitro Evaluation of a Novel Chitosan–Glutathione Conjugate.* Pharmaceutical Research, 2005. **22**(9): p. 1480-1488.
130. Kafedjiiski, K., et al., *Improved synthesis and in vitro characterization of chitosan–thioethylamidine conjugate.* Biomaterials, 2006. **27**(1): p. 127-135.
131. Bernkop-Schnürch, A., M. Hornof, and T. Zoidl, *Thiolated polymers—thiomers: synthesis and in vitro evaluation of chitosan–2-iminothiolane conjugates.* International Journal of Pharmaceutics, 2003. **260**(2): p. 229-237.
132. Jintapattanakit, A., V.B. Junyaprasert, and T. Kissel, *The role of mucoadhesion of trimethyl chitosan and PEGylated trimethyl chitosan nanocomplexes in insulin uptake.* Journal of Pharmaceutical Sciences, 2009. **98**(12): p. 4818-4830.
133. Sandri, G., et al., *Buccal penetration enhancement properties of N-trimethyl chitosan: Influence of quaternization degree on absorption of a high molecular weight molecule.* International Journal of Pharmaceutics, 2005. **297**(1–2): p. 146-155.

134. Andreas, B.-S., *Mucoadhesive Polymers*, in *Polymeric Biomaterials, Revised and Expanded*. 2001, CRC Press.
135. Kesavan, K., G. Nath, and J.K. Pandit, *Sodium Alginate Based Mucoadhesive System for Gatifloxacin and Its In Vitro Antibacterial Activity.* Scientia Pharmaceutica, 2010. **78**(4): p. 941-957.
136. Ahn, J.S., H.K. Choi, and C.S. Cho, *A novel mucoadhesive polymer prepared by template polymerization of acrylic acid in the presence of chitosan.* Biomaterials, 2001. **22**(9): p. 923-8.
137. Leitner, V.M., M.K. Marschutz, and A. Bernkop-Schnurch, *Mucoadhesive and cohesive properties of poly(acrylic acid)-cysteine conjugates with regard to their molecular mass.* Eur J Pharm Sci, 2003. **18**(1): p. 89-96.
138. Jones, D.S., et al., *An examination of the rheological and mucoadhesive properties of poly(acrylic acid) organogels designed as platforms for local drug delivery to the oral cavity.* J Pharm Sci, 2007. **96**(10): p. 2632-46.
139. Choi, H.-K., et al., *A novel mucoadhesive polymer prepared by template polymerization of acrylic acid in the presence of poly (ethylene glycol).* Journal of Applied Polymer Science, 1999. **73**(13): p. 2749-2754.
140. Kim, T.H., et al., *A novel mucoadhesive polymer film composed of carbopol, poloxamer and hydroxypropylmethylcellulose.* Arch Pharm Res, 2007. **30**(3): p. 381-6.
141. Karavas, E., E. Georgarakis, and D. Bikiaris, *Application of PVP/HPMC miscible blends with enhanced mucoadhesive properties for adjusting drug release in predictable pulsatile chronotherapeutics.* European Journal of Pharmaceutics and Biopharmaceutics, 2006. **64**(1): p. 115-126.
142. Park, J.S., et al., *In situ gelling and mucoadhesive polymer vehicles for controlled intranasal delivery of plasmid DNA.* J Biomed Mater Res, 2002. **59**(1): p. 144-51.
143. Mongia, N.K., K.S. Anseth, and N.A. Peppas, *Mucoadhesive poly(vinyl alcohol) hydrogels produced by freezing/thawing processes: applications in the development of wound healing systems.* J Biomater Sci Polym Ed, 1996. **7**(12): p. 1055-64.
144. Wang, J., et al., *Evaluation of gastric mucoadhesive properties of aminated gelatin microspheres.* Journal of Controlled Release, 2001. **73**(2–3): p. 223-231.
145. Bonferoni, M.C., et al., *Carrageenan–gelatin mucoadhesive systems for ion-exchange based ophthalmic delivery: in vitro and preliminary in vivo studies.* European Journal of Pharmaceutics and Biopharmaceutics, 2004. **57**(3): p. 465-472.
146. Majithiya, R.J. and R.S. Murthy, *Chitosan-based mucoadhesive microspheres of clarithromycin as a delivery system for antibiotic to stomach.* Curr Drug Deliv, 2005. **2**(3): p. 235-42.
147. Yin, L., et al., *Drug permeability and mucoadhesion properties of thiolated trimethyl chitosan nanoparticles in oral insulin delivery.* Biomaterials, 2009. **30**(29): p. 5691-700.
148. Millotti, G., et al., *In Vivo Evaluation of Thiolated Chitosan Tablets for Oral Insulin Delivery.* Journal of Pharmaceutical Sciences, 2014. **103**(10): p. 3165-3170.
149. Bernkop-Schnürch, A., *Thiomers: A new generation of mucoadhesive polymers.* Advanced Drug Delivery Reviews, 2005. **57**(11): p. 1569-1582.
150. Ahmed, A., et al., *Mucoadhesive Nanoparticulate System for Oral Drug Delivery: A Review.* Current Drug Therapy, 2002. **7**: p. 42-55.

151. Alur, H.H., et al., *Evaluation of a novel, natural oligosaccharide gum as a sustained-release and mucoadhesive component of calcitonin buccal tablets.* Journal of Pharmaceutical Sciences, 1999. **88**(12): p. 1313-1319.
152. Charde, S., et al., *Development and Evaluation of Buccoadhesive Controlled Release Tablets of Lercanidipine.* AAPS PharmSciTech, 2008. **9**(1): p. 182-190.
153. Kohda, Y., et al., *Controlled release of lidocaine hydrochloride from buccal mucosa-adhesive films with solid dispersion.* International Journal of Pharmaceutics, 1997. **158**(2): p. 147-155.
154. Burgalassi, S., et al., *Development and in vitro/in vivo testing of mucoadhesive buccal patches releasing benzydamine and lidocaine.* International Journal of Pharmaceutics, 1996. **133**(1–2): p. 1-7.
155. Cavallari, C., A. Fini, and F. Ospitali, *Mucoadhesive multiparticulate patch for the intrabuccal controlled delivery of lidocaine.* Eur J Pharm Biopharm, 2012.
156. Jacques, Y., et al., *In vivo evaluation of hydrophilic and hydrophobic mucoadhesive semi-solid formulations containing sucralfate and lidocaine for intraoral use.* European Journal of Pharmaceutics and Biopharmaceutics, 1997. **43**(1): p. 59-63.
157. Park, C.R. and D.L. Munday, *Development and evaluation of a biphasic buccal adhesive tablet for nicotine replacement therapy.* International Journal of Pharmaceutics, 2002. **237**(1–2): p. 215-226.
158. Ìkinci, G., et al., *Development of a buccal bioadhesive nicotine tablet formulation for smoking cessation.* International Journal of Pharmaceutics, 2004. **277**(1–2): p. 173-178.
159. Rao, S., et al., *A novel tri-layered buccal mucoadhesive patch for drug delivery: assessment of nicotine delivery.* Journal of Pharmacy and Pharmacology, 2011. **63**(6): p. 794-799.
160. Abu-Huwaij, R., et al., *Formulation and In Vitro Evaluation of Xanthan Gum or Carbopol 934-Based Mucoadhesive Patches, Loaded with Nicotine.* AAPS PharmSciTech, 2011. **12**(1): p. 21-27.
161. Abruzzo, A., et al., *Mucoadhesive chitosan/gelatin films for buccal delivery of propranolol hydrochloride.* Carbohydrate Polymers, 2012. **87**(1): p. 581-588.
162. Patel, V.M., et al., *Mucoadhesive bilayer tablets of propranolol hydrochloride.* AAPS PharmSciTech, 2007. **8**(3): p. E77.
163. Maurya, S.K., V. Bali, and K. Pathak, *Bilayered transmucosal drug delivery system of pravastatin sodium: statistical optimization, in vitro, ex vivo, in vivo and stability assessment.* Drug Deliv, 2012. **19**(1): p. 45-57.
164. Li, C., P.P. Bhatt, and T.P. Johnston, *Transmucosal delivery of oxytocin to rabbits using a mucoadhesive buccal patch.* Pharm Dev Technol, 1997. **2**(3): p. 265-74.
165. Alur, H.H., et al., *Transmucosal sustained-delivery of chlorpheniramine maleate in rabbits using a novel, natural mucoadhesive gum as an excipient in buccal tablets.* Int J Pharm, 1999. **188**(1): p. 1-10.
166. Han, R.Y., et al., *Mucoadhesive buccal disks for novel nalbuphine prodrug controlled delivery: effect of formulation variables on drug release and mucoadhesive performance.* Int J Pharm, 1999. **177**(2): p. 201-9.
167. Nafee, N.A., et al., *Mucoadhesive buccal patches of miconazole nitrate: in vitro/in vivo performance and effect of ageing.* Int J Pharm, 2003. **264**(1-2): p. 1-14.
168. Perioli, L., et al., *Novel mucoadhesive buccal formulation containing metronidazole for the treatment of periodontal disease.* Journal of Controlled Release, 2004. **95**(3): p. 521-533.

169. Diaz del Consuelo, I., et al., *Ex vivo evaluation of bioadhesive films for buccal delivery of fentanyl.* Journal of Controlled Release, 2007. **122**(2): p. 135-140.
170. Perioli, L., et al., *Development of mucoadhesive patches for buccal administration of ibuprofen.* Journal of Controlled Release, 2004. **99**(1): p. 73-82.
171. Choi, H.-G., et al., *Formulation and in vivo evaluation of omeprazole buccal adhesive tablet.* Journal of Controlled Release, 2000. **68**(3): p. 405-412.
172. Jay, S., et al., *Transmucosal delivery of testosterone in rabbits using novel bi-layer mucoadhesive wax-film composite disks.* J Pharm Sci, 2002. **91**(9): p. 2016-25.
173. Cilurzo, F., et al., *A new mucoadhesive dosage form for the management of oral lichen planus: Formulation study and clinical study.* European Journal of Pharmaceutics and Biopharmaceutics, 2010. **76**(3): p. 437-442.
174. Wu, X., et al., *Mucoadhesive Fenretinide Patches for Site-Specific Chemoprevention of Oral Cancer: Enhancement of Oral Mucosal Permeation of Fenretinide by Coincorporation of Propylene Glycol and Menthol.* Molecular Pharmaceutics, 2012. **9**(4): p. 937-945.
175. Choi, H.-G., Y.-K. Oh, and C.-K. Kim, *In situ gelling and mucoadhesive liquid suppository containing acetaminophen: enhanced bioavailability.* International Journal of Pharmaceutics, 1998. **165**(1): p. 23-32.
176. Ryu, J.-M., et al., *Increased bioavailability of propranolol in rats by retaining thermally gelling liquid suppositories in the rectum.* Journal of Controlled Release, 1999. **59**(2): p. 163-172.
177. Choi, H.-G., et al., *Development of in situ-gelling and mucoadhesive acetaminophen liquid suppository.* International Journal of Pharmaceutics, 1998. **165**(1): p. 33-44.
178. Ramadan, E.M., T.M. Borg, and M.O. Elkayal, *Formulation and evaluation of novel mucoadhesive ketorolac tromethamine liquid suppository.* African Journal of Pharmacy and Pharmacology, 2009. **3**(4): p. 124-132.
179. Ban, E. and C.-K. Kim, *Design and evaluation of ondansetron liquid suppository for the treatment of emesis.* Archives of Pharmacal Research, 2013. **36**(5): p. 586-592.
180. Attama, A., M. Adikwu, and O. Okpi, *Bioavailability Of Metronidazole From In Situ Gelling And Mucoadhesive Suppositories Formulated With Carbopol ETD 2020.* Bio-Research, 2004. **2**(1): p. 75-81.
181. Barakat, N.S., *In Vitro and In Vivo Characteristics of a Thermogelling Rectal Delivery System of Etodolac.* AAPS PharmSciTech, 2009. **10**(3): p. 724-731.
182. Waite, J.H. and M.L. Tanzer, *Polyphenolic Substance of Mytilus edulis: Novel Adhesive Containing L-Dopa and Hydroxyproline.* Science, 1981. **212**(4498): p. 1038-40.
183. Lin, Q., et al., *Adhesion mechanisms of the mussel foot proteins mfp-1 and mfp-3.* Proceedings of the National Academy of Sciences, 2007. **104**(10): p. 3782-3786.
184. Lee, H., N.F. Scherer, and P.B. Messersmith, *Single-molecule mechanics of mussel adhesion.* Proc Natl Acad Sci U S A, 2006. **103**(35): p. 12999-3003.
185. Silverman, H. and F. Roberto, *Understanding Marine Mussel Adhesion.* Marine Biotechnology, 2007. **9**(6): p. 661-681.
186. Waite, J.H. and X. Qin, *Polyphosphoprotein from the adhesive pads of Mytilus edulis.* Biochemistry, 2001. **40**(9): p. 2887-93.
187. Lee, H., et al., *Mussel-inspired surface chemistry for multifunctional coatings.* Science, 2007. **318**(5849): p. 426-30.

188. Lee, B.P., et al., *Mussel-Inspired Adhesives and Coatings.* Annu Rev Mater Res, 2011. **41**: p. 99-132.
189. Waite, J.H., et al., *Mussel Adhesion: Finding the Tricks Worth Mimicking.* The Journal of Adhesion, 2005. **81**(3-4): p. 297-317.
190. Deming, T.J., *Mussel byssus and biomolecular materials.* Current Opinion in Chemical Biology, 1999. **3**(1): p. 100-105.
191. Suhre, M.H., et al., *Structural and functional features of a collagen-binding matrix protein from the mussel byssus.* Nat Commun, 2014. **5**: p. 3392.
192. Lee, B., J. Dalsin, and P. Messersmith, *Biomimetic Adhesive Polymers Based on Mussel Adhesive Proteins*, in *Biological Adhesives*, A. Smith and J. Callow, Editors. 2006, Springer Berlin Heidelberg. p. 257-278.
193. Schweigert, N., A.J.B. Zehnder, and R.I.L. Eggen, *Chemical properties of catechols and their molecular modes of toxic action in cells, from microorganisms to mammals.* Environmental Microbiology, 2001. **3**(2): p. 81-91.
194. Yu, J., et al., *Adhesion of Mussel Foot Protein-3 to TiO2 Surfaces: the Effect of pH.* Biomacromolecules, 2013.
195. Wu, J., et al., *Mussel-Inspired Chemistry for Robust and Surface-Modifiable Multilayer Films.* Langmuir, 2011. **27**(22): p. 13684-13691.
196. Holten-Andersen, N., et al., *pH-induced metal-ligand cross-links inspired by mussel yield self-healing polymer networks with near-covalent elastic moduli.* Proceedings of the National Academy of Sciences of the United States of America, 2011. **108**(7): p. 2651-2655.
197. Zeng, H., et al., *Strong reversible Fe(3+)-mediated bridging between dopa-containing protein films in water.* Proceedings of the National Academy of Sciences of the United States of America, 2010. **107**(29): p. 12850-12853.
198. Monahan, J. and J.J. Wilker, *Cross-Linking the Protein Precursor of Marine Mussel Adhesives: Bulk Measurements and Reagents for Curing.* Langmuir, 2004. **20**(9): p. 3724-3729.
199. Coombs, T.L. and P.J. Keller, *Mytilus byssal threads as an environmental marker for metals.* Aquatic Toxicology, 1981. **1**(5–6): p. 291-300.
200. Waite, J.H. and C.C. Broomell, *Changing environments and structure–property relationships in marine biomaterials.* The Journal of Experimental Biology, 2012. **215**(6): p. 873-883.
201. Ayyadurai, N., et al., *Bioconjugation of L-3,4-dihydroxyphenylalanine containing protein with a polysaccharide.* Bioconjug Chem, 2011. **22**(4): p. 551-5.
202. Nunes, C., et al., *Chitosan–caffeic acid–genipin films presenting enhanced antioxidant activity and stability in acidic media.* Carbohydrate Polymers, 2013. **91**(1): p. 236-243.
203. Brzonova, I., et al., *Enzymatic synthesis of catechol and hydroxyl-carboxic acid functionalized chitosan microspheres for iron overload therapy.* European Journal of Pharmaceutics and Biopharmaceutics, 2011. **79**(2): p. 294-303.
204. Yang, K., et al., *Polydopamine-mediated surface modification of scaffold materials for human neural stem cell engineering.* Biomaterials, 2012. **33**(29): p. 6952-6964.
205. Matos-Pérez, C.R., J.D. White, and J.J. Wilker, *Polymer Composition and Substrate Influences on the Adhesive Bonding of a Biomimetic, Cross-Linking Polymer.* Journal of the American Chemical Society, 2012. **134**(22): p. 9498-9505.

206. Yamada, K., et al., *Chitosan Based Water-Resistant Adhesive. Analogy to Mussel Glue.* Biomacromolecules, 2000. **1**(2): p. 252-258.
207. Lee, B.P., et al., *Rapid Gel Formation and Adhesion in Photocurable and Biodegradable Block Copolymers with High DOPA Content.* Macromolecules, 2006. **39**(5): p. 1740-1748.
208. Guvendiren, M., P.B. Messersmith, and K.R. Shull, *Self-Assembly and Adhesion of DOPA-Modified Methacrylic Triblock Hydrogels.* Biomacromolecules, 2007. **9**(1): p. 122-128.
209. Ochs, C.J., et al., *Dopamine-Mediated Continuous Assembly of Biodegradable Capsules.* Chemistry of Materials, 2011. **23**(13): p. 3141-3143.
210. Waite, J.H., *Surface chemistry: Mussel power.* Nat Mater, 2008. **7**(1): p. 8-9.
211. Sileika, T.S., et al., *Antibacterial performance of polydopamine-modified polymer surfaces containing passive and active components.* ACS Appl Mater Interfaces, 2011. **3**(12): p. 4602-10.
212. Feng, J.-J., et al., *One-step synthesis of monodisperse polydopamine-coated silver core-shell nanostructures for enhanced photocatalysis.* New Journal of Chemistry, 2012. **36**(1): p. 148-154.
213. Akin, M.S., et al., *Large area uniform deposition of silver nanoparticles through bio-inspired polydopamine coating on silicon nanowire arrays for practical SERS applications.* Journal of Materials Chemistry B, 2014. **2**(30): p. 4894-4900.
214. Huang, K.-J., et al., *Electrochemical biosensor based on silver nanoparticles–polydopamine–graphene nanocomposite for sensitive determination of adenine and guanine.* Talanta, 2013. **114**(0): p. 43-48.
215. Lee, B.P., J.L. Dalsin, and P.B. Messersmith, *Synthesis and Gelation of DOPA-Modified Poly(ethylene glycol) Hydrogels.* Biomacromolecules, 2002. **3**(5): p. 1038-1047.
216. Min, Y. and P.T. Hammond, *Catechol-Modified Polyions in Layer-by-Layer Assembly to Enhance Stability and Sustain Release of Biomolecules: A Bioinspired Approach.* Chemistry of Materials, 2011. **23**(24): p. 5349-5357.
217. Fullenkamp, D.E., et al., *Mussel-inspired silver-releasing antibacterial hydrogels.* Biomaterials, 2012. **33**(15): p. 3783-3791.
218. Oh, Y.J., et al., *Bio-inspired catechol chemistry: a new way to develop a re-moldable and injectable coacervate hydrogel.* Chemical Communications, 2012. **48**(97): p. 11895-11897.
219. Lee, B.P., et al., *Mussel-Inspired Adhesives and Coatings.* Annual Review of Materials Research, 2011. **41**(1): p. 99-132.
220. Schnurrer, J. and C.-M. Lehr, *Mucoadhesive properties of the mussel adhesive protein.* International Journal of Pharmaceutics, 1996. **141**(1–2): p. 251-256.
221. Deacon, M.P., et al., *Structure and mucoadhesion of mussel glue protein in dilute solution.* Biochemistry, 1998. **37**(40): p. 14108-12.
222. Schweigert, N., et al., *DNA degradation by the mixture of copper and catechol is caused by DNA-copper-hydroperoxo complexes, probably DNA-Cu(I)OOH.* Environ Mol Mutagen, 2000. **36**(1): p. 5-12.
223. Mitsuda, H., K. Murakami, and F. Kawai, *Effect of Chlorophenol Analogues on the Oxidative Phosphorylation in Rat Liver Mitochondria.* Agricultural and Biological Chemistry, 1963. **27**(5): p. 366-372.
224. Brubaker, C.E., et al., *Biological performance of mussel-inspired adhesive in extrahepatic islet transplantation.* Biomaterials, 2010. **31**(3): p. 420-7.
225. Hong, S., et al., *Attenuation of the in vivo toxicity of biomaterials by polydopamine surface modification.* Nanomedicine, 2011. **6**(5): p. 793-801.

226. Toegel, S., et al., *Lectin binding studies on C-28/I2 and T/C-28a2 chondrocytes provide a basis for new tissue engineering and drug delivery perspectives in cartilage research.* Journal of Controlled Release, 2007. **117**(1): p. 121-129.
227. Serra, L., J. Doménech, and N. Peppas, *Engineering Design and Molecular Dynamics of Mucoadhesive Drug Delivery Systems as Targeting Agents.* European journal of pharmaceutics and biopharmaceutics : official journal of Arbeitsgemeinschaft fur Pharmazeutische Verfahrenstechnik e.V, 2009. **71**(3): p. 519-528.
228. Liu, Y., et al., *Bioadhesion and enhanced bioavailability by wheat germ agglutinin-grafted lipid nanoparticles for oral delivery of poorly water-soluble drug bufalin.* Int J Pharm, 2011. **419**(1-2): p. 260-5.
229. das Neves, J., et al., *Mucoadhesive nanomedicines: characterization and modulation of mucoadhesion at the nanoscale.* Expert Opinion on Drug Delivery, 2011. **8**(8): p. 1085-1104.
230. Davidovich-Pinhas, M. and H. Bianco-Peled, *Mucoadhesion: a review of characterization techniques.* Expert Opinion on Drug Delivery, 2010. **7**(2): p. 259-271.
231. Andrews, G.P., T.P. Laverty, and D.S. Jones, *Mucoadhesive polymeric platforms for controlled drug delivery.* European Journal of Pharmaceutics and Biopharmaceutics, 2009. **71**(3): p. 505-518.
232. Bonferoni, M.C., et al., *Chitosan and its salts for mucosal and transmucosal delivery.* Expert Opinion on Drug Delivery, 2009. **6**(9): p. 923-939.
233. Chaudhury, A. and S. Das, *Recent Advancement of Chitosan-Based Nanoparticles for Oral Controlled Delivery of Insulin and Other Therapeutic Agents.* AAPS PharmSciTech, 2011. **12**(1): p. 10-20.
234. George, M. and T.E. Abraham, *Polyionic hydrocolloids for the intestinal delivery of protein drugs: Alginate and chitosan — a review.* Journal of Controlled Release, 2006. **114**(1): p. 1-14.
235. Leitner, V.M., G.F. Walker, and A. Bernkop-Schnürch, *Thiolated polymers: evidence for the formation of disulphide bonds with mucus glycoproteins.* European Journal of Pharmaceutics and Biopharmaceutics, 2003. **56**(2): p. 207-214.
236. Barthelmes, J., et al., *Development of a mucoadhesive nanoparticulate drug delivery system for a targeted drug release in the bladder.* International Journal of Pharmaceutics, 2011. **416**(1): p. 339-345.
237. Talaei, F., et al., *Thiolated chitosan nanoparticles as a delivery system for antisense therapy: evaluation against EGFR in T47D breast cancer cells.* International Journal of Nanomedicine, 2011. **6**: p. 1963-1975.
238. Yang, L.-q., et al., *Ophthalmic drug-loaded N,O-carboxymethyl chitosan hydrogels: synthesis, in vitro and in vivo evaluation.* Acta Pharmacol Sin, 2010. **31**(12): p. 1625-1634.
239. Waite, J.H., *Nature's underwater adhesive specialist.* International Journal of Adhesion and Adhesives, 1987. **7**(1): p. 9-14.
240. Lee, H., N.F. Scherer, and P.B. Messersmith, *Single-molecule mechanics of mussel adhesion.* Proceedings of the National Academy of Sciences of the United States of America, 2006. **103**(35): p. 12999-13003.
241. Fan, X., et al., *Biomimetic Anchor for Surface-Initiated Polymerization from Metal Substrates.* Journal of the American Chemical Society, 2005. **127**(45): p. 15843-15847.

242. Jewett, S.L., L.J. Eddy, and P. Hochstein, *Is the autoxidation of catecholamines involved in ischemia-reperfusion injury?* Free Radical Biology and Medicine, 1989. **6**(2): p. 185-188.
243. Yu, J., et al., *Effects of Interfacial Redox in Mussel Adhesive Protein Films on Mica.* Advanced Materials, 2011. **23**(20): p. 2362-2366.
244. Alegria, A.E., et al., *Thiols oxidation and covalent binding of BSA by cyclolignanic quinones are enhanced by the magnesium cation.* Free radical research, 2008. **42**(1): p. 70-81.
245. Guvendiren, M., et al., *Adhesion of DOPA-Functionalized Model Membranes to Hard and Soft Surfaces.* The Journal of adhesion, 2009. **85**(9): p. 631-645.
246. Li, J. and B.M. Christensen, *Effect of pH on the oxidation pathway of dopamine and dopa.* Journal of Electroanalytical Chemistry, 1994. **375**(1–2): p. 219-231.
247. Bisaglia, M., S. Mammi, and L. Bubacco, *Kinetic and Structural Analysis of the Early Oxidation Products of Dopamine.* Journal of Biological Chemistry, 2007. **282**(21): p. 15597-15605.
248. Barreto, W.J., S. Ponzoni, and P. Sassi, *A Raman and UV-Vis study of catecholamines oxidized with Mn(III).* Spectrochimica Acta Part A: Molecular and Biomolecular Spectroscopy, 1998. **55**(1): p. 65-72.
249. Peppas, N.A., *Hydrogels and drug delivery.* Current Opinion in Colloid & Interface Science, 1997. **2**(5): p. 531-537.
250. Park, H., K. Park, and D. Kim, *Preparation and swelling behavior of chitosan-based superporous hydrogels for gastric retention application.* Journal of Biomedical Materials Research Part A, 2006. **76A**(1): p. 144-150.
251. Solano-Muñoz, F., R. Peñafiel, and J.D. Galindo, *An electrometric method for the determination of tyrosinase activity.* Biochemical Journal, 1985. **229**(3): p. 573-578.
252. Land, E.J., C.A. Ramsden, and P.A. Riley, *Ortho-quinone Amines and Derivatives: The Influence of Structure on the Rates and Modes of Intramolecular Reaction.* ARKIVOC (Gainesville, FL, United States), 2007: p. 23-36.
253. Ritger, P.L. and N.A. Peppas, *A simple equation for description of solute release I. Fickian and non-fickian release from non-swellable devices in the form of slabs, spheres, cylinders or discs.* Journal of Controlled Release, 1987. **5**(1): p. 23-36.
254. LeWitt, P.A., J. Dubow, and C. Singer, *Is levodopa toxic? Insights from a brain bank.* Neurology, 2011. **77**(15): p. 1414-5.
255. Basma, A.N., et al., *l-DOPA Cytotoxicity to PC12 Cells in Culture Is via Its Autoxidation.* Journal of Neurochemistry, 1995. **64**(2): p. 825-832.
256. Koshimura, K., et al., *Effects of dopamine and L-DOPA on survival of PC12 cells.* Journal of Neuroscience Research, 2000. **62**(1): p. 112-119.
257. Moridani, M.Y., et al., *Quantitative structure toxicity relationships for catechols in isolated rat hepatocytes.* Chemico-Biological Interactions, 2004. **147**(3): p. 297-307.
258. Hong, S., et al., *Non-Covalent Self-Assembly and Covalent Polymerization Co-Contribute to Polydopamine Formation.* Advanced Functional Materials, 2012: p. n/a-n/a.
259. Ku, S.H. and C.B. Park, *Human endothelial cell growth on mussel-inspired nanofiber scaffold for vascular tissue engineering.* Biomaterials, 2010. **31**(36): p. 9431-9437.
260. Proudfoot, G. and I. Ritchie, *A cyclic voltammetric study of some 4-substituted Benzene-1,2-diols.* Australian Journal of Chemistry, 1983. **36**(5): p. 885-894.

261. Graham, D.G. and P.W. Jeffs, *The role of 2,4,5-trihydroxyphenylalanine in melanin biosynthesis.* J Biol Chem, 1977. **252**(16): p. 5729-34.
262. Li, J., F.-J. Zhang, and B.M. Christensen, *Involvement of lactones in the formation of 6-hydroxydopa and 6-hydroxyhydrocaffeic acid during oxidation of dopa and hydrocaffeic acid.* Journal of Electroanalytical Chemistry, 1996. **412**(1–2): p. 19-29.
263. Agha, A., D. Makris, and P. Kefalas, *Hydrocaffeic acid oxidation by a peroxidase homogenate from onion solid wastes.* European Food Research and Technology, 2008. **227**(5): p. 1379-1386.
264. Jones, D.S., A.D. Woolfson, and A.F. Brown, *Textural, viscoelastic and mucoadhesive properties of pharmaceutical gels composed of cellulose polymers.* International Journal of Pharmaceutics, 1997. **151**(2): p. 223-233.
265. Thirawong, N., et al., *Mucoadhesive properties of various pectins on gastrointestinal mucosa: An in vitro evaluation using texture analyzer.* European Journal of Pharmaceutics and Biopharmaceutics, 2007. **67**(1): p. 132-140.
266. das Neves, J., M.H. Amaral, and M.F. Bahia, *Performance of an in vitro mucoadhesion testing method for vaginal semisolids: Influence of different testing conditions and instrumental parameters.* European Journal of Pharmaceutics and Biopharmaceutics, 2008. **69**(2): p. 622-632.
267. Leung, S.-H.S. and J.R. Robinson, *Polymer structure features contributing to mucoadhesion. II.* Journal of Controlled Release, 1990. **12**(3): p. 187-194.
268. Yamada, K., et al., *Application of enzymatically gelled chitosan solutions to water-resistant adhesives.* Journal of Applied Polymer Science, 2007. **104**(3): p. 1818-1827.
269. Vold, I.M. and B.E. Christensen, *Periodate oxidation of chitosans with different chemical compositions.* Carbohydr Res, 2005. **340**(4): p. 679-84.
270. Wilson, D.S., et al., *Orally delivered thioketal nanoparticles loaded with TNF-α–siRNA target inflammation and inhibit gene expression in the intestines.* Nat Mater, 2010. **9**(11): p. 923-928.
271. Smart, J.D., *Buccal drug delivery.* Expert Opinion on Drug Delivery, 2005. **2**(3): p. 507-517.
272. Shojaei, A.H., *Buccal mucosa as a route for systemic drug delivery: a review.* J Pharm Pharm Sci, 1998. **1**(1): p. 15-30.
273. Squier, C.A. and M.J. Kremer, *Biology of Oral Mucosa and Esophagus.* JNCI Monographs, 2001. **2001**(29): p. 7-15.
274. Lesch, C.A., et al., *The Permeability of Human Oral Mucosa and Skin to Water.* Journal of Dental Research, 1989. **68**(9): p. 1345-1349.
275. Patel, V.F., F. Liu, and M.B. Brown, *Modeling the oral cavity: In vitro and in vivo evaluations of buccal drug delivery systems.* Journal of Controlled Release, 2012. **161**(3): p. 746-756.
276. Patel, V.F., F. Liu, and M.B. Brown, *Advances in oral transmucosal drug delivery.* Journal of Controlled Release, 2011. **153**(2): p. 106-116.
277. Darwish, M., et al., *Absolute and relative bioavailability of fentanyl buccal tablet and oral transmucosal fentanyl citrate.* J Clin Pharmacol, 2007. **47**(3): p. 343-50.
278. Xu, H.B., et al., *Hypoglycaemic effect of a novel insulin buccal formulation on rabbits.* Pharmacol Res, 2002. **46**(5): p. 459-67.

279. El-Samaligy, M.S., N.N. Afifi, and E.A. Mahmoud, *Increasing bioavailability of silymarin using a buccal liposomal delivery system: preparation and experimental design investigation.* Int J Pharm, 2006. **308**(1-2): p. 140-8.
280. Rana, P. and R.S.R. Murthy, *Formulation and evaluation of mucoadhesive buccal films impregnated with carvedilol nanosuspension: a potential approach for delivery of drugs having high first-pass metabolism.* Drug Delivery, 2013. **20**(5): p. 224-235.
281. Aksungur, P., et al., *Chitosan delivery systems for the treatment of oral mucositis: in vitro and in vivo studies.* Journal of Controlled Release, 2004. **98**(2): p. 269-279.
282. Codd, J.E. and P.B. Deasy, *Formulation development and in vivo evaluation of a novel bioadhesive lozenge containing a synergistic combination of antifungal agents.* International Journal of Pharmaceutics, 1998. **173**(1–2): p. 13-24.
283. Sudhakar, Y., K. Kuotsu, and A.K. Bandyopadhyay, *Buccal bioadhesive drug delivery — A promising option for orally less efficient drugs.* Journal of Controlled Release, 2006. **114**(1): p. 15-40.
284. Morales, J.O. and J.T. McConville, *Manufacture and characterization of mucoadhesive buccal films.* Eur J Pharm Biopharm, 2011. **77**(2): p. 187-99.
285. Yehia, S.A., O.N. El-Gazayerly, and E.B. Basalious, *Fluconazole mucoadhesive buccal films: in vitro/in vivo performance.* Curr Drug Deliv, 2009. **6**(1): p. 17-27.
286. Peh, K.K. and C.F. Wong, *Polymeric films as vehicle for buccal delivery: swelling, mechanical, and bioadhesive properties.* J Pharm Pharm Sci, 1999. **2**(2): p. 53-61.
287. Jaipal, A., et al., *Interaction of calcium sulfate with xanthan gum: Effect on in vitro bioadhesion and drug release behavior from xanthan gum based buccal discs of buspirone.* Colloids and Surfaces B: Biointerfaces, 2013. **111**(0): p. 644-650.
288. Langoth, N., et al., *Thiolated chitosans: design and in vivo evaluation of a mucoadhesive buccal peptide drug delivery system.* Pharm Res, 2006. **23**(3): p. 573-9.
289. Martin, L., et al., *Sustained buccal delivery of the hydrophobic drug denbufylline using physically cross-linked palmitoyl glycol chitosan hydrogels.* Eur J Pharm Biopharm, 2003. **55**(1): p. 35-45.
290. Remunan-Lopez, C., et al., *Design and evaluation of chitosan/ethylcellulose mucoadhesive bilayered devices for buccal drug delivery.* J Control Release, 1998. **55**(2-3): p. 143-52.
291. Rinaudo, M., *Chitin and chitosan: Properties and applications.* Progress in Polymer Science, 2006. **31**(7): p. 603-632.
292. Sogias, I.A., A.C. Williams, and V.V. Khutoryanskiy, *Why is Chitosan Mucoadhesive?* Biomacromolecules, 2008. **9**(7): p. 1837-1842.
293. Bernkop-Schnurch, A. and J. Freudl, *Comparative in vitro study of different chitosan-complexing agent conjugates.* Pharmazie, 1999. **54**(5): p. 369-71.
294. Snyder, G.H., et al., *Use of local electrostatic environments of cysteines to enhance formation of a desired species in a reversible disulfide exchange reaction.* Biochim Biophys Acta, 1983. **749**(3): p. 219-26.
295. Leitner, V.M., M.K. Marschütz, and A. Bernkop-Schnürch, *Mucoadhesive and cohesive properties of poly(acrylic acid)-cysteine conjugates with regard to their molecular mass.* European Journal of Pharmaceutical Sciences, 2003. **18**(1): p. 89-96.
296. Lee, H., et al., *Mussel-Inspired Surface Chemistry for Multifunctional Coatings.* Science, 2007. **318**: p. 5.

297. Lee, C., et al., *Bioinspired, Calcium-Free Alginate Hydrogels with Tunable Physical and Mechanical Properties and Improved Biocompatibility.* Biomacromolecules, 2013. **14**(6): p. 2004-2013.
298. Zhang, H., et al., *Mussel-inspired hyperbranched poly(amino ester) polymer as strong wet tissue adhesive.* Biomaterials, 2014. **35**(2): p. 711-719.
299. Xu, J., et al., *Mollusk Glue Inspired Mucoadhesives for Biomedical Applications.* Langmuir, 2012. **28**(39): p. 14010-14017.
300. Kawai, R., S. Fujita, and T. Suzuki, *Simultaneous quantitation of lidocaine and its four metabolites by high-performance liquid chromatography: application to studies on in vitro and in vivo metabolism of lidocaine in rats.* J Pharm Sci, 1985. **74**(11): p. 1219-24.
301. Thompson, S.W., *Selected histochemical and histopathological methods*. 1966: C.C. Thomas.
302. Sheehan, D.C. and B.B. Hrapchak, *Theory and Practice of Histotechnology*. 1987: Battelle Press.
303. Bland, J.M. and D.G. Altman, *Survival probabilities (the Kaplan-Meier method).* BMJ, 1998. **317**(7172): p. 1572-1580.
304. Mi, F.-L., H.-W. Sung, and S.-S. Shyu, *Release of indomethacin from a novel chitosan microsphere prepared by a naturally occurring crosslinker: Examination of crosslinking and polycation–anionic drug interaction.* Journal of Applied Polymer Science, 2001. **81**(7): p. 1700-1711.
305. Butler, M.F., Y.-F. Ng, and P.D.A. Pudney, *Mechanism and kinetics of the crosslinking reaction between biopolymers containing primary amine groups and genipin.* Journal of Polymer Science Part A: Polymer Chemistry, 2003. **41**(24): p. 3941-3953.
306. Mi, F.-L., et al., *Synthesis and characterization of biodegradable TPP/genipin co-crosslinked chitosan gel beads.* Polymer, 2003. **44**(21): p. 6521-6530.
307. Kawadkar, J. and M.K. Chauhan, *Intra-articular delivery of genipin cross-linked chitosan microspheres of flurbiprofen: preparation, characterization, in vitro and in vivo studies.* Eur J Pharm Biopharm, 2012. **81**(3): p. 563-72.
308. Chen, H., et al., *Reaction of chitosan with genipin and its fluorogenic attributes for potential microcapsule membrane characterization.* J Biomed Mater Res A, 2005. **75**(4): p. 917-27.
309. Ofner, J., et al., *Physico-chemical characterization of SOA derived from catechol and guaiacol – a model substance for the aromatic fraction of atmospheric HULIS.* Atmos. Chem. Phys., 2011. **11**.
310. Heux, L., et al., *Solid State NMR for Determination of Degree of Acetylation of Chitin and Chitosan.* Biomacromolecules, 2000. **1**(4): p. 746-751.
311. Zhang, M., et al., *Structure of insect chitin isolated from beetle larva cuticle and silkworm (Bombyx mori) pupa exuvia.* International Journal of Biological Macromolecules, 2000. **27**(1): p. 99-105.
312. Fründ, R., et al., *Comparison of the solid state CPMAS and solution carbon-13-NMR spectra of humic acids extracted from composted municipal refuse.* Zeitschrift für Naturforschung, 1987. **42**: p. 205-208.
313. Wyman, C.E., *Aqueous pretreatment of plant biomass for biological and chemical conversion to fuels and chemicals*. 2013: John Wiley & Sons.

314. Ritger, P.L. and N.A. Peppas, *A simple equation for description of solute release II. Fickian and anomalous release from swellable devices.* Journal of Controlled Release, 1987. **5**(1): p. 37-42.
315. Moura, M.J., M.M. Figueiredo, and M.H. Gil, *Rheological Study of Genipin Cross-Linked Chitosan Hydrogels.* Biomacromolecules, 2007. **8**(12): p. 3823-3829.
316. Sung, H.W., et al., *In vitro evaluation of cytotoxicity of a naturally occurring cross-linking reagent for biological tissue fixation.* J Biomater Sci Polym Ed, 1999. **10**(1): p. 63-78.
317. Okamoto, H., et al., *Development of polymer film dosage forms of lidocaine for buccal administration: I. Penetration rate and release rate.* Journal of Controlled Release, 2001. **77**(3): p. 253-260.
318. Leopold, A., et al., *Pharmacokinetics of lidocaine delivered from a transmucosal patch in children.* Anesth Prog, 2002. **49**(3): p. 82-7.
319. Routledge, P.A., et al., *Lidocaine plasma protein binding.* Clin Pharmacol Ther, 1980. **27**(3): p. 347-51.
320. Collinsworth, K.A., S.M. Kalman, and D.C. Harrison, *The clinical pharmacology of lidocaine as an antiarrhythymic drug.* Circulation, 1974. **50**(6): p. 1217-30.
321. Hersh, E., et al., *Analgesic efficacy and safety of an intraoral lidocaine patch.* The Journal of the American Dental Association, 1996. **127**(11): p. 1626-1634.
322. Danese, S. and C. Fiocchi, *Ulcerative Colitis.* New England Journal of Medicine, 2011. **365**(18): p. 1713-1725.
323. Molodecky, N.A., et al., *Increasing Incidence and Prevalence of the Inflammatory Bowel Diseases With Time, Based on Systematic Review.* Gastroenterology, 2012. **142**(1): p. 46-54.e42.
324. Kornbluth, A. and D.B. Sachar, *Ulcerative colitis practice guidelines in adults: American College Of Gastroenterology, Practice Parameters Committee.* Am J Gastroenterol, 2010. **105**(3): p. 501-23; quiz 524.
325. Varshosaz, J., A. Jaffarian Dehkordi, and S. Golafshan, *Colon-specific delivery of mesalazine chitosan microspheres.* Journal of Microencapsulation, 2006. **23**(3): p. 329-339.
326. Lichtenstein, G.R. and M.A. Kamm, *Review article: 5-aminosalicylate formulations for the treatment of ulcerative colitis – methods of comparing release rates and delivery of 5-aminosalicylate to the colonic mucosa.* Alimentary Pharmacology & Therapeutics, 2008. **28**(6): p. 663-673.
327. Riley, S.A., *What dose of 5-aminosalicylic acid (mesalazine) in ulcerative colitis?* Gut, 1998. **42**(6): p. 761-3.
328. Tozaki, H., et al., *Chitosan capsules for colon-specific drug delivery: enhanced localization of 5-aminosalicylic acid in the large intestine accelerates healing of TNBS-induced colitis in rats.* Journal of Controlled Release, 2002. **82**(1): p. 51-61.
329. Sandborn, W.J., *Rational selection of oral 5-aminosalicylate formulations and prodrugs for the treatment of ulcerative colitis.* Am J Gastroenterol, 2002. **97**(12): p. 2939-2941.
330. Sandborn, W.J. and S.B. Hanauer, *The pharmacokinetic profiles of oral mesalazine formulations and mesalazine pro-drugs used in the management of ulcerative colitis.* Alimentary Pharmacology & Therapeutics, 2003. **17**(1): p. 29-42.
331. Schroeder, K.W., W.J. Tremaine, and D.M. Ilstrup, *Coated oral 5-aminosalicylic acid therapy for mildly to moderately active ulcerative colitis. A randomized study.* N Engl J Med, 1987. **317**(26): p. 1625-9.

332. Sninsky, C.A., et al., *Oral mesalamine (Asacol) for mildly to moderately active ulcerative colitis. A multicenter study.* Ann Intern Med, 1991. **115**(5): p. 350-5.
333. Kamm, M.A., et al., *Effect of extended MMX mesalamine therapy for acute, mild-to-moderate ulcerative colitis.* Inflamm Bowel Dis, 2009. **15**(1): p. 1-8.
334. Kamm, M.A., et al., *Randomised trial of once- or twice-daily MMX mesalazine for maintenance of remission in ulcerative colitis.* Gut, 2008. **57**(7): p. 893-902.
335. Dick, A.P., et al., *Controlled trial of sulphasalazine in the treatment of ulcerative colitis.* Gut, 1964. **5**(5): p. 437-442.
336. Baron, J.H., et al., *Sulphasalazine and salicylazosulphadimidine in ulcerative colitis.* Lancet, 1962. **1**(7239): p. 1094-6.
337. Marteau, P., et al., *Combined oral and enema treatment with Pentasa (mesalazine) is superior to oral therapy alone in patients with extensive mild/moderate active ulcerative colitis: a randomised, double blind, placebo controlled study.* Gut, 2005. **54**(7): p. 960-5.
338. Lee, F.I., et al., *A randomised trial comparing mesalazine and prednisolone foam enemas in patients with acute distal ulcerative colitis.* Gut, 1996. **38**(2): p. 229-33.
339. Loew, B.J. and C.A. Siegel, *Foam preparations for the treatment of ulcerative colitis.* Curr Drug Deliv, 2012. **9**(4): p. 338-44.
340. Whitlow, C.B., *Ulcerative Proctitis.* Clinics in Colon and Rectal Surgery, 2004. **17**(1): p. 21-27.
341. Smart, J.D., *Theories of Mucoadhesion*, in *Mucoadhesive Materials and Drug Delivery Systems*. 2014, John Wiley & Sons, Ltd. p. 159-174.
342. Umejima, H., et al., *Application with bioadhesive Eudispert gel preparations containing ONO-4057, a new drug for ulcerative colitis, for rectal drug delivery.* Drug Delivery System, 1994. **9**(5): p. 363-369.
343. Dash, A.K., et al., *Development of a rectal nicotine delivery system for the treatment of ulcerative colitis.* International Journal of Pharmaceutics, 1999. **190**(1): p. 21-34.
344. Sedó, J., et al., *Catechol-Based Biomimetic Functional Materials.* Advanced Materials, 2013. **25**(5): p. 653-701.
345. Xu, J., et al., *Genipin-crosslinked catechol-chitosan mucoadhesive hydrogels for buccal drug delivery.* Biomaterials, 2015. **37**(0): p. 395-404.
346. Laroui, H., et al., *Dextran sodium sulfate (DSS) induces colitis in mice by forming nano-lipocomplexes with medium-chain-length fatty acids in the colon.* PLoS One, 2012. **7**(3): p. e32084.
347. Okayasu, I., et al., *A novel method in the induction of reliable experimental acute and chronic ulcerative colitis in mice.* Gastroenterology, 1990. **98**(3): p. 694-702.
348. Shimono, N., et al., *Chitosan dispersed system for colon-specific drug delivery.* International Journal of Pharmaceutics, 2002. **245**(1–2): p. 45-54.
349. van der Burg, T., *Injection Force of SoloSTAR(®) Compared with Other Disposable Insulin Pen Devices at Constant Volume Flow Rates.* Journal of Diabetes Science and Technology, 2011. **5**(1): p. 150-155.
350. Cilurzo, F., et al., *Injectability Evaluation: An Open Issue.* AAPS PharmSciTech, 2011. **12**(2): p. 604-609.
351. Diaz-Granados, N., et al., *Dextran Sulfate Sodium-Induced Colonic Histopathology, but not Altered Epithelial Ion Transport, Is Reduced by Inhibition of Phosphodiesterase Activity.* The American Journal of Pathology, 2000. **156**(6): p. 2169-2177.

352. Sayer, B., et al., *Dextran sodium sulphate-induced colitis perturbs muscarinic cholinergic control of colonic epithelial ion transport.* British Journal of Pharmacology, 2002. **135**(7): p. 1794-1800.
353. Perše, M. and A. Cerar, *Dextran Sodium Sulphate Colitis Mouse Model: Traps and Tricks.* Journal of Biomedicine and Biotechnology, 2012. **2012**: p. 13.
354. Geboes, K., *Histopathology of Crohn's disease and ulcerative colitis.* Inflammatory Bowel Disease. Edinburgh, London, Melbourne: Churchill Livingstone, 2003: p. 255-276.
355. Zhou, S.Y., et al., *Intestinal metabolism and transport of 5-aminosalicylate.* Drug Metab Dispos, 1999. **27**(4): p. 479-85.
356. Punchard, N.A., S.M. Greenfield, and R.P.H. Thompson, *Mechanism of action of 5-arninosalicylic acid.* Mediators of Inflammation, 1992. **1**(3): p. 151-165.
357. Joshi, R., et al., *Free radical scavenging reactions of sulfasalazine, 5-aminosalicylic acid and sulfapyridine: Mechanistic aspects and antioxidant activity.* Free Radical Research, 2005. **39**(11): p. 1163-1172.
358. Tozaki, H., et al., *Chitosan capsules for colon-specific drug delivery: Improvement of insulin absorption from the rat colon.* Journal of Pharmaceutical Sciences, 1997. **86**(9): p. 1016-1021.
359. De Jong, W.H. and P.J.A. Borm, *Drug delivery and nanoparticles: Applications and hazards.* International Journal of Nanomedicine, 2008. **3**(2): p. 133-149.
360. Panyam, J. and V. Labhasetwar, *Biodegradable nanoparticles for drug and gene delivery to cells and tissue.* Advanced Drug Delivery Reviews, 2003. **55**(3): p. 329-347.
361. Hoare, T.R. and D.S. Kohane, *Hydrogels in drug delivery: Progress and challenges.* Polymer, 2008. **49**(8): p. 1993-2007.
362. Kim, K., et al., *Chitosan-catechol: A polymer with long-lasting mucoadhesive properties.* Biomaterials, 2015. **52**(0): p. 161-170.